

UNCLASSIFIED

AD NUMBER

AD488080

LIMITATION CHANGES

TO:

Approved for public release; distribution is unlimited.

FROM:

Distribution authorized to U.S. Gov't. agencies and their contractors;  
Administrative/Operational Use; APR 1966. Other requests shall be referred to Army Materiel Command, Washington, DC 20310.

AUTHORITY

USAARDC ltr 29 Aug 1978

THIS PAGE IS UNCLASSIFIED

THIS REPORT HAS BEEN DELIMITED  
AND CLEARED FOR PUBLIC RELEASE  
UNDER DOD DIRECTIVE 5200.20 AND  
NO RESTRICTIONS ARE IMPOSED UPON  
ITS USE AND DISCLOSURE,

DISTRIBUTION STATEMENT A

APPROVED FOR PUBLIC RELEASE;  
DISTRIBUTION UNLIMITED,

488080

BRL R 1319

# BRL

AD

REPORT NO. 1319

## TERRAIN EFFECTS ON BLAST WAVE PARAMETERS

by

J. H. Keefer

J. D. Day

April 1966

This document is subject to special export controls and each transmittal to foreign governments or foreign nationals may be made only with prior approval of U.S. Army Materiel Command, ATTN: AMCMU-IS, Washington, D.C.

U. S. ARMY MATERIEL COMMAND  
**BALLISTIC RESEARCH LABORATORIES**  
ABERDEEN PROVING GROUND, MARYLAND

Destroy this report when it is no longer needed.  
Do not return it to the originator.

The findings in this report are not to be construed as an official Department of the Army position, unless so designated by other authorized documents.

BALLISTIC RESEARCH LABORATORIES

REPORT NO. 1319

APRIL 1966

This document is subject to special export controls and each transmittal to foreign governments or foreign nationals may be made only with prior approval of U.S. Army Materiel Command, ATTN: AMCMU-IS, Washington, D.C.

TERRAIN EFFECTS ON BLAST WAVE PARAMETERS

J. H. Keefer  
J. D. Day

Terminal Ballistics Laboratory

Work was partially supported by the  
Defense Atomic Support Agency.

RDT&E Project No. 1P014501A33E

ABERDEEN PROVING GROUND, MARYLAND

BALLISTIC RESEARCH LABORATORIES

REPORT NO. 1319

JHKeefe/JDDay/blw  
Aberdeen Proving Ground, Md.  
April 1966

TERRAIN EFFECTS ON BLAST WAVE PARAMETERS

ABSTRACT

This report presents the results from large scale model terrain features exposed to the blast wave from a 100 ton TNT surface burst and a small scale terrain model exposed to the blast wave from the Ballistic Research Laboratories (BRL) high pressure shock tube.

The large scale model terrain study utilized five terrain features exposed to the blast at various pressure levels. The terrain features were equipped with various types of overpressure and dynamic pressure instrumentation. Ratios obtained from the pressure measured on the flat terrain and that measured on the rising and falling slopes are presented.

For the small scale model test, pressures were measured over the rising and falling slopes of a  $30^{\circ}$  model hill exposed to the blast wave from the mouth of the BRL detonation driven shock tube. The pressure time records measured are presented. The results compare favorably to previously reported model data.

## TABLE OF CONTENTS

	Page
ABSTRACT . . . . .	3
LIST OF TABLES . . . . .	7
LIST OF FIGURES . . . . .	9
CHAPTER 1 INTRODUCTION . . . . .	13
1.1 Objectives . . . . .	13
1.2 Background . . . . .	13
1.3 Theory and Prediction . . . . .	14
CHAPTER 2 PROCEDURE . . . . .	26
2.1 Experimental Plan . . . . .	26
2.2 Site Activities . . . . .	33
2.3 Instrumentation . . . . .	33
2.4 Description of Data . . . . .	38
CHAPTER 3 RESULTS . . . . .	40
3.1 Terrain Feature A . . . . .	40
3.2 Terrain Feature B . . . . .	52
3.3 Terrain Feature C . . . . .	52
3.4 Terrain Feature D . . . . .	54
3.5 Terrain Feature E . . . . .	54
CHAPTER 4 DISCUSSION AND CONCLUSIONS . . . . .	57
4.1 Pulse Shape . . . . .	57
4.2 Comparison with Other Terrain Studies . . . . .	63
REFERENCES . . . . .	65

TABLE OF CONTENTS (contd)

	Page
APPENDIX A SHOCK PRESSURE DISTRIBUTION OVER A $30^{\circ}$ MODEL HILL. . .	67
APPENDIX B PRESSURE TIME PLOTS. . . . .	83
DISTRIBUTION LIST. . . . .	119



# LIST OF TABLES

<u>Table No.</u>		<u>Page</u>
1.1	PREDICTED MAXIMUM OVERPRESSURE RATIOS FOR VARIOUS PRESSURE LEVELS. . . . .	21
2.1a	INSTRUMENTATION PLAN FOR TERRAIN FEATURE A . . . . .	22
2.1b	INSTRUMENTATION PLAN FOR TERRAIN FEATURE B . . . . .	23
2.1c	INSTRUMENTATION PLAN FOR TERRAIN FEATURE C . . . . .	24
2.1d	INSTRUMENTATION PLAN FOR TERRAIN FEATURE D AND E . . . . .	25
3.1	RESULTS, CONTROL LINE BLAST PARAMETERS . . . . .	41
3.2	RESULTS, TERRAIN FEATURE A . . . . .	42
3.3	RESULTS, TERRAIN FEATURE B . . . . .	43
3.4	RESULTS, TERRAIN FEATURE C . . . . .	44
3.5	RESULTS, TERRAIN FEATURE D . . . . .	45
3.6	DYNAMIC PRESSURE RESULTS . . . . .	46
3.7	COMPARISON OF PRESSURE RATIOS. . . . .	48
A-I	OBSERVED PRESSURES - 30° MODEL HILL. . . . .	74
A-II	CALCULATIONS FOR A RISING SLOPE. . . . .	79

PREVIOUS PAGE WAS BLANK, THEREFORE WAS NOT FILMED

LIST OF FIGURES

<u>Figure No.</u>		<u>Page</u>
1.1	PREDICTED MAXIMUM OVERPRESSURE FOR 100 TON HE SURFACE BURST. . . . .	15
1.2	STAGNATION PRESSURE VERSUS PEAK OVERPRESSURE . . . .	16
1.3	MAXIMUM PRESSURE RATIOS FOR RISING SLOPES FOLLOWING FLAT TERRAIN, AS A FUNCTION OF SLOPE ANGLE AND INCIDENT MAXIMUM PRESSURE. . . . .	18
1.4	MAXIMUM PRESSURE RATIOS FOR FALLING SLOPES FOLLOWING FLAT TERRAIN, AS A FUNCTION OF SLOPE ANGLE AND INCIDENT MAXIMUM PRESSURE. . . . .	19
2.1	FIELD LAYOUT OF TERRAIN FEATURES . . . . .	27
2.2	STATION LAYOUT ON TERRAIN FEATURES A, B, C and D . .	28
2.3	GAGE LAYOUT ON TERRAIN FEATURES A, B, and C. . . . .	29
2.4	TERRAIN FEATURE A. . . . .	30
2.5	TERRAIN FEATURE B. . . . .	30
2.6	TERRAIN FEATURE C. . . . .	32
2.7	PRESSURE TRANSDUCERS . . . . .	32
2.8	TYPICAL GAGE STATION ON TERRAIN FEATURE. . . . .	36
2.9	SURFACE STAGNATION MOUNT . . . . .	36
2.10	PITOT PROBE MOUNTS, 12 and 36 INCHES IN HEIGHT . . .	37
3.1	MEASURED OVERPRESSURE ON THE FLAT CONTROL LINE . . .	49
3.2	MEASURED DYNAMIC PRESSURE ON THE FLAT CONTROL LINE .	50
3.3	MEASURED PRESSURES ON TERRAIN FEATURE A COMPARED WITH THE CONTROL LINE . . . . .	51
3.4	MEASURED PRESSURES ON TERRAIN FEATURE B COMPARED WITH THE CONTROL LINE . . . . .	53
3.5	MEASURED PRESSURES ON TERRAIN FEATURE C COMPARED WITH THE CONTROL LINE . . . . .	55

# LIST OF FIGURES (Contd)

Figure No.		Page
3.6	MEASURED PRESSURE ON TERRAIN FEATURES D AND E COMPARED WITH THE CONTROL LINE. . . . .	56
4.1	OVERPRESSURE - TIME ON TERRAIN FEATURE B COMPARED WITH CONTROL LINE . . . . .	58
4.2	OVERPRESSURE - TIME ON TERRAIN FEATURE C COMPARED WITH CONTROL LINE . . . . .	59
4.3	STAGNATION PRESSURE - TIME ON TERRAIN FEATURE B COMPARED WITH CONTROL LINE. . . . .	61
4.4	STAGNATION PRESSURE - TIME ON TERRAIN FEATURE C COMPARED WITH CONTROL LINE. . . . .	62
A1	A SKETCH OF THE MODEL HILL WITH GAGE POSITIONS. . . .	71
A2	PRESSURE-TIME RESULTS . . . . .	72
A3	PRESSURE-TIME RESULTS . . . . .	73
A4	MEASURED OVERPRESSURE ON TERRAIN MODEL COMPARED WITH FREE FIELD. . . . .	75
A5	MEASURED STAGNATION PRESSURE TERRAIN MODEL COMPARED WITH FREE FIELD . . . . .	76
A6	MEASURED OVERPRESSURE ON TERRAIN MODEL COMPARED WITH FREE FIELD. . . . .	77
A7	MEASURED STAGNATION ON TERRAIN MODEL COMPARED WITH FREE FIELD. . . . .	78
B1	FREE FIELD OVERPRESSURE MEASUREMENTS. . . . .	85
B2	FREE FIELD OVERPRESSURE MEASUREMENTS. . . . .	86
B3	FREE FIELD PRESSURE MEASUREMENTS AT 279 FEET, STATION 8.5 . . . . .	87
B4	FREE FIELD PRESSURE MEASUREMENTS AT 299 FEET, STATION 8.6 . . . . .	88
B5	FREE FIELD PRESSURE MEASUREMENTS AT 334 FEET, STATION 8.7 . . . . .	89

# LIST OF FIGURES (Contd)

Figure No.		Page
B6	FREE FIELD PRESSURE MEASUREMENTS AT 413 FEET, STATION 8.8 . . . . .	90
B7	FREE FIELD PRESSURE MEASUREMENTS AT 443 FEET, STATION 8.9 . . . . .	91
B8	FREE FIELD PRESSURE MEASUREMENTS IN FRONT OF TERRAIN FEATURE A, STATION P1 . . . . .	92
B9	PRESSURE MEASUREMENTS ON 15° RISING SLOPE OF TERRAIN FEATURE A, STATION P2 . . . . .	93
B10	PRESSURE MEASUREMENTS ON 15° RISING SLOPE OF TERRAIN FEATURE A, STATION P3 . . . . .	94
B11	FREE FIELD PRESSURE MEASUREMENTS IN FRONT OF TERRAIN FEATURE B, STATION P1 . . . . .	95
B12	PRESSURE MEASUREMENTS ON 15° RISING SLOPE OF TERRAIN FEATURE B, STATION P2 . . . . .	96
B13	PRESSURE MEASUREMENTS ON 15° RISING SLOPE OF TERRAIN FEATURE B, STATION P2 SURFACE LEVEL STAGNATION BLOCK. .	97
B14	PRESSURE MEASUREMENTS ON 15° RISING SLOPE OF TERRAIN FEATURE B, STATION P3 . . . . .	98
B15	PRESSURE MEASUREMENTS ON 15° RISING SLOPE OF TERRAIN FEATURE B, STATION P3 SURFACE LEVEL STAGNATION BLOCK. .	99
B16	PRESSURE MEASUREMENTS ON 15° FALLING SLOPE OF TERRAIN FEATURE B, STATION P5 . . . . .	100
B17	PRESSURE MEASUREMENTS ON 15° FALLING SLOPE OF TERRAIN FEATURE B, STATION P5 SURFACE LEVEL STAGNATION BLOCK. .	101
B18	PRESSURE MEASUREMENTS IN BACK OF TERRAIN FEATURE B, STATION P6 . . . . .	102
B19	FREE FIELD PRESSURE MEASUREMENTS IN FRONT OF TERRAIN FEATURE C, STATION P1 . . . . .	103
B20	PRESSURE MEASUREMENTS ON 30° RISING SLOPE OF TERRAIN FEATURE C, STATION P2 . . . . .	104

# LIST OF FIGURES (Contd)

<u>Figure No.</u>		<u>Page</u>
B21	PRESSURE MEASUREMENTS ON 30° RISING SLOPE OF TERRAIN FEATURE C, STATION P2 SURFACE LEVEL STAGNATION BLOCK .	105
B22	PRESSURE MEASUREMENTS ON 30° RISING SLOPE OF TERRAIN FEATURE C, STATION P3. . . . .	106
B23	PRESSURE MEASUREMENTS ON 30° RISING SLOPE OF TERRAIN FEATURE C, STATION P3 SURFACE LEVEL STAGNATION BLOCK .	107
B24	PRESSURE MEASUREMENTS ON 30° FALLING SLOPE OF TERRAIN FEATURE C, STATION P4. . . . .	108
B25	PRESSURE MEASUREMENTS ON 30° FALLING SLOPE OF TERRAIN FEATURE C, STATION P4 SURFACE LEVEL STAGNATION BLOCK .	109
B26	PRESSURE MEASUREMENTS ON 30° FALLING SLOPE OF TERRAIN FEATURE C, STATION P5. . . . .	110
B27	PRESSURE MEASUREMENTS ON 30° FALLING SLOPE OF TERRAIN FEATURE C, STATION P5 SURFACE LEVEL STAGNATION BLOCK .	111
B28	PRESSURE MEASUREMENTS IN BACK OF TERRAIN FEATURE C, STATION P6 . . . . .	112
B29	SELF-RECORDING OVERPRESSURE-TIME RECORDS FROM TERRAIN FEATURE A. . . . .	113
B30	SELF-RECORDING OVERPRESSURE-TIME RECORDS FROM TERRAIN FEATURE B. . . . .	114
B31	SELF-RECORDING OVERPRESSURE-TIME RECORDS FROM TERRAIN FEATURE C. . . . .	115
B32	SELF-RECORDING OVERPRESSURE-TIME RECORDS FROM TERRAIN FEATURE D. . . . .	116
B33	SELF-RECORDING OVERPRESSURE-TIME RECORDS FROM TERRAIN FEATURE E. . . . .	117

## CHAPTER 1

### INTRODUCTION

During the period from 1959 to 1964, the Canadian Government was conducting a comprehensive program for measuring air blast parameters from various size charges of TNT (from 8 to 1,000,000 pounds) detonated on the ground. Projects from the United Kingdom (UK) and the United States, as well as those from Canada, participated in the study of air blast phenomenology and blast effects. U.S. Project Number 8, carried out by personnel from the U.S. Army Ballistic Research Laboratories (BRL), was sponsored by the Defense Atomic Support Agency on a 100 ton test in 1961 to study how terrain effects can alter an air blast wave.

To correlate the results obtained by measuring the effects produced by full scale topographic features with small scale topography effects, scaled models of terrain features were tested in the BRL Shock Tube Facility.

#### 1.1 Objectives

(a) To determine the effects of topography (rising and falling slopes) on the dynamic pressure resulting from the detonation of a 100 ton TNT charge.

(b) To correlate the information obtained with current and previous studies.

#### 1.2 Background

Terrain effects received little attention before the advent of nuclear weapons. The blast waves from small yield conventional weapons do not cover sufficient area to encounter large surface variations. However, the greater the yield, the larger the area of blast effectiveness and this area is more likely to include significant topographic features. For a one kiloton nuclear device, burst at the optimum height over a level surface, the peak shock overpressure of about 4 psi - adequate to cause a large amount of damage to many man-made structures - is experienced as far from ground zero as 1/2 of a mile. For a one-megaton weapon this distance becomes about 5 miles<sup>1\*</sup>.

---

\* *Superscript numbers denote references which may be found on page 65.*

Natural topographic features such as hills and dales can provide various degrees of protection for drag-sensitive targets. Studies have been conducted to determine the effect of rising and falling slopes on peak overpressure, but very little work has been done on dynamic pressure. The peak overpressure studies varied from full-scale terrain measurements in the low-pressure region during nuclear tests, to small models exposed to a wide range of pressures from small charges.<sup>2</sup> Interferometer studies of models with various angles in the shock tube have also contributed to the understanding of how slopes effect blast wave parameters.<sup>3</sup>

Prior to Shot Smoky, during Operation Plumbbob, 1957, no known studies of terrain effects on dynamic pressure had been conducted.<sup>4</sup> For Shot Smoky, the surface of the terrain varied a great deal from station to station, both in slope angle and surface roughness; thus, it was difficult to generalize the information that was obtained. Since then, Broadview Research Corporation and BRL have conducted small-scale model experiments to learn more about the change in dynamic pressure as the blast wave encounters rising and falling slopes.<sup>5</sup> The results from these model studies show an increase in the dynamic pressure for a 30° rising slope and a broadening of the pulse width with increasing distance up the front slope. Both these phenomena agree with previous observations of side-on pressure changes on the front slope.

### 1.3 Theory and Prediction

The free-field maximum peak overpressure to be expected at a particular measurement station was obtained from the curve predicted for the 100 tons of HE (Figure 1.1). A curve giving the total head pressure (stagnation pressure) was then established from standard Rankine-Hugoniot classical relationships and is shown in Figure 1.2. This curve predicts the measured total head pressure. To obtain dynamic pressure, the side-on or static overpressure is subtracted from the total head pressure; in addition a compressibility correction is necessary. With these two curves, the gage ranges were established for all free-field stations.

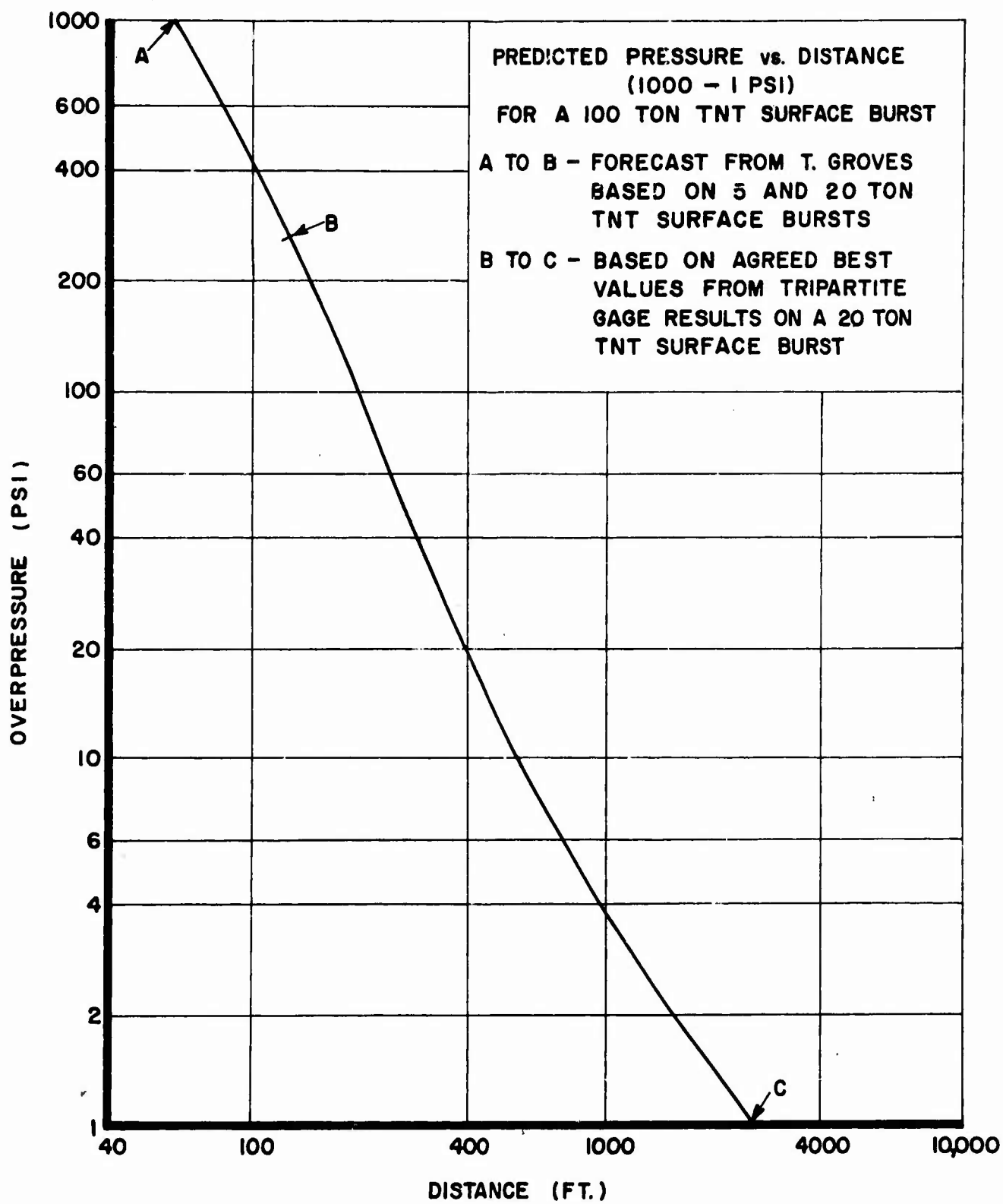


FIGURE 1.1 PREDICTED MAXIMUM OVERPRESSURE FOR 100 TON HE SURFACE BURST



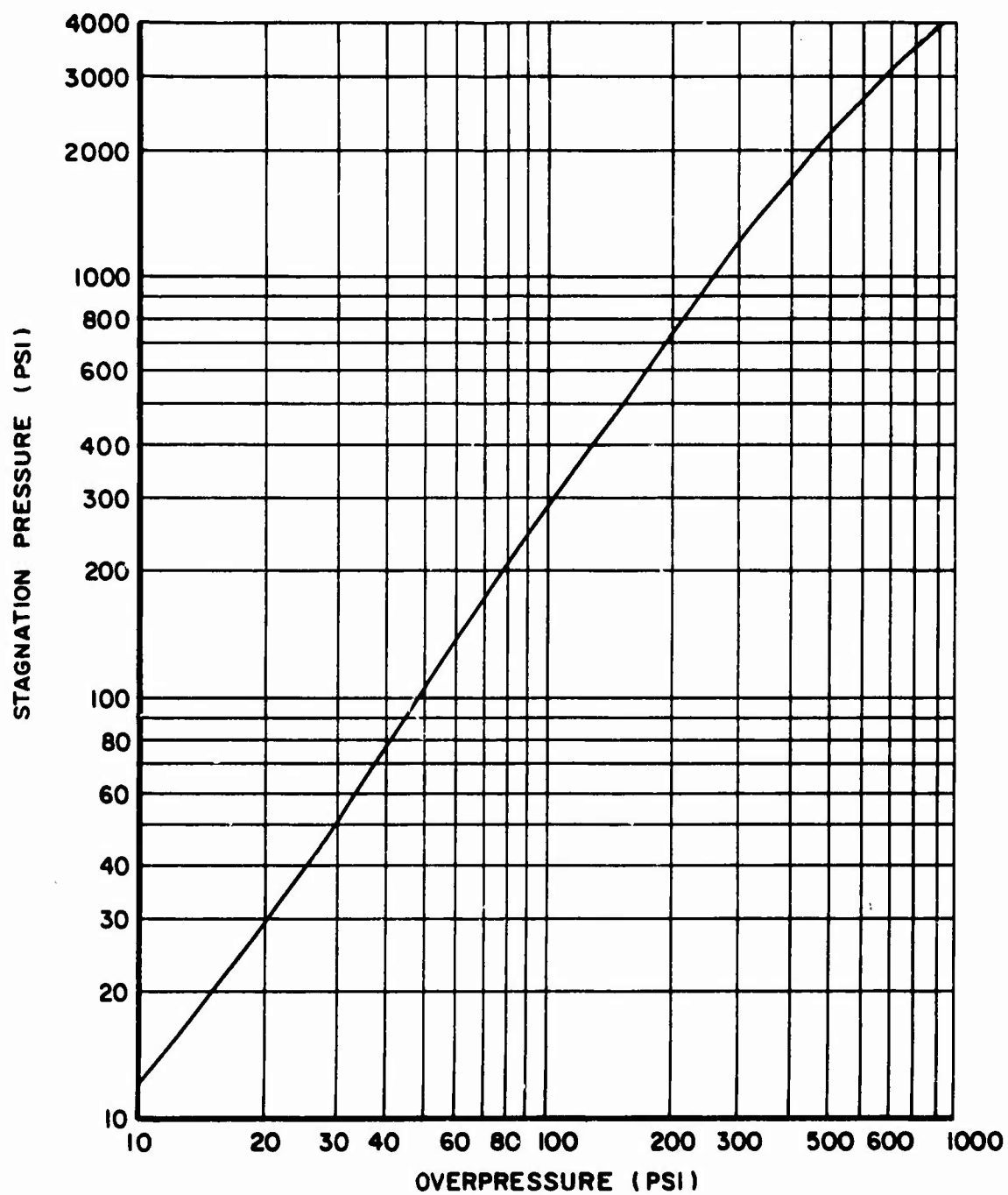


FIGURE 1.2 STAGNATION PRESSURE VERSUS PEAK OVERPRESSURE

On the forward rising slopes where a Mach stem forms the maximum overpressure was predicted from Figure 1.3.<sup>2</sup> The maximum overpressure ratio or amplification factor is defined as the ratio of pressure on the slope to the pressure at the same distance over flat terrain. This ratio or amplification factor remains more or less constant for a particular slope. Shadowgraph analysis of shock waves incident on model terrains has shown that the increase in maximum pressure on a rising slope exists right down to the beginning of the slope even though on several tests pressures measured at the first station were lower than pressures measured at points along the rest of the slope.<sup>6</sup> The gages used in these measurements in many cases are believed to have missed the very short pressure spike that exists near the beginning of the slope. For rising slopes the results in Reference 6 are given by the following empirical equation:

$$A = 1 + 2.63 \tan \theta \left(1 - \frac{r_0}{r} \cos 2\theta\right)$$

where

- A - is the ratio of overpressure on the rising slope to the overpressure at the same distance over flat terrain
- $\theta$  - is the slope angle of the topographical shape
- r - is the slant distance from the point of detonation to the start of the slope
- $r_0$  - is a characteristic distance dependent on the cube root of the charge weight.

Where Mach reflection occurs on the rising slope of a symmetrical ridge, the interaction processes occurring on the falling slope are generally quite similar to those found on isolated falling slopes. The reason for this similarity is that the increase in pressure due to the Mach reflection on the rising slope is approximately counteracted by the additional reduction in pressure due to the greater angle through which the Mach stem must diffract as it passes onto the falling slope. The falling slope maximum overpressures are given in Figure 1.4. For symmetrical ridges the following empirical equation has been obtained by Todd,<sup>6</sup>

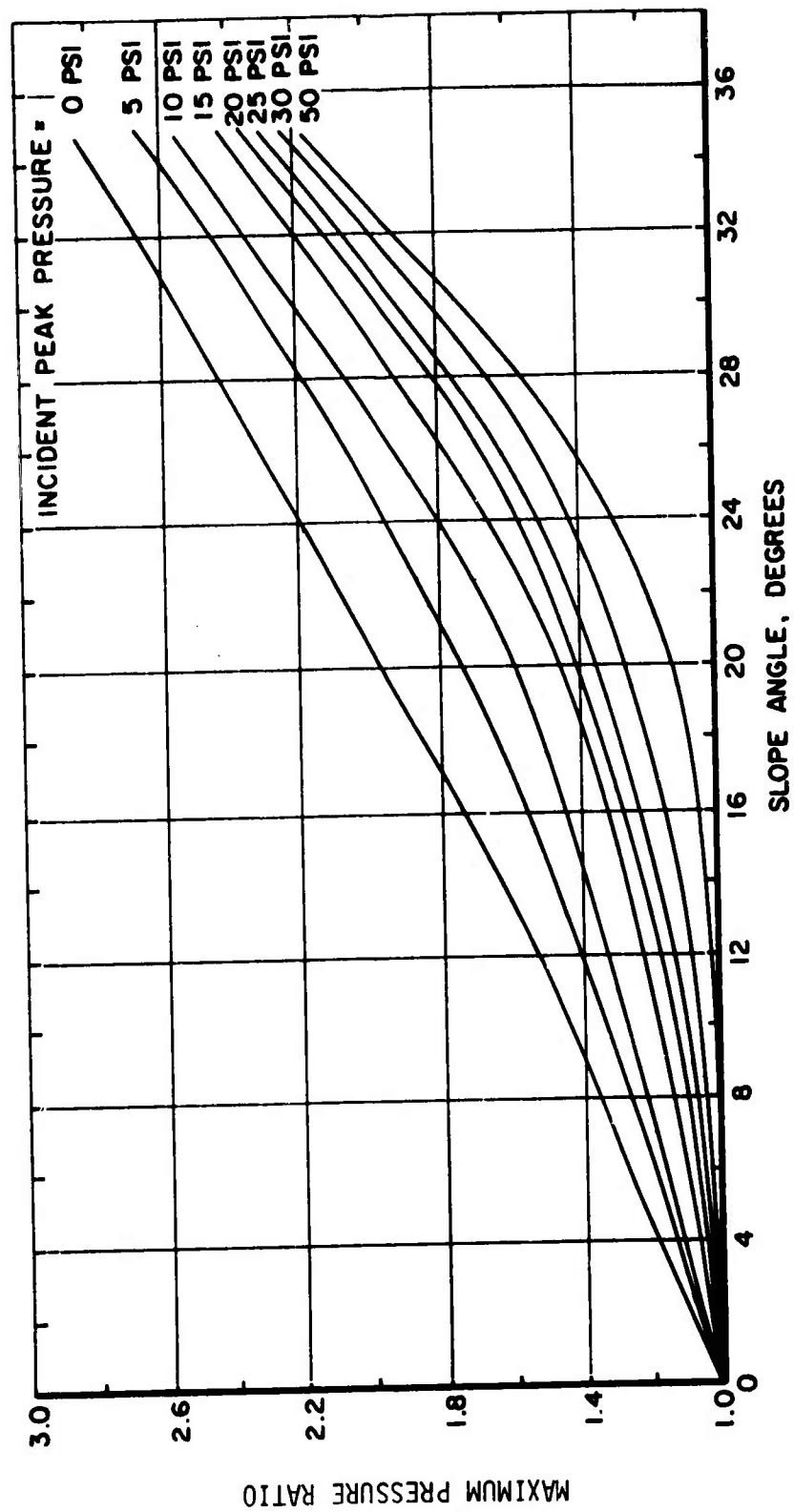


FIGURE 1.3 MAXIMUM PRESSURE RATIOS FOR RISING SLOPES FOLLOWING FLAT TERRAIN, AS A FUNCTION OF SLOPE ANGLE AND INCIDENT MAXIMUM PRESSURE

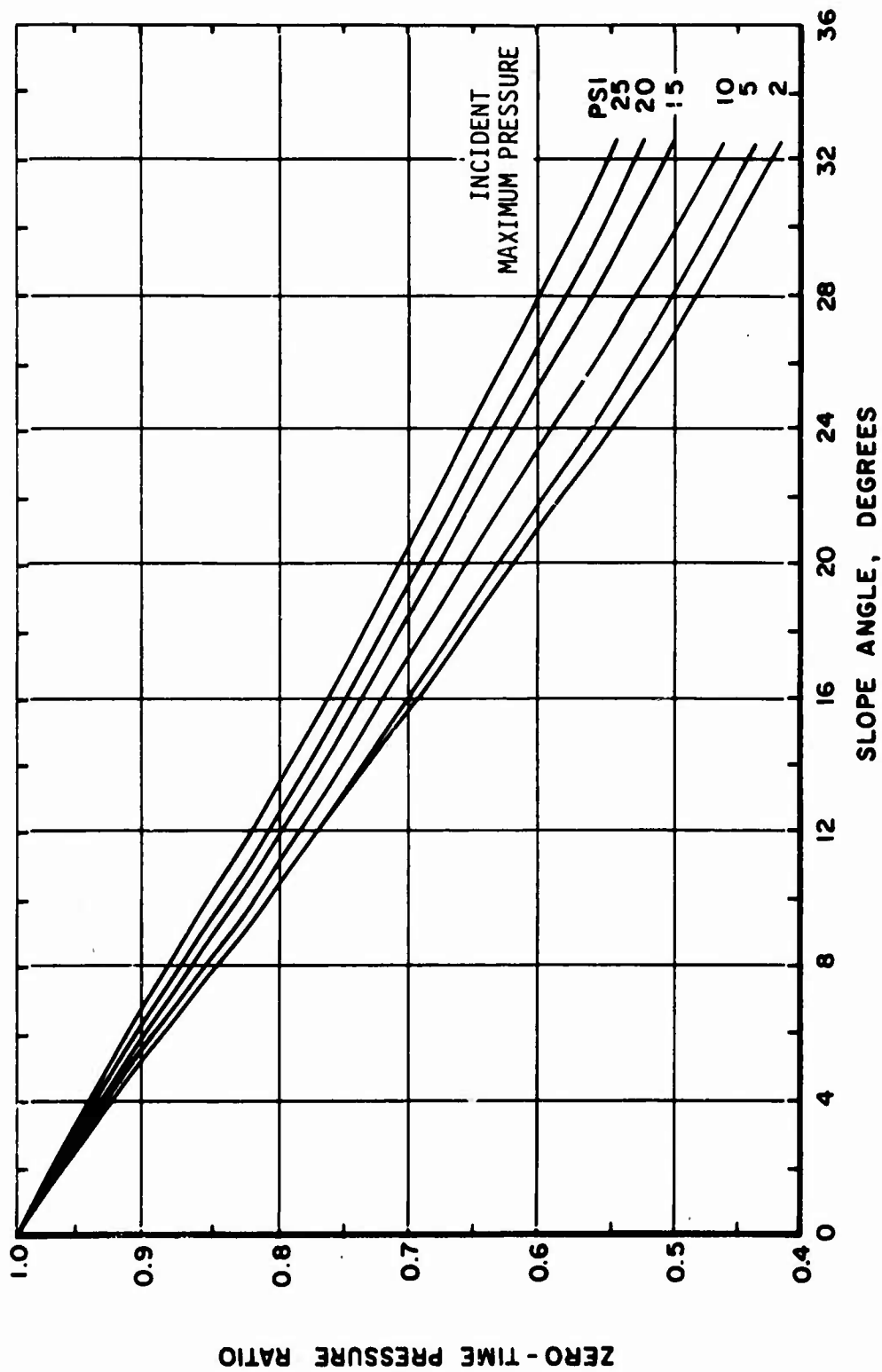


FIGURE 1.4 MAXIMUM PRESSURE RATIOS FOR FALLING SLOPES FOLLOWING FLAT TERRAIN, AS A FUNCTION OF SLOPE ANGLE AND INCIDENT MAXIMUM PRESSURE

$$A = 1 - 0.61 \sin 2\theta$$

where      A - is the ratio of maximum overpressure on the falling slope to the maximum overpressure on flat terrain at equal horizontal distance

$\theta$  - is the falling slope angle.

Table 1.1 gives the maximum overpressure ratios predicted for various overpressure levels for both the rising and falling slopes.

Stagnation pressures on the slopes were established by using the predicted peak overpressures and classical shock relations between overpressure and dynamic pressure. The assumption was made that the blast wave would be perpendicular to the surface of the slopes at all positions instrumented. The predicted maximum overpressure and stagnation pressures for all positions on the terrain features are given in Table 2.1.

TABLE 1.1 PREDICTED MAXIMUM OVERPRESSURE RATIOS FOR  
VARIOUS PRESSURE LEVELS

Pressure Level	Slope Angle	Rising Slope Ratio	Falling Slope Ratio	Terrain Feature
psi	degree			
50	15	1.05	0.85	A
20	15	1.25	0.76	B
20	30	1.96	0.55	C
10	15	1.40	0.73	D
25	26	-	0.63	E

TABLE 2.1 (a) INSTRUMENTATION PLAN FOR TERRAIN FEATURE A

Position	Distance From Ground Zero feet	Type Station	Type Gage	Recorder	Type Measurement	Predicted Pressure psi
8A-P1-40	255.4	Free field in front of terrain feature	Piezo	Miller	Total	125.0
60			Piezo	Miller	Side-on	56.0
60			Piezo	Miller	Side-on	56.0
70			Mechanical	Self-recording	Side-on	56.0
8A-P2-40	271.0	15° rising slope	Piezo	Miller	Total (12")	112.0
60			Piezo	Miller	Side-on	52.2
65			Detroit	Leach	Total (surface)	112.0
70			Mechanical	Self-recording	Side-on	52.2
8A-P3-40	273.8	15° rising slope	Piezo	Miller	Total (12")	104.0
60			Piezo	Miller	Side-on	49.0
65			Detroit	Leach	Total (surface)	104.0
70			Mechanical	Self-recording	Side-on	49.0
8A-P4-40	290.4	15° falling slope	Piezo	Miller	Total (12")	62.0
60			Piezo	Miller	Side-on	34.4
65			Detroit	Leach	Total (surface)	62.0
70			Mechanical	Self-recording	Side-on	34.4
8A-P5-40	298.1	15° falling slope	Piezo	Miller	Total (12")	56.0
60			Piezo	Miller	Side-on	32.3
65			Detroit	Leach	Total (surface)	56.0
70			Mechanical	Self-recording	Side-on	32.3
8A-P6-40	313.8	Free field in back of terrain feature	Piezo	Miller	Total (12")	56.0
60			Piezo	Miller	Side-on	32.0
70			Mechanical	Self-recording	Side-on	32.0

TABLE 2.1 (b) INSTRUMENTATION PLAN FOR TERRAIN FEATURE B

Position	Distance From Ground Zero feet	Type Station	Type Gage	Recorder	Type Measurement	Predicted Pressure psi
8B-P1-40	391.1	Free field in front of terrain feature	Detroit	20 kc	Total (12")	31.0
60			Detroit	20 kc	Side-on	21.2
70			Mechanical	Self-recording	Side-on	21.2
8B-P2-40	406.8	15° rising slope	Detroit	20 kc	Total (12")	37.0
60			Detroit	20 kc	Side-on	23.9
65			Detroit	Miller	Total (surface)	37.0
70			Mechanical	Self-recording	Side-on	23.9
8B-P3-40	414.5	15° rising slope	Detroit	20 kc	Total (12")	34.0
60			Detroit	20 kc	Side-on	22.6
65			Detroit	Miller	Total (surface)	34.0
70			Mechanical	Self-recording	Side-on	22.6
8B-P4-40	426.1	15° falling slope	Detroit	20 kc	Total (12")	17.0
60			Detroit	20 kc	Side-on	13.4
65			Detroit	Miller	Total (surface)	17.0
70			Mechanical	Self-recording	Side-on	13.4
8B-P5-40	433.8	15° falling slope	Detroit	20 kc	Total (12")	16.0
60			Detroit	20 kc	Side-on	12.6
65			Detroit	Miller	Total (surface)	16.0
70			Mechanical	Self-recording	Side-on	12.6
8B-P6-40	449.5	Free field in back of terrain feature	Detroit	20 kc	Total (12")	20.0
60			Detroit	20 kc	Side-on	15.5
70			Mechanical	Self-recording	Side-on	15.5



TABLE 2.1 (c) INSTRUMENTATION PLAN FOR TERRAIN FEATURE C

Position	Distance From Ground Zero feet	Type Station	Type Gage	Recorder	Type Measurement	Predicted Pressure psi
8C-P1-40	390.1	Free field in front of terrain feature	CEC	3 kc	Total (12")	31.0
60			CEC	3 kc	Side-on	21.5
70			Mechanical	Self-recording	Side-on	21.5
8C-P2-40	405.2	30° rising slope	CEC	20 kc	Total (12")	68.0
60			CEC	20 kc	Side-on	37.6
65			Detroit	20 kc	Total (surface)	68.0
70			Mechanical	Self-recording	Side-on	37.6
8C-P3-40	412.1	30° rising slope	CEC	20 kc	Total (12")	63.0
60			CEC	20 kc	Side-on	35.7
65			Detroit	3 kc	Total (surface)	63.0
70			Mechanical	Self-recording	Side-on	35.7
8C-P4-40	422.5	30° falling slope	CEC	20 kc	Total (12")	11.5
60			CEC	20 kc	Side-on	9.5
65			Detroit	20 kc	Total (surface)	11.5
70			Mechanical	Self-recording	Side-on	9.5
8C-P5-40	429.4	30° falling slope	CEC	20 kc	Total (12")	11.0
60			CEC	20 kc	Side-on	9.2
65			Detroit	3 kc	Total (surface)	11.0
70			Mechanical	Self-recording	Side-on	9.2
8C-P6-40	444.4	Free field in back of terrain feature	CEC	20 kc	Total (12")	23.0
60			CEC	20 kc	Side-on	16.9
70			Mechanical	Self-recording	Side-on	16.9

TABLE 2.1 (d) INSTRUMENTATION PLAN FOR TERRAIN FEATURE D and E

Position	Distance From Ground Zero feet	Type Station	Type Gage	Recorder	Type Measurement	Predicted Pressure psi
8D-P1-70	255.4	Free field in front of terrain feature	Mechanical	Self-recording	Side-on	11.2
8D-P2-70	271.0	15° rising slope	Mechanical	Self-recording	Side-on	14.6
8D-P3-70	278.8	15° rising slope	Mechanical	Self-recording	Side-on	14.0
8D-P4-70	290.4	15° falling slope	Mechanical	Self-recording	Side-on	7.1
8D-P5-70	298.1	15° falling slope	Mechanical	Self-recording	Side-on	6.9
8D-P6-70	313.8	Free field in back of terrain feature	Mechanical	Self-recording	Side-on	9.2
8E-P1-70	353.7	26° falling slope	Mechanical	Self-recording	Side-on	16.7
8E-P2-70	356.4	26° falling slope	Mechanical	Self-recording	Side-on	16.4

## CHAPTER 2

### PROCEDURE

Symmetrical terrain features were constructed of earth; various types of blast instrumentation were installed at significant points on the features. The blast sensors were mounted on concrete pads, as shown in Figure 2.1. This terrain study utilized fine terrain features exposed to the blast at several overpressure levels. An extensive number of ground baffle overpressure gages, both electronic and mechanical were used on the primary terrain features. On the secondary terrain features mechanical overpressure gages were used. Electronic stagnation pressure gages were used on the three primary terrain features.

#### 2.1 Experimental Plan

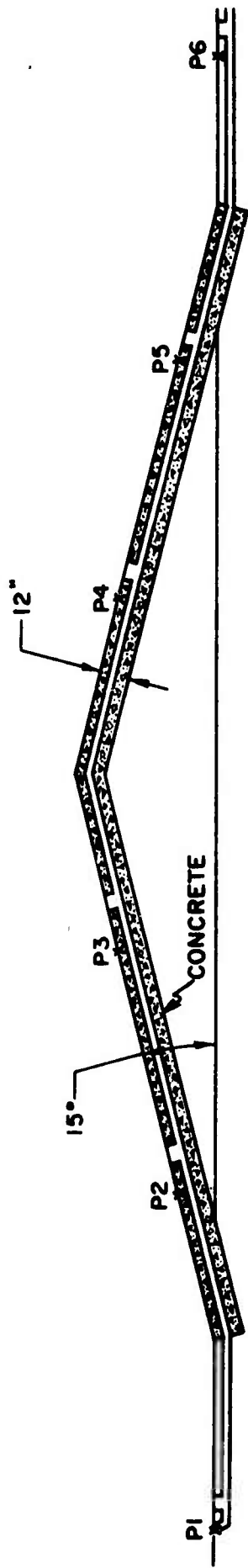
A blast line or control line was located between the structures for Projects US-7 and US-8, and the information obtained from this was utilized by both projects as input data.<sup>7</sup> There were three primary features, Terrain Features A, B, and C, and two auxiliary ones, Terrain Features D and E. The field layout of terrain features, measurement station positions, and the gage locations are shown in Figures 2.2 and 2.3. The instrumentation is summarized in Table 2.1.

Terrain Feature A was a symmetrical hill or ridge located in the 50 psi overpressure region; the rising and falling slopes were at 15 degrees. Thirteen channels of high frequency piezo gages with a cathode ray recording system were used to measure the ground baffle side-on pressures and the total head pressures from the pitot probes. Four channels of bonded strain gages recording on a 10-kc response magnetic tape system were used for the surface stagnation measurements. Six mechanical, self-recording gages were used as ground baffle gages to make side-on pressure measurements on all hills. Figure 2.4 shows Feature A.

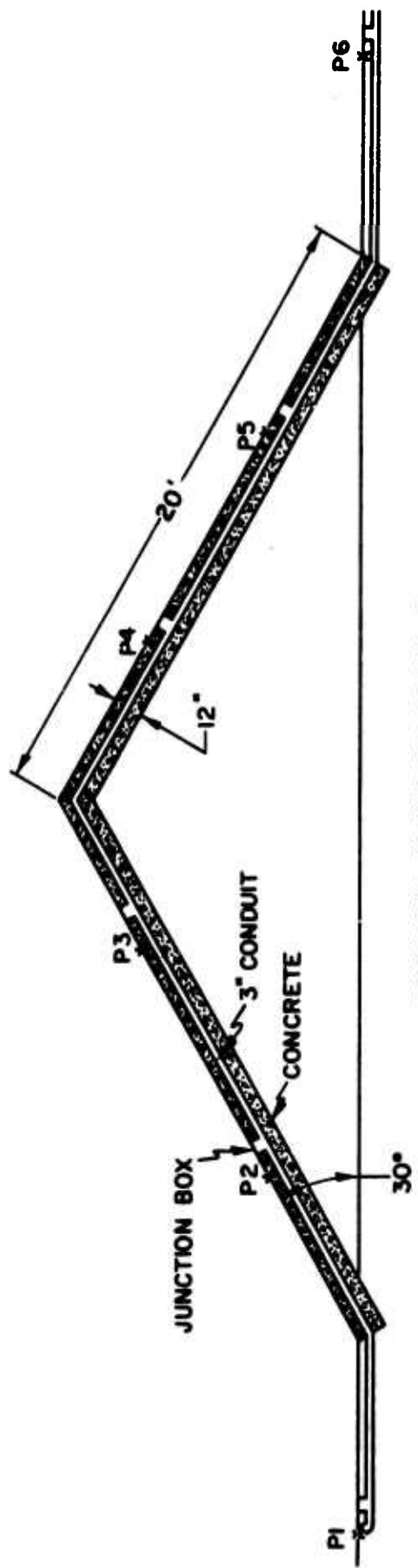
Terrain Feature B was a 15 degree slope identical to Feature A; however, B was positioned in the 20 psi region. Twelve channels of bonded strain gages with a 20 kc carrier frequency recording system were used



FIGURE 2.1 FIELD LAYOUT OF TERRAIN FEATURES



TERRAIN FEATURE TYPE A, B AND D



TERRAIN FEATURE TYPE C

FIGURE 2.2 STATION LAYOUT ON TERRAIN FEATURES A, B, C AND D

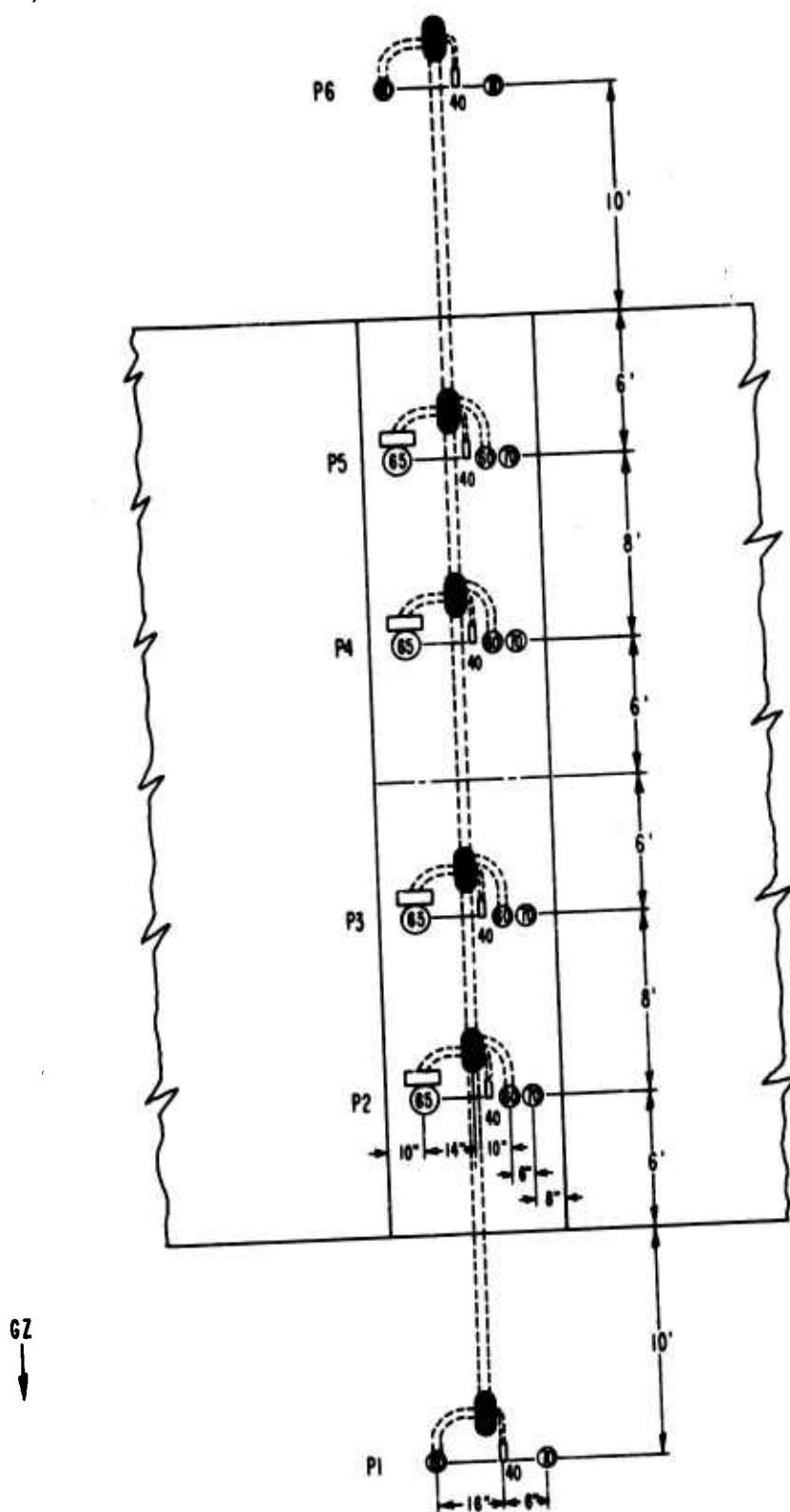


FIGURE 2.3 GAGE LAYOUT ON TERRAIN FEATURES A, B, AND C

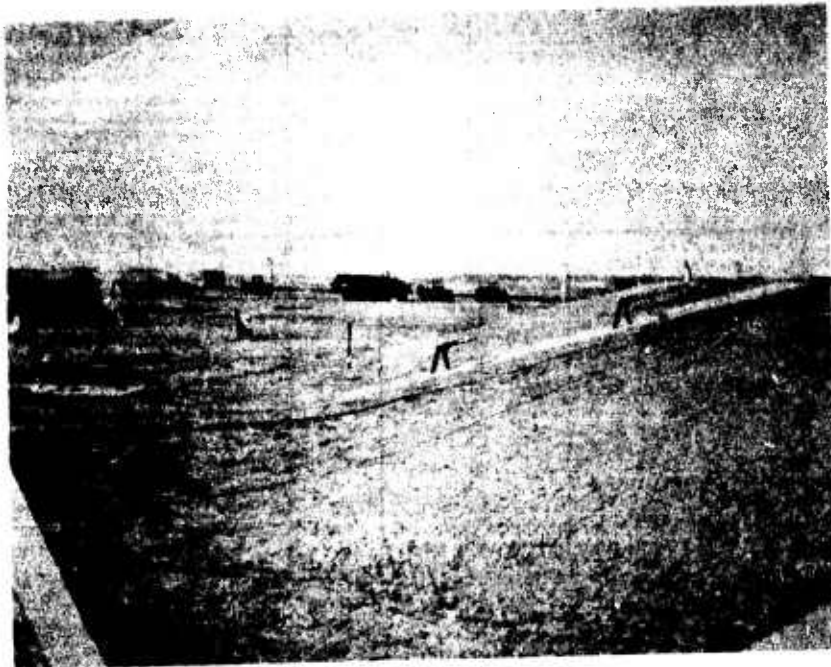


FIGURE 2.4 TERRAIN FEATURE A



FIGURE 2.5 TERRAIN FEATURE B

to measure the ground baffle overpressure and the total head pressures. Four channels of bonded strain gages with a cathode ray recording system were used to measure the surface stagnation pressures. Feature B is shown in Figure 2.5.

Terrain Feature C was a symmetrical ridge with front and back slopes inclined 30 degrees; it was positioned in the 20 psi overpressure region. Ten channels of unbonded strain gages with a 20 kc carrier frequency recording system were used to measure the ground baffle side-on overpressures and the total head pressures from the pitot probes. Two channels of bonded strain gages with the 20 kc carrier frequency recording system were used for two of the surface stagnation measurements, and two channels of bonded strain gages with a 3 kc carrier frequency recording system were used for the other surface stagnation measurements. Two channels of unbonded strain gages with a 3 kc carrier frequency recorder completed the ground baffle and pitot probe measurements. Figure 2.6 shows Feature C.

Terrain Feature D was the earth covered lateral portion of the Project US-7 tunnel. This earth berm was fashioned into a symmetrical ridge with 15 degree front and back slopes. This feature was in the 10 psi region and was instrumented solely with self-recording gages.

Terrain Feature E, located in the 25 psi region, was a field fortification of Project US-5. This feature was an excavation, as opposed to the hill structures. The leading downward slope was inclined at 26 degrees and was instrumented with two self-recording gages.

The blast line had seven ground baffles and five pitot probes; channels at these stations consisted of five channels of piezo gages with cathode ray recording, three channels of bonded strain gages with cathode ray recording, and four channels of bonded strain gages with 10 kc magnetic tape recording.





FIGURE 2.6 TERRAIN FEATURE C

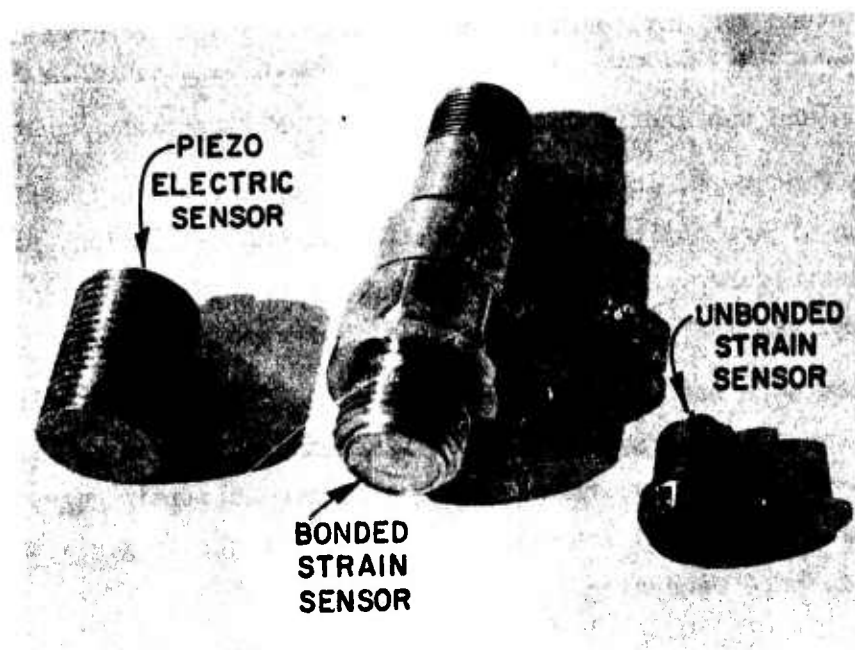


FIGURE 2.7 PRESSURE TRANSDUCERS

## 2.2 Site Activities

Project personnel began arriving at the test site approximately five weeks before shot day. Much of the heavy construction work had been completed by this time. The artificial hills had been built and the concrete pads had been poured. The final grades and surfacing were completed under project supervision. The majority of cable ditching had been dug; all short connecting ditches were finished within several days. Special care was taken to ensure that the coaxial cables and splices were enclosed in conduit and buried at least 36 inches. This precaution was taken since the cable is susceptible to impulsive loading. Random signal fluctuations result in many cases with unprotected cables. By the second week in the field, cables, conduit, and gage housings had been installed and in-place calibrations of transducers had begun.

The field calibration of all electronic gages was considered important and the most critical phase of the site activities. Laboratory calibrations had been carried out on all equipment before the project went to the field, because much more exhaustive examinations could be made concerning response, damping, mounting techniques, and static-dynamic output under the controlled conditions of the laboratory. For these calibrations of the electronic equipment to be meaningful, the field calibrations must show that the system gain has remained constant and can be duplicated at shot time by electrical methods. Approximately two weeks were devoted to in-place calibrations. The week immediately preceding the shot was used for gage installation for any recalibration necessary.

## 2.3 Instrumentation

2.3.1 Transducers. Since the primary objective of this project was the determination of the effects of terrain on air blast propagation, transducers that had the necessary output and response to monitor the pressure fluctuations had to be selected. The specific transducers selected are shown in Figure 2.7; namely, a piezo-electric crystal gage,

a bonded strain gage pressure pickup, and an unbonded strain gage. At the higher pressure level (50 psi), the high frequency piezo gages were used, and the strain gage pressure pickups were used at the 20 psi level.

The piezo-electric gages had lead-metaniobate crystals as the sensitive element. They were designed especially for use on Feature A where the pressures were higher and fluctuations more rapid than on B or C. The charge sensitivity averaged about 80  $\mu$ coulombs/psi. The resonant frequency of the gages occurred between 35-50 kc.

The bonded strain gage pressure pickup was manufactured by the Detroit Controls Division of the American Standard Corporation. This gage had an output of 50 mv at full scale and the output was flat from 0 to 20,000 cps. It is a temperature-stabilized, 4-arm bridge strain element bonded to a cylinder. This cylinder is attached to a corrugated diaphragm and the diaphragm is flush-mounted in the structure. As the overpressure deflects the diaphragm, the cylinder is compressed and the voltage changes proportionally.

The unbonded strain gage pickup, a 4-arm bridge type, was manufactured by the Consolidated Electrodynamic Corporation (CEC). The output of this transducer is 20 mv/v of excitation voltage; the transducer has a natural frequency of approximately 15,000 cps. Its sensing mechanism consists of a wire-wound flexible core which is in contact with a diaphragm. When the gage is mounted flush with the structure, pressure exerted on the diaphragm will expand the core, thereby unbalancing the 4-arm bridge proportionally. This mechanical linkage limits the response frequency, but the gage is quite stable and linear.

The mechanical self-recording gage used on Project US-8 was designed and developed for medium pressure ranges. It has been used with much success under many conditions. The transducer is a corrugated capsule which expands as the result of incident pressure. A stylus attached to the capsule scribes a line which represents the capsule deflection

on a revolving aluminized glass disk driven by a governed dc motor. The pressure fluctuations versus time are recorded. The sensitivity of the capsule is 50 mils/full scale and the natural frequency is approximately 250 cps.

The electronic gages were used both as the surface level gages and the pitot probe gages. The self-recording gages were always used in the flush mounted ground baffles for side-on pressure measurements, Figure 2.8. Surface stagnation pressures were measured by means of a block which stagnated the flow, mounted directly behind a flush ground baffle, Figure 2.9. The ground gage monitored the stagnation pressure. The pitot probes on the terrain were 12 inches above the surface, whereas those on the blast line were mounted 36 inches above the surface, Figure 2.10.

Field calibrations were accomplished by two methods. Those strain gages utilizing the carrier systems were statically calibrated by applying air at a pressure controlled by a series of regulators and flow valves contained in a calibration console. The pressure source was a small portable high pressure air bottle which fed the regulator console. The gage was mounted in the console and the proper pressures applied. Dynamic calibrations were applied to the crystal gages and the strain gages recording on the cathode ray recorders. This type calibration was used for two reasons. One, the crystal gages cannot maintain a constant output when statically loaded and two, the cathode followers used with crystal gages are subject to drift over long time periods. The dynamic calibration was accomplished by quickly releasing a predetermined pressure pulse into the gage by means of a quick-acting 3-way solenoid actuated valve. Actual bottle pressures were measured by a precision-calibrated Heise dial gage.

2.3.2 Recording Systems. Project US-8 used four recording systems. The most sensitive and responsive were the cathode ray oscillographs manufactured by Miller Instruments, now a part of CEC. There were thirty-two channels available and their responses went up to 125 kcps. The thirty-two signal inputs are amplified by direct coupled amplifiers

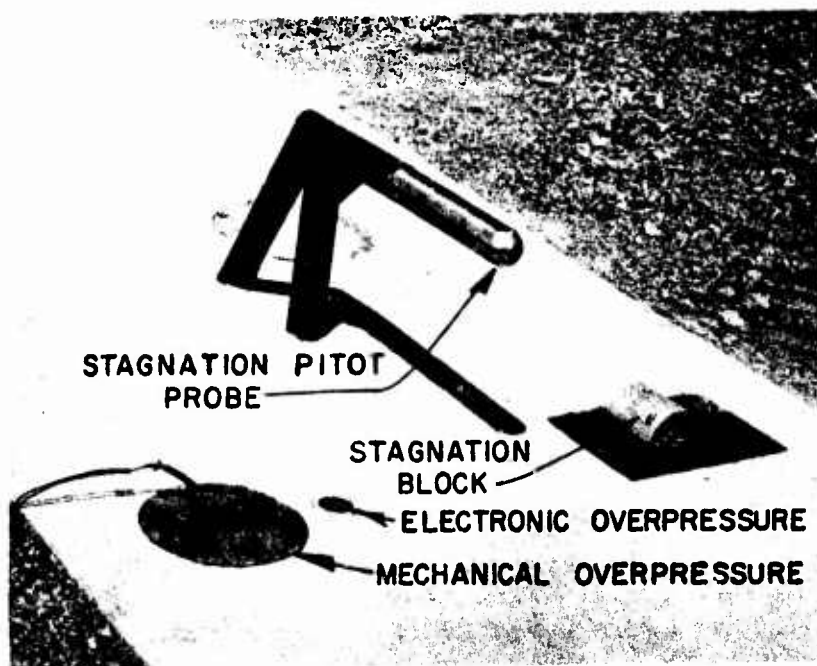


FIGURE 2.8 TYPICAL GAGE STATION ON TERRAIN FEATURE

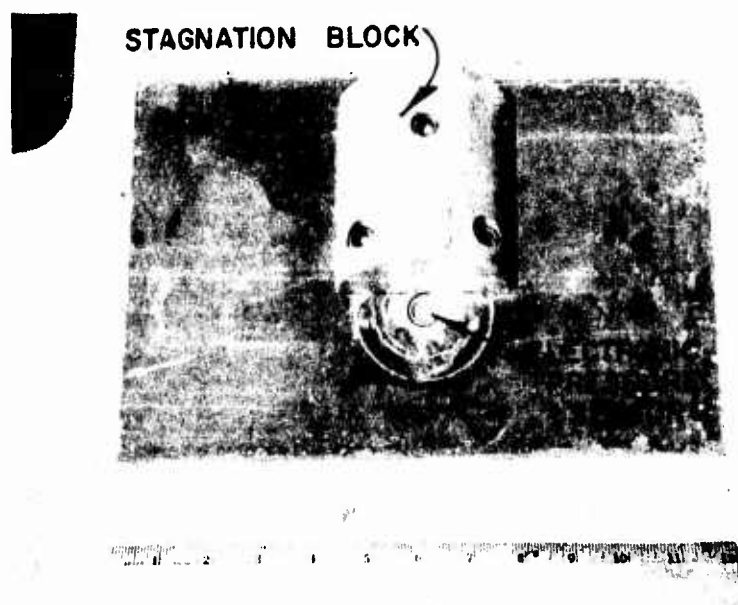


FIGURE 2.9 SURFACE STAGNATION MOUNT

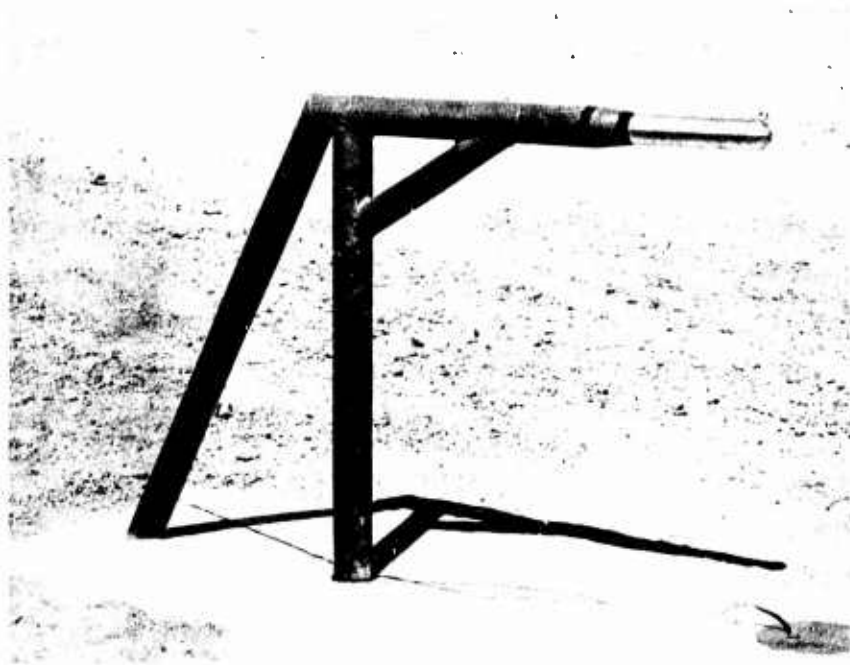


FIGURE 2.10 PITOT PROBE MOUNTS, 12 and 36 INCHES IN HEIGHT

and are fed into the deflection plate of the cathode ray tube. The deflections are photographed by optically focusing the 16 traces on photo-sensitive paper moving at rates up to 400 inches per second. Timing is provided at 1000 cps from a signal generator.

A rugged, miniature, FM magnetic tape recorder was also used by US-8. This system, manufactured by the Leach Corporation, is a small self-contained unit designed to be buried close to the transducers. It is 10 inches in diameter, 6.5 feet long, and weighs 200 pounds. The system has 14 wide band deviation,  $\pm 40$  percent, frequency modulated channels. Center frequency is 54 kc. Frequency response of the system is from 0-10 kc. Self-contained batteries power the electronics for 30 minutes; total tape recording time is two minutes. An auxiliary rack-mounted check-out unit contains all networks necessary for sensor calibration, monitoring, and playback.

The remaining two recording systems used by Project US-8 were manufactured by CEC. Both systems are amplitude modulated and are quite similar; the only difference being one has a 3 kc carrier frequency (System D), the other a 20 kc carrier frequency (System E). The carrier amplifiers were mounted in groups of four in a common case. Each amplifier has controls for balancing, setting sensitivity, metering output, and calibrating. Filament current, regulated plate voltage, and carrier current were supplied from a common power supply-oscillator unit. The amplifiers were designed for operation with two or four element resistive bridge transducers and for several other type transducers which operate in the neighborhood of 3 or 20 kc. The outputs from the amplifiers were fed into precision galvanometers of the oscillographic recorders and the deflections were photographed on moving photosensitive paper.

#### 2.4 Description of Data

The actual format of the data on the oscillographic paper is as follows: (1) field calibration with a precise electrically simulated signal, (2) preshot electrical signal, (3) zero time marker, (4) gage

signal at blast arrival, (5) post-shot electrical signal, and (6) 1-kc timing during the entire event. A sequence timer was used to program the proper function in the correct order.

The data from the terrain features, as well as that obtained from the blast or control line, were processed by the Computing Laboratory of BRL. This process consisted of reading both the calibrations and the shot record on a Universal Telereader, digitizing them on a Telercordex and punching the information on IBM cards. Once on the cards, the data were fed into a high speed digital computer which linearized and converted the data into units of pressure and time. The output from the computer was fed into a fully automatic line plotter and the final results are the plots presented in Appendix B.



## CHAPTER 3

### RESULTS

The results from the control line and each of the terrain features are presented in Tables 3.1-3.6. The plots of the pertinent parameters versus time are presented in Appendix B. Using both the tables and the plots, one can assess the phenomena being examined. The overall effectiveness of the instrumentation can also be reviewed.

The free-field pressure versus time records are felt to be quite reliable with but two exceptions. The one exception is the decay rate in the latter portion of the electronic overpressure record at station 8.6 and the second one is the peak recorded on the electronic overpressure record at Station 8.8. In Figure 3.1 the free-field measurements from the flat control line are compared with predicted values. Figure 3.2 shows the dynamic pressures measured on the control line compared to predicted values.

#### 3.1 Terrain Feature A

3.1.1 Overpressure. A comparison of pressure versus ground range (distance from ground zero) is made in Figure 3.3. The pressures obtained from the free-field or control line are presented as a solid line and are shown in order to graphically display the effects produced by the changing terrain. A fairly good picture of pressure fluctuations up the front slopes is given; however, all electronic traces from the back slope went off scope before or at blast arrival time; therefore, there were no electronic measurements recorded from the back slope. The mechanical gages recorded pressure pulses, but the values appear questionable. The gage at Position 4 gives a reasonable maximum overpressure value, but the wave form is poor. All gages were apparently affected by the strong vortex action emanating from the crest and traveling down the back slope. Ratios obtained between level terrain pressures and changing terrain pressures, as well as those obtained from theory, are given in Table 3.7. The ratios of the measured values are higher than those predicted.

TABLE 3.1

## RESULTS, CONTROL LINE BLAST PARAMETERS

Position	Ground Range feet	Type Measurement	Arrival Time msec	Maximum Pressure psi	Positive Duration msec	Positive Impulse psi-msec
8.4	232	Static	-	82.0	84.0	991
8.5	279	Total	64.3	106.0	115.0	2413
		Static		56.0	112.0	1081
8.6	299	Total	73.3	76.0	102.0	
		Static		42.0		
		Static		38.0	787.0	
8.7	334	Total	89.1	56.0	98.0	
		Static		34.0	121.0	818
		Static		30.0	85.0	642
8.8	413	Total	134.4	27.0	100.0	
		Static		30.0	117.0	670
		Static		18.0	104.0	540
8.9	443	Total	148.2	24.0	117.0	
		Static		17.0	132.0	560
		Static		15.8	121.0	549
8.10	525	Static	204.4	11.5	-	-
		Static		12.3	130.0	465

TABLE 3.2

## RESULTS, TERRAIN FEATURE A

Position	Ground Range ft	Type Measurement	Arrival Time msec	Maximum Pressure psi	Positive Duration msec	Positive Impulse psi - msec
8A-P1-40 60 60(SIES) 70	255.4	Total (12") Static Static Static	54.4	107.0 52.0 54.0	16.6 - 41.1 75.0	600 - 605 952
8A-P2-40 65 60 70	271.0	Total (12") Total (Surface) Static Static	61.0 59.1	132.0 - 74.0 63.0	- - 26 80	- - 670 948
8A-P3-40 65 60 70	278.8	Total (12") Total (Surface) Static Static	64.2 62.6	136.0 132.0 62.0 59.0	- - - 78.0	- - 445 991
8A-P4-40 65 60 70	290.4	Total (12") Total (Surface) Static Static	69.7 68.1	65 65 - 38.0	- - - 81	- - - 312
8A-P5-40 65 60 70	298.1	Total (12") Total (Surface) Static Static	72.5 72.5	- 55 34.0 53.5	- - - 76	- - - 1304
8A-P6-40 60 70	313.8	Total (12") Static Static	81.9	62 - 45.0	- - 75	- - 702

TABLE 3.3

## RESULTS, TERRAIN FEATURE B

Position	Ground Range ft	Type Measurement	Arrival Time msec	Maximum Pressure psi	Positive Duration msec	Positive Impulse psi - msec
8B-P1-40 60 70	391.1	Total (12") Static Static	121.8	37.0 26.0 22.0	108 113 110	840 710 623
8B-P2-40 65 60 70	406.8	Total (12") Total (Surface) Static Static	131.1 131.1	42.0 39.0 26.0 23.3	106 - 111 108	850 - 713 657
8B-P3-40 65 60 70	414.5	Total (12") Total (Surface) Static Static	139.7 135.3	42.0 41.0 21.5 22.6	104 119 112 110	827 - 660 709
8B-P4-40 65 60 70	426.1	Total (12") Total (Surface) Static Static	142.4 142.4	- 20.0 18.0 15.4	- 94 116 106	- 482 632 395
8B-P5-40 65 60 70	433.8	Total (12") Total (Surface) Static Static	146.9 147.6	18.0 17.0 13.5 14.3	110 124 124 116	671 885 692 603
8B-P6-40 60 70	449.5	Total (12") Static Static	157.4	24.0 17.0 17.1	87 90 114	545 742 578

TABLE 3.4

## RESULTS, TERRAIN FEATURE C

Position	Ground Range ft.	Type Measurement	Arrival Time msec	Maximum Pressure psi	Positive Duration msec	Positive Impulse psi - msec
8C-P1-40	390.1	Total (12")	124.2	35.0	75	882
		Static		22.5	80	558
		Static		22.5	114	670
8C-P2-40	405.2	Total (12")	129.6	50.0	110	872
		Total (Surface)		60.0	96	1050
		Static		36.0	102	706
8C-P3-40	412.1	Static	130.1	31.2	110	780
		Total (12")		60.0	103	764
		Total (Surface)		60.0	77	685
8C-P4-40	422.5	Static	134.6	34.0	90	564
		Static		30.9	105	635
		Total (12")		16.5	116	230
8C-P5-40	429.4	Total (Surface)	140.8	13.8	128	356
		Static		13.3	113	276
		Static		14.5	112	111
8C-P6-40	444.4	Total (12")	144.9	15.0	121	585
		Total (Surface)		15.3	98	507
		Static		12.3	121	535
8C-P6-40	444.4	Static	154.3	12.9	116	519
		Total (12")		23.5	118	746
		Static		15.6	122	609
8C-P6-40	444.4	Static	154.3	15.7	118	530
		Total (12")		23.5	118	746
		Static		15.6	122	609

TABLE 3.5

## RESULTS, TERRAIN FEATURE D

Position	Ground Range feet	Type Measurement	Maximum Pressure psi	Positive Duration msec	Positive Impulse psi-msec
8D-P1-70	537.3	Static	11.3	133.0	484
8D-P2-70	551.5	Static	13.6	127.0	436
8D-P3-70	561.4	Static	12.5	132.0	441
8D-P4-70	572.2	Static	9.0	133.0	371
8D-P5-70	580.5	Static	8.2	130.0	397
8D-P6-70	596.6	Static	9.3	137.0	442

## RESULTS TERRAIN FEATURE E

Position	Ground Range feet	Type Measurement	Maximum Pressure psi	Positive Duration msec	Positive Impulse psi-msec
8E-P1-70	353.7	Static	21.4	134.0	608
8E-P2-70	356.4	Static	22.5	133.0	674

TABLE 3.6 DYNAMIC PRESSURE RESULTS

Position	Ground Range feet	Type Station	Maximum Dynamic Pressure psi	Remarks
Control Line				
P5	279	Free field	40.0	Good Record
P6	298	" "	29.0	Good Record
P7	334	" "	17.0	Good Record
P8	413	" "	7.3	Poor Rise on side-on
P9	443	" "	6.3	Good Record
Terrain Feature A				
P1	255.4	Free field in front of terrain feature 15° rising slope	44.0	Poor Record
P2	271.0		56.0	Good Record
P3	278.8	15° rising slope	55.5	Poor Record
P4	290.4	15° falling slope	55.0	Good Record
P5	298.1	15° falling slope	-	Poor Record
P6	313.8	15° falling slope	-	Poor Side-on Record
			-	" " "
			-	" " "
			-	" " "
			-	" " "
		Free field in back of terrain feature	-	Poor Total Head Record
Terrain Feature B				
P1	391.1	Free field in front of terrain feature 15° rising slope	10.0	Good Record
P2	406.8		13.3	Good Record
P3	414.5	15° rising slope	14.0	Good Record
P4	426.1	15° falling slope	16.0	Good Record
P5	433.8	15° falling slope	16.0	Poor Record
			-	No Record
			-	Poor Record
			4.8	Good Record
			4.0	Poor Record

TABLE 3.6 (Contd.)

Position	Ground Range feet	Type Station	Maximum Dynamic Pressure psi	Remarks
P6	449.5	Free field in back of terrain feature	6.0	Poor Record
Terrain Feature C				
P1	390.1	Free field in front of terrain feature	9.5	Good Record
P2	405.2	30° rising slope	13.0	Poor Record
P3	412.1	30° rising slope	18.0	Good Record
P4	422.5	30° falling slope	18.0	Poor Record
P5	429.4	30° falling slope	19.0	Good Record
			3.0	Fair Record
			2.0	Fair Record
			2.7	Good Record
			3.0	Good Record
P6	444.4	Free field in back of terrain feature	6.0	Good Record



TABLE 3.7 COMPARISON OF PRESSURE RATIOS

TERRAIN	TYPE OF RATIO		P1	P2	P3	P4	P5	P6
A	Overpressure	Calculated	1.00	1.05	1.05	0.85	0.85	1.00
		Electronic	0.85	1.42*	1.29	-	.83	-
		Mechanical	0.89	1.21	1.23	0.86	1.30*	1.22
	Dynamic Pressure	Pitot	0.94	1.49	1.68	-	-	-
		Surface	-	-	1.66	-	-	-
B	Overpressure	Calculated	1.00	1.25	1.25	0.76	0.76	1.00
		Electronic	1.13	1.27	1.10	0.98	0.76	1.02
		Mechanical	0.96	1.14	1.16	0.84	0.81	1.03
	Dynamic Pressure	Pitot	1.00	1.62	2.11	-	0.76	1.07
		Surface	-	1.71	2.11	-	0.64	-
C	Overpressure	Calculated	1.00	1.96	1.96	0.55	0.55	1.00
		Electronic	0.95	1.70	1.68	0.70	0.66	0.90
		Mechanical	0.95	1.50	1.53	0.76	0.70	0.91
	Dynamic Pressure	Pitot	0.90	1.48	2.25	0.41	0.40	1.00
		Surface	-	2.05	2.38	0.27	0.45	-
D	Overpressure	Calculated	1.00	1.40	1.40	0.73	0.73	1.00
		Mechanical	1.00	1.27	1.21	0.90	0.85	1.00
E	Overpressure	Calculated	0.63	0.63				
		Mechanical	0.74	0.79				

\* Questionable Value

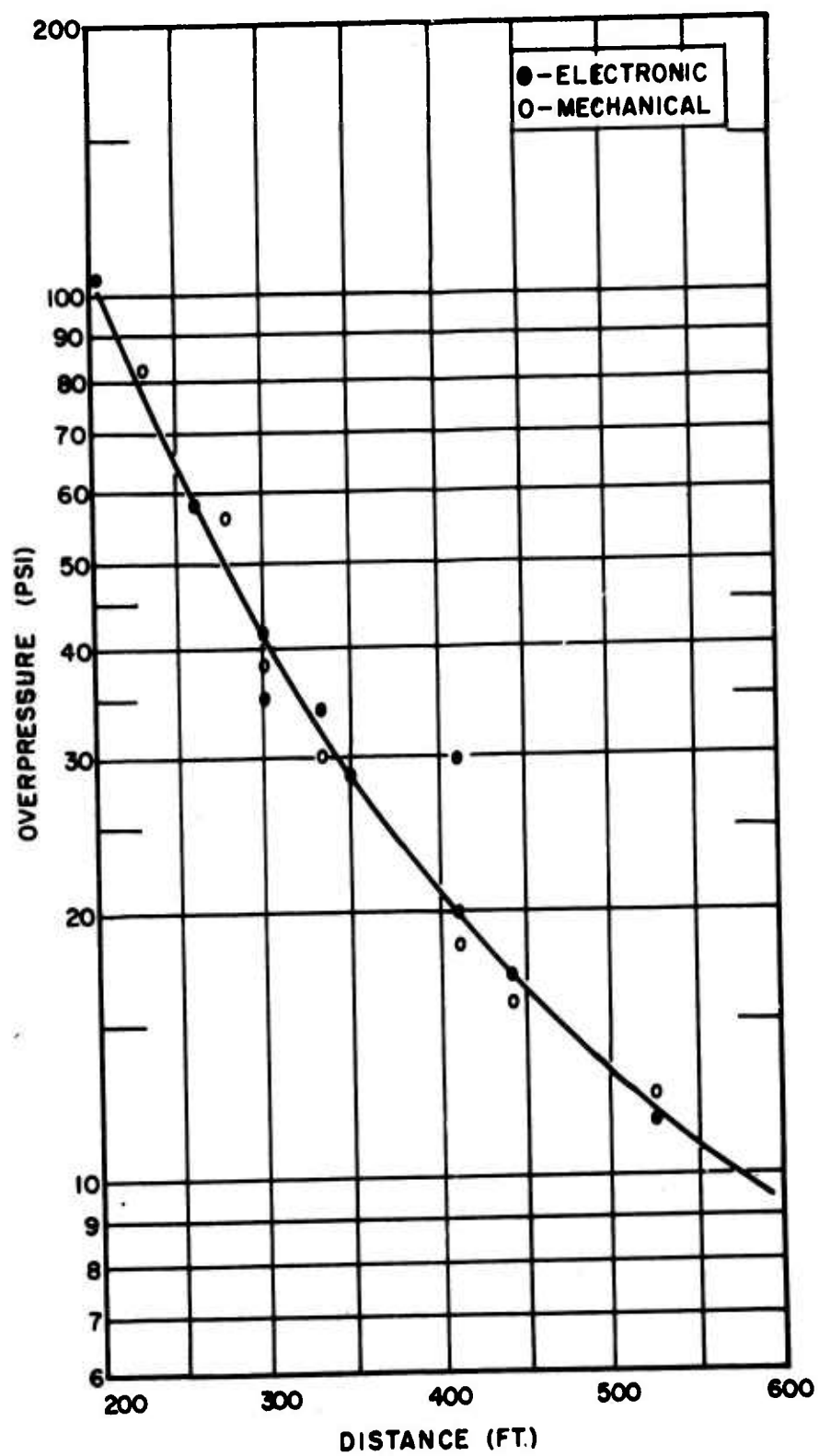


FIGURE 3.1 MEASURED OVERPRESSURE ON THE FLAT CONTROL LINE

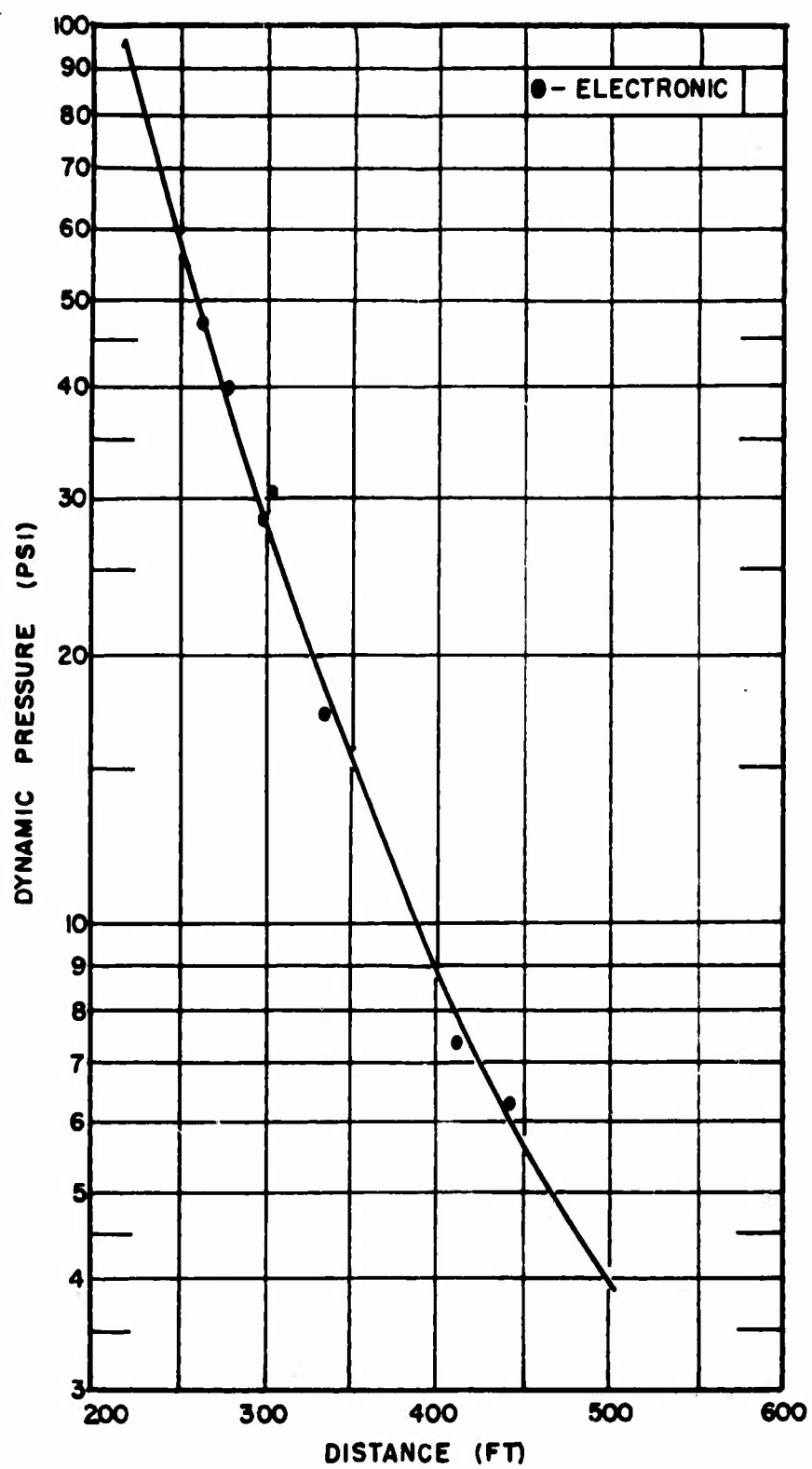


FIGURE 3.2 MEASURED DYNAMIC PRESSURE ON THE FLAT CONTROL LINE

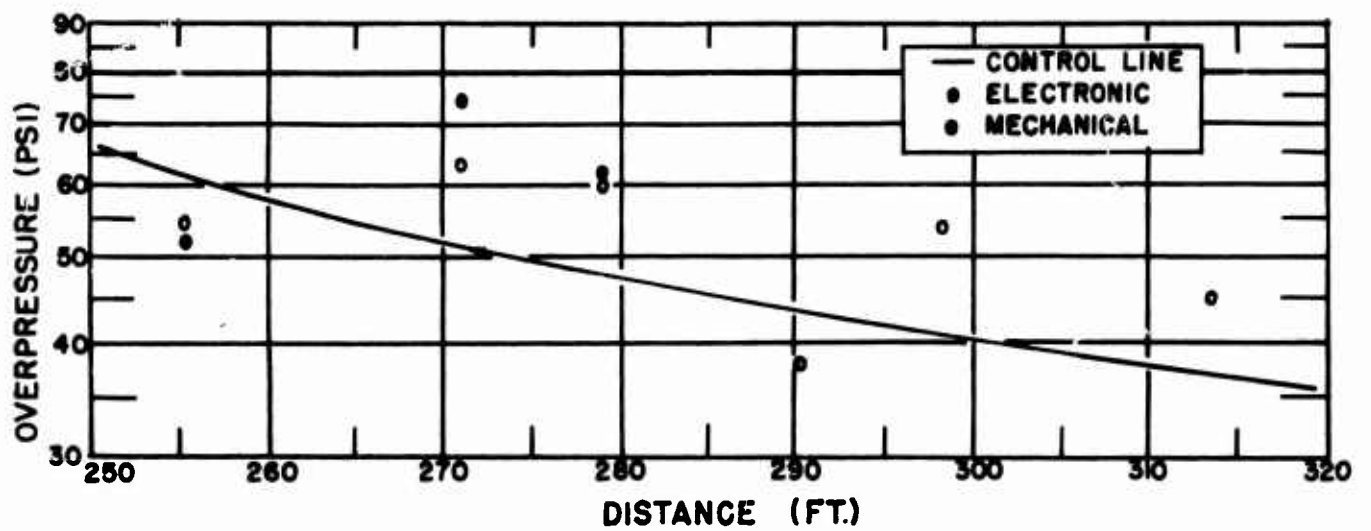
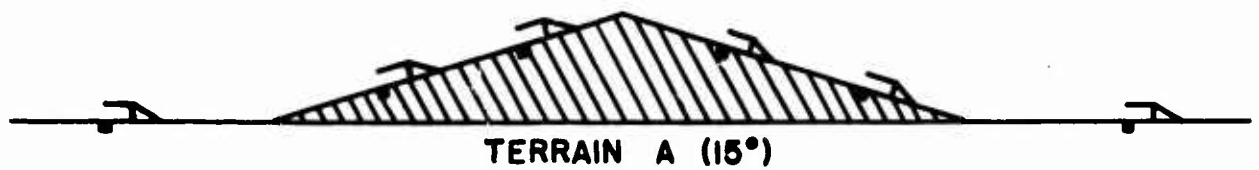
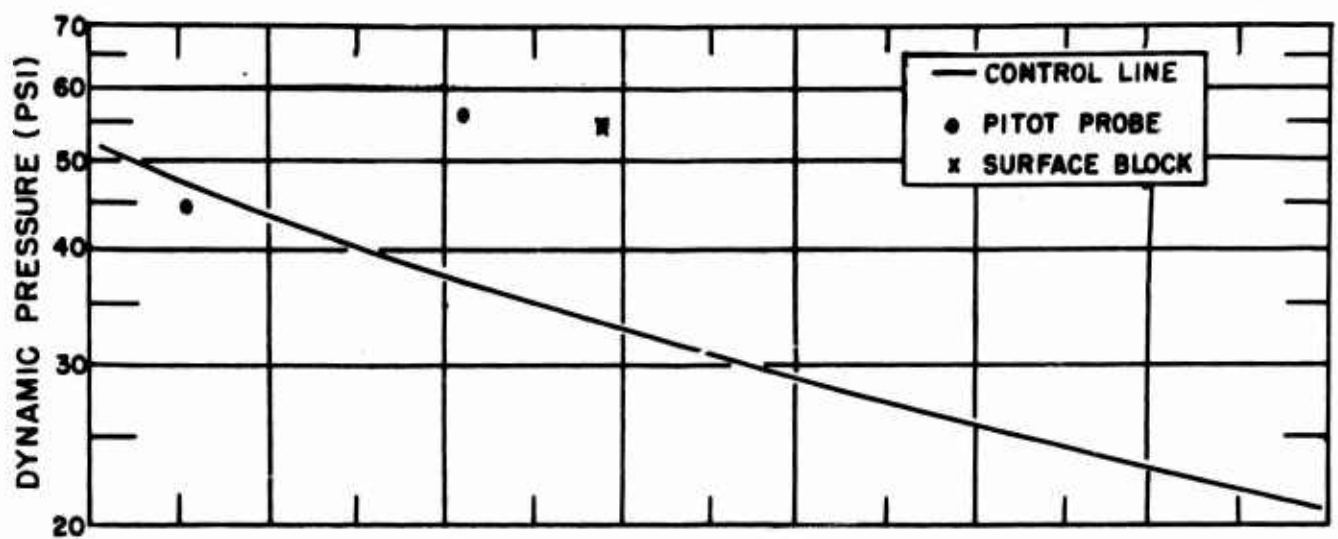


FIGURE 3.3 MEASURED PRESSURES ON TERRAIN FEATURE A COMPARED WITH THE CONTROL LINE

3.1.2 Dynamic Pressure. Figure 3.3 also compares dynamic pressure values provided by measurements made on level and hilly terrain. As would be expected, since no valid overpressures were obtained on the back slope, no values are plotted for Positions 4, 5, and 6. Those ratios obtained for the front slope indicate significant enhancement of dynamic pressure.

### 3.2 Terrain Feature B

3.2.1 Overpressure. Pressure-distance relationships for Terrain B are plotted in Figure 3.4. Instrumentation performance was very good on this feature. Front slope ratio values, given in Table 3.7, show a possible deviation at Position 3. The gages at this position recorded a shock wave which did not exhibit a typical form. A local surface roughness could have buffered the wave front at the surface and caused a slight lowering of pressure. Rear slope measurements are good. Here again, turbulence from the vortex shedding contributed to data scatter.

3.2.2 Dynamic Pressure. As was the case on Feature A, these measurements reflect any anomalies present in the overpressure values. Positions 1 and 2 show good data while Position 3 shows the large difference obtained from a low overpressure record and a normal pitot record. The record from the P4 pitot probe was lost because of a bad amplifier. The surface stagnation record was lowered by the vortex; this combination allowed no dynamic pressure calculation. P5 was similarly affected, however, values were obtained.

### 3.3 Terrain Feature C

3.3.1 Overpressure. The results from "C" were most gratifying. All instrument channels yielded very good records. This is in part explained by two factors. First, the hill itself was a radical departure from flat terrain which would tend to accentuate pressure fluctuations; and second, the electronic gages and systems, while being of lower response frequency, were quite dependable.

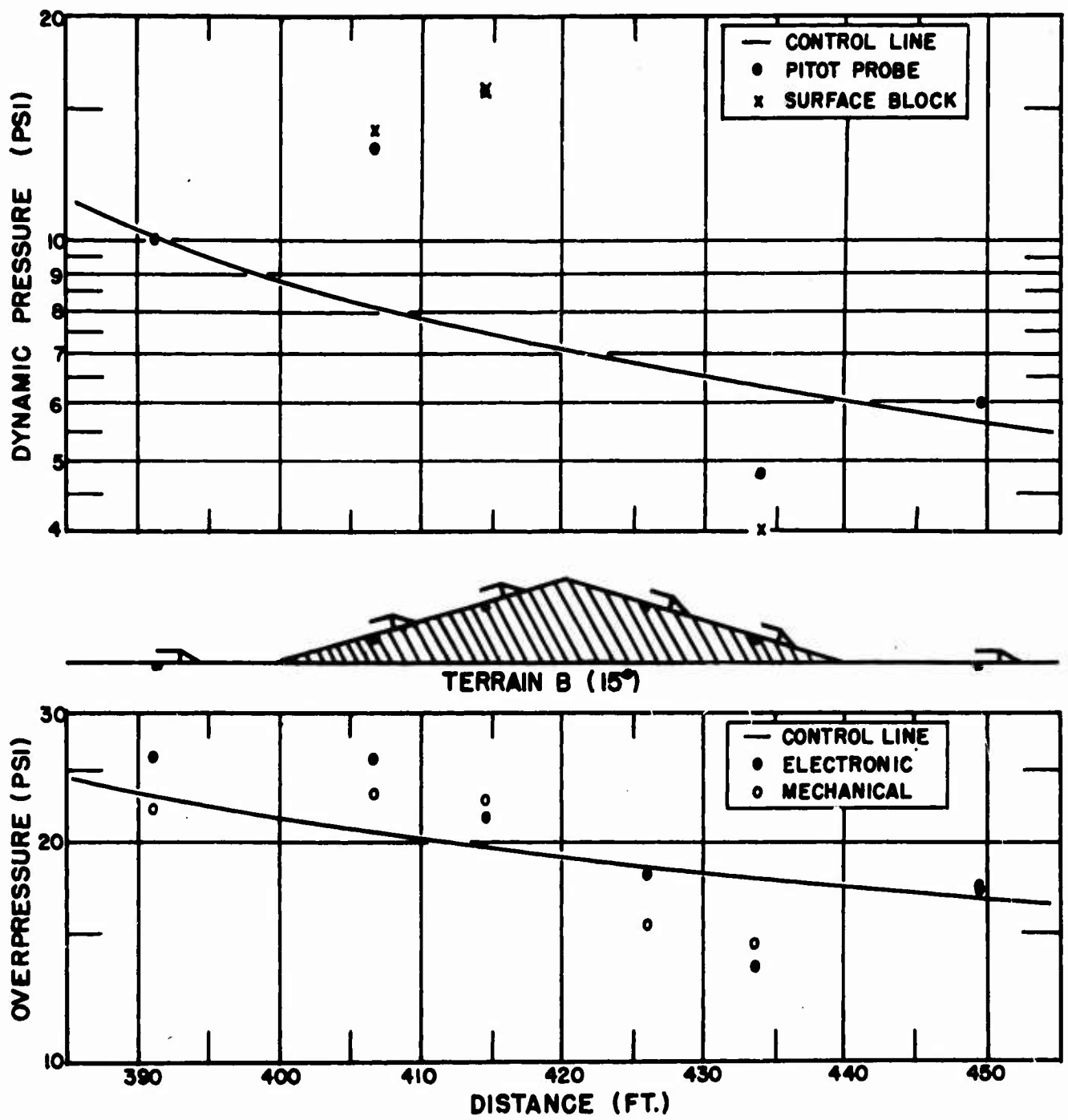


FIGURE 3.4 MEASURED PRESSURES ON TERRAIN FEATURE B COMPARED WITH THE CONTROL LINE

The data are plotted in Figure 3.5 and the resulting ratios are given in Table 3.7. The plot of overpressure versus distance shows the close agreement between the electronic and mechanical gages. Although the ratios of pressures are not as radical as those computed, a strong correlation exists.

3.3.2 Dynamic Pressure. The values plotted in Figure 3.5 are considered valid. The value obtained using the pitot probe at Position 2 is low because the triple point passed just under the probe. At Position 4, the value from the surface stagnation gage is low because of low flow conditions at the surface just behind the hill crest. For a 30 degree slope, dynamic pressure ratios indicate a significant departure from level terrain conditions.

#### 3.4 Terrain Feature D

The results from the mechanical gages used on Feature D are plotted in Figure 3.6. These values reflect the general case of pressure amplification on the front slope and attenuation on the back slope. The ratios listed in Table 3.7 show that the changes measured were below those predicted by the theoretical calculations.

#### 3.5 Terrain Feature E

The initial maximum overpressure values recorded on Feature E are plotted in Figure 3.6. Ratios are given in Table 3.7. These values, although reduced, are not as low as expected. The narrow width of the field fortifications probably restricted the expansion of the shock wave.

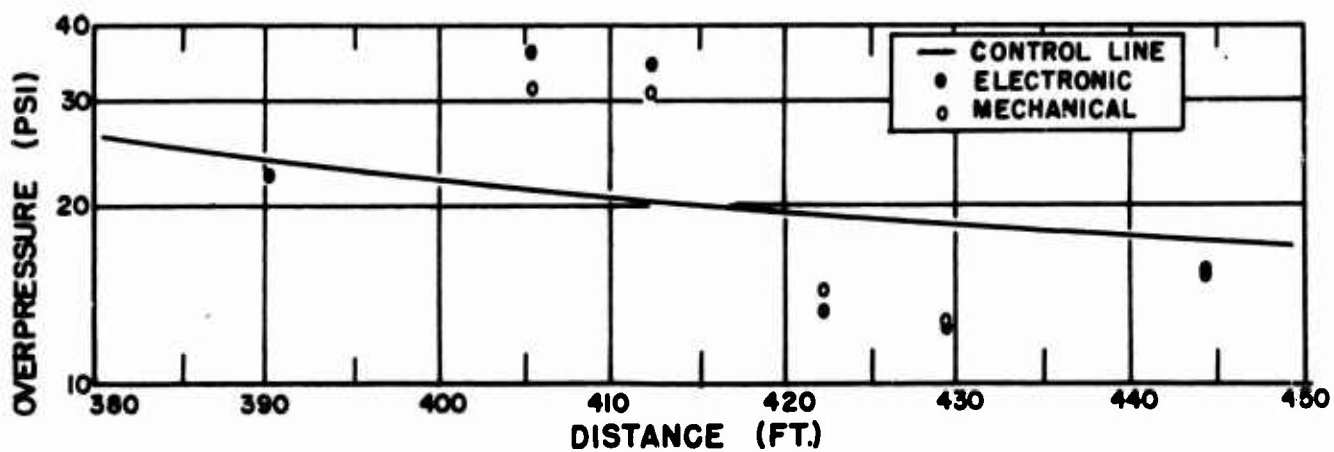
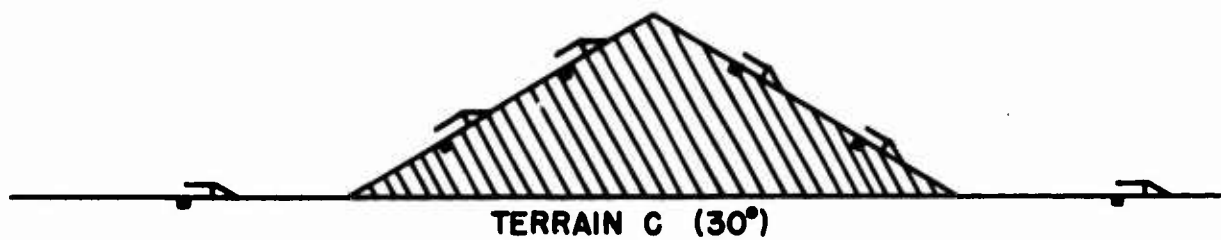
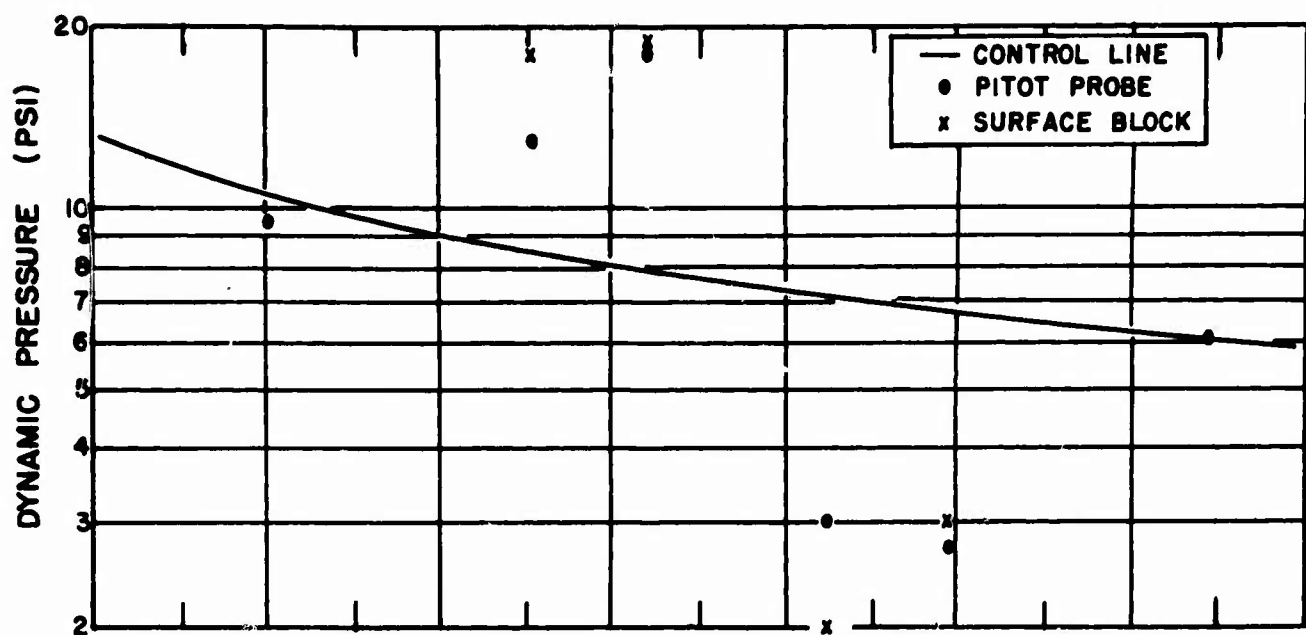


FIGURE 3.5 MEASURED PRESSURES ON TERRAIN FEATURE C COMPARED WITH THE CONTROL LINE



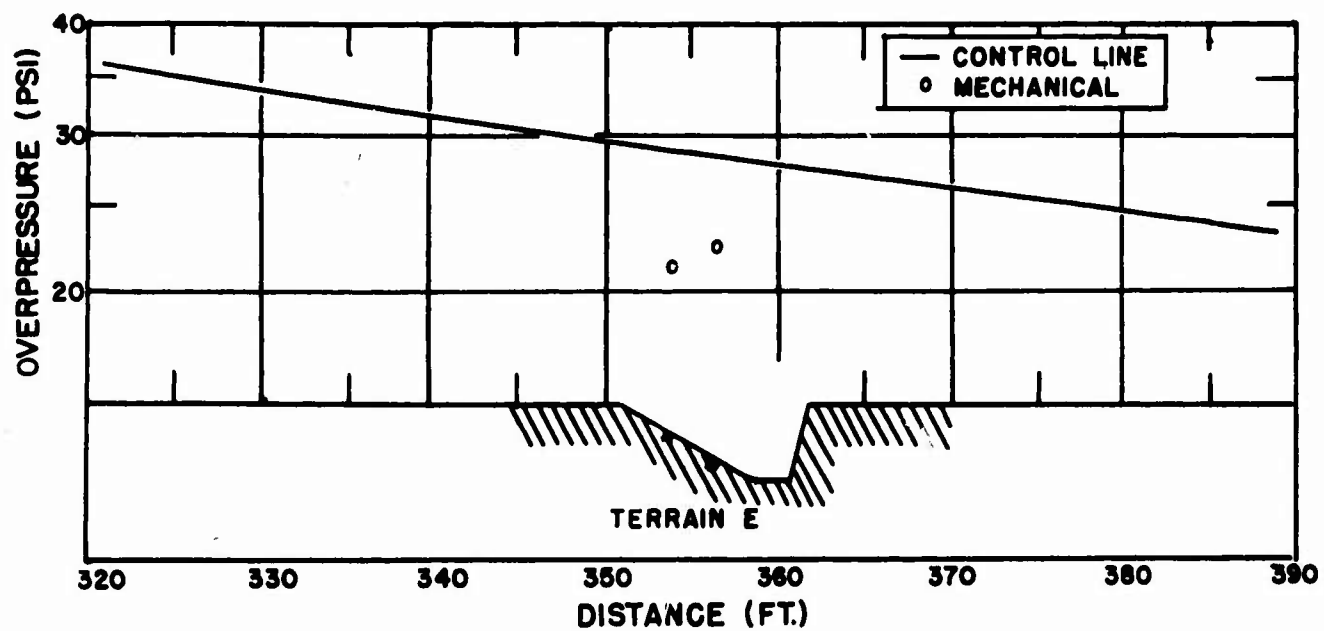
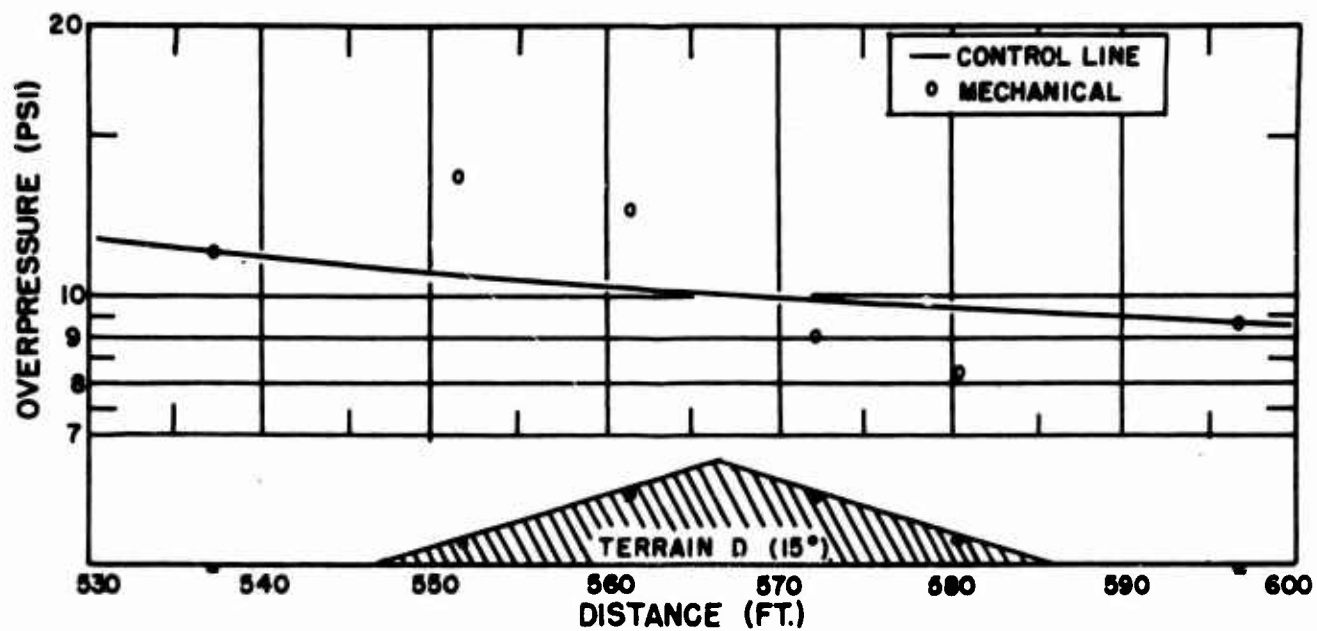


FIGURE 3.6 MEASURED PRESSURE ON TERRAIN FEATURES D AND E COMPARED WITH THE CONTROL LINE

## CHAPTER 4

### DISCUSSION AND CONCLUSIONS

The reliability of the pressure ratios, presented in the previous chapter, depends directly on the accuracy with which both the overpressure and the stagnation pressure could be measured. In large scale experiments such as the 100 ton test, many things influence the overall accuracy. To establish the effects certain parameters had on the system accuracy, many tests were conducted in the Laboratory before going to the field. Acceleration effects induced by the pressure acting on the electronic transducers were checked in the shock tube and were found to be negligible when the transducer was mounted in an accurately machined brass adapter. Temperature effects on the gages were also checked and found to be less than 2 percent. To minimize error due to changes in gage sensitivity, all piezo gages were calibrated as close to shot time as possible. All the pressure gages used were dynamically calibrated and tested in the BRL Shock Tube prior to field use. The probable error of gage calibration for all the data was established to be less than  $\pm 6$  percent.

#### 4.1 Pulse Shape

Terrain effects play their most important role for large yield detonations, and thus it is important to consider the terrain effects on the entire pressure time profile. Selecting the 15 and 30 degree terrain features at the 20 psi level as typical, one can compare the complete pressure time wave shape for rising and falling slopes with the wave shape for flat terrain. The overpressure wave forms are compared in Figures 4.1 and 4.2. On the rising slopes the initial portion of the pressure time record is considerably higher than for the flat terrain conditions; the biggest increase occurs on the 30 degree slope. The measured peak overpressures are in agreement with predictions. On terrain Feature C, Figure 4.2, the enhanced portion of the pressure time record accounts for about the first third of the record. For the latter two thirds of the records on the rising slope, the pressure is less than for the flat terrain. This crossover causes a smaller overpressure impulse ratio than peak overpressure ratio. A peak overpressure

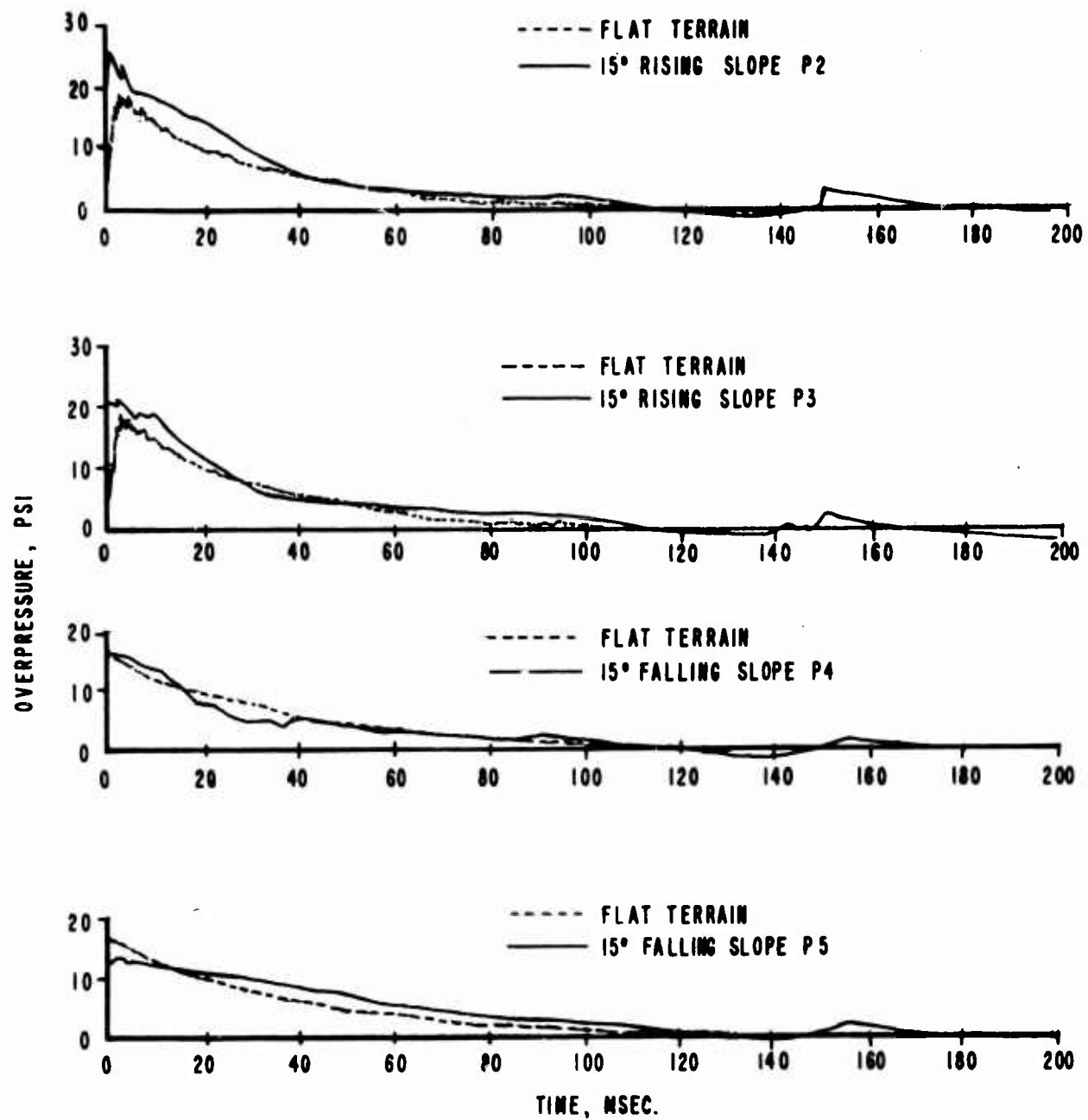


FIGURE 4.1 OVERPRESSURE - TIME ON TERRAIN FEATURE B COMPARED WITH CONTROL LINE

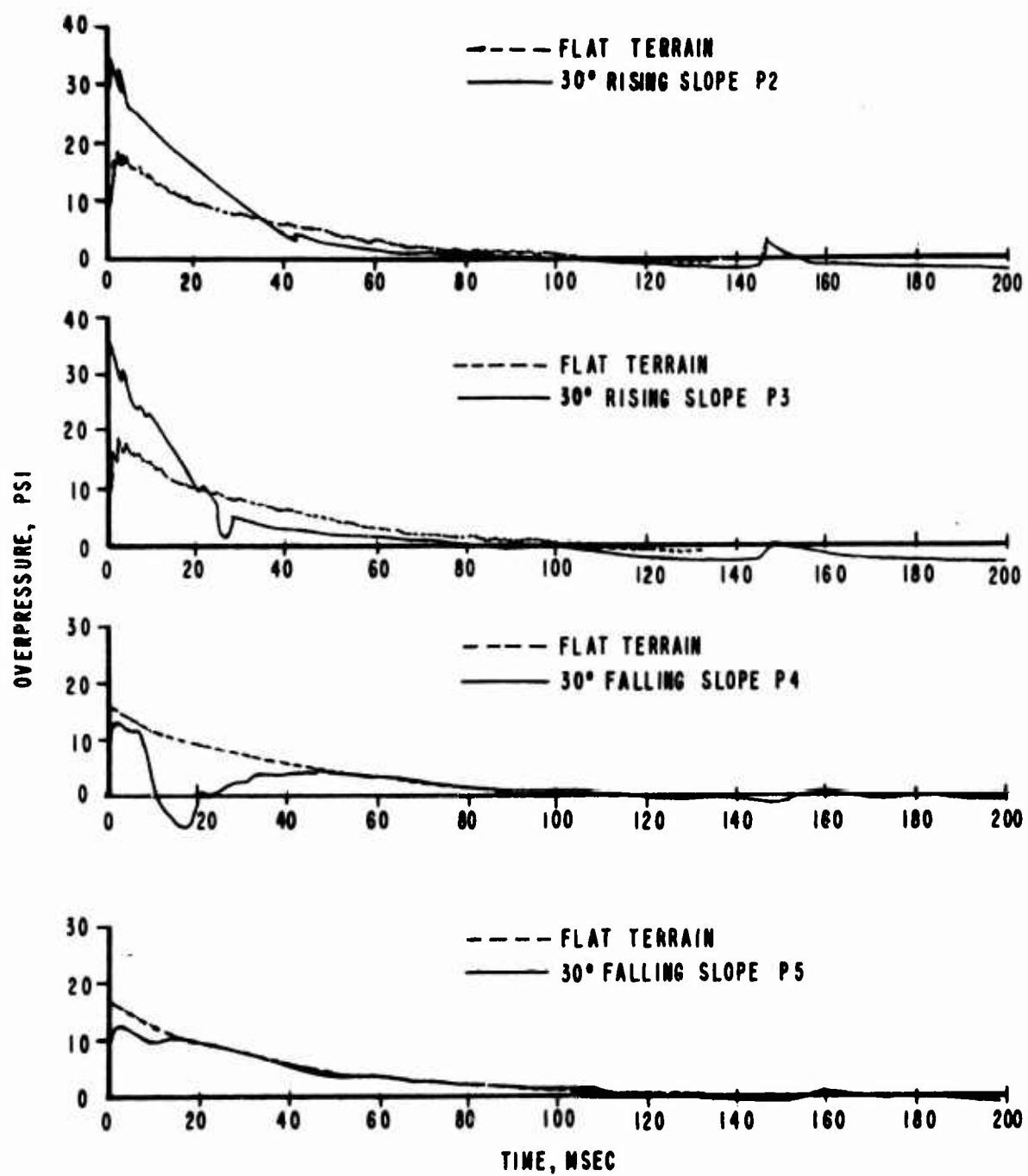


FIGURE 4.2 OVERPRESSURE - TIME ON TERRAIN FEATURE C COMPARED WITH CONTROL LINE

ratio of 1.6, measured on the rising slopes, compares with an overpressure impulse ratio of 1.1 for the 30 degree rising slope. On the back slope of the 30 degree terrain feature, the same trend was observed. Initially, an average reduction of 25 percent was recorded for both positions on the back slope. A larger reduction in pressure was observed on all terrain features at the first measurement position over the crest. This reduction is a function of the distance from the crest and the contour of the crest. This effect is not believed to be significant in the overall analysis of natural terrain features. The second station, P5, on the back slope is more representative of back slope conditions. Here a few milliseconds after the passage of the shock wave the back slope pressures equal the flat terrain pressures. A reduction of only 5 percent in the overpressure impulse was recorded at station P5 on the 30 degree falling slope. On the 15 degree back slope an increase of 15 percent was measured in the overpressure impulse when compared with the control line, even though a reduction of 25 percent in maximum overpressure was observed; this reduction had been predicted.

The stagnation pressures which include the dynamic and static pressures are compared for the same two terrain features discussed above (Figures 4.3 and 4.4). The stagnation pressure waveforms are modified in much the same way as the side-on pressure pulses. The shock front dynamic pressure for both the rising and falling slopes can be predicted from the shock front side-on pressure by the Rankine-Hugoniot relationship.

Using P2 as the most representative station on the front slope, it is observed that as the angle increases, the enhancement of peak overpressure increases and the time to decay to free field overpressure value on flat terrain conditions decreases, thus resulting in a smaller percentage of increase in total impulse. Position P4 on the back slope is affected by the vortex action from the crest and the pressure time wave shape from this position would change if the crest were slightly

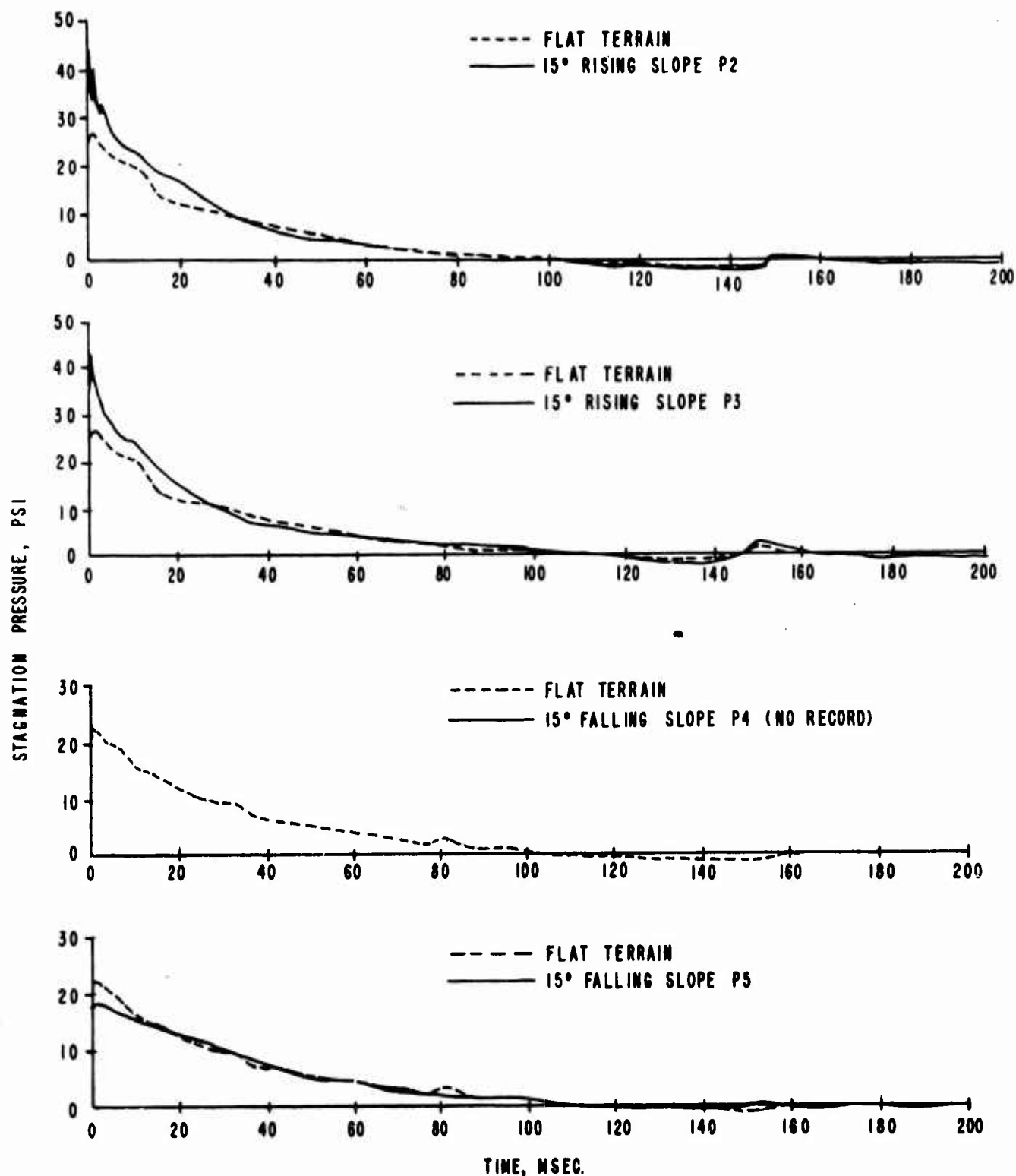


FIGURE 4.3 STAGNATION PRESSURE - TIME ON TERRAIN FEATURE B COMPARED WITH CONTROL LINE

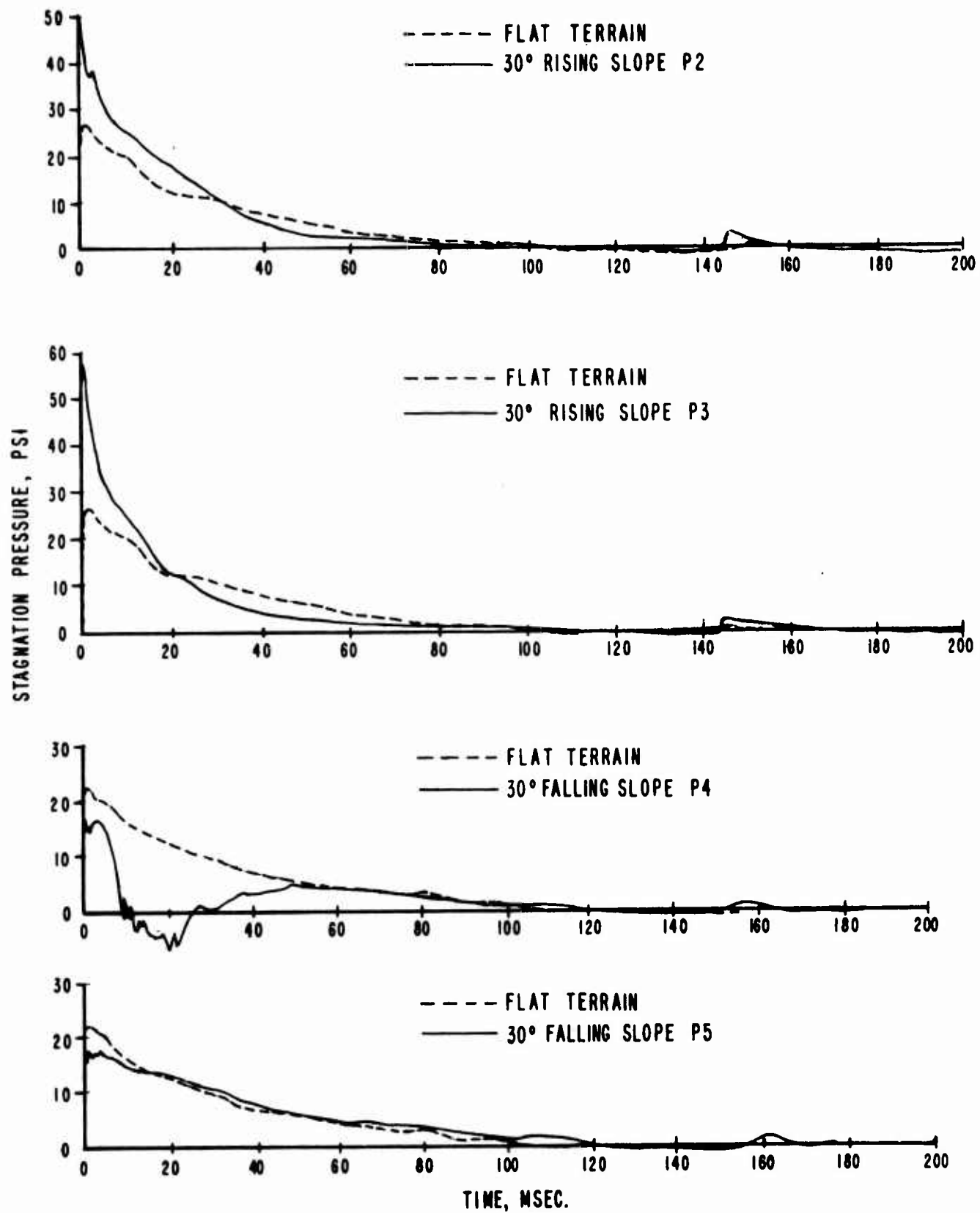


FIGURE 4.4 STAGNATION PRESSURE - TIME ON TERRAIN FEATURE C COMPARED WITH CONTROL LINE

altered. Position P5 best represents the average pressure over the back slope and the pressure value measured at this station would be best for scaling to larger slopes.

#### 4.2 Comparison with Other Terrain Studies

The peak overpressures measured on the rising and falling slopes of the large artificial terrain features on the 100 ton test are in good agreement with small scale model data. Pressure wave forms from small scale model tests are very limited, and the scaling of feedback effects from the crest over the front slopes and vortices action over the back slopes makes direct comparisons extremely difficult. The dynamic pressure measurements from shock tube tests are in agreement with the 100 ton results. See Appendix A. The correlation of the 100 ton data with the nuclear full scale data is difficult because of the non-classical nature of the nuclear blast wave. The terrain features on the nuclear shot altered the blast waves by thermal and mechanical action. More thermal energy is incident on the front slopes, which normally in precursor formation would decrease the overpressures. However, the mechanical action of the terrain, causing reflection of blast waves, resulted in a slight increase of overpressure.

The analysis of the 100 ton results indicate that, although terrain effects can drastically alter the initial portion of the pressure time histories, the change in total impulse is not as significant.

#### ACKNOWLEDGEMENTS

Appreciation is expressed to the Suffield Experimental Station Staff who provided almost daily assistance and held throughout the field phase of this report.

The excellent advice and guidance of J. J. Meszaros and C. N. Kingery of Ballistic Research Laboratories is greatly appreciated.



Particular recognition is given for the outstanding work of the following BRL personnel, E. G. Schwartz, R. E. Reisler, D. P. Lefevre, R. L. Peterson, G. D. Teel, W. O. Ewing, T. R. Watson, L. Giglio-Tos and T. F. Stipa.

JOHN H. KEEFER

J. DONALD DAY

#### REFERENCES

1. Samuel Glasstone, Editor. The Effects of Nuclear Weapons. U.S. Atomic Energy Commission, June 1957.
2. A. B. Willoughby, K. Kaplan and R. I. Condit. Effects of Topography on Shock Waves in Air. AFSWC-TR-57-9, August 1956.
3. D. R. White. An Experimental Survey of the Mach Reflection of Shock Waves. Princeton University, AT1-195417, August 1951.
4. E. J. Bryant and J. H. Keefer. Project 1.8a, L. M. Swift and D. C. Sachs - Project 1.8c; Effects of Rough and Sloping Terrain on Air-blast Phenomena. Final Report - WT-1407, 5 July 1962.
5. N. R. Wallace and A. B. Willoughby. Effects of Topography on Dynamic Pressure. DASA-1262, October 1961.
6. J. Todd, Jr. A Scale Model Study of the Effects of Symmetric Ridges on Blast Overpressures. SC-3335(TR), 3 May 1954, Sandia Corporation, Albuquerque, New Mexico.
7. C. N. Kingery; J. H. Keefer and J. D. Day. Surface Air Blast Measurements From a 100-Ton TNT Detonation. Ballistic Research Laboratories Memorandum Report No. 1410, June 1962.

PREVIOUS PAGE WAS BLANK, THEREFORE WAS NOT FILMED

APPENDIX A

SHOCK PRESSURE DISTRIBUTION OVER A  $30^{\circ}$  MODEL HILL

George A. Coulter

PREVIOUS PAGE WAS BLANK, THEREFORE WAS NOT FILMED

#### INTRODUCTION

Under Weapons Effects Board Project Number 02.043 a study is being made of the effects of topography upon a blast wave. In particular, data were obtained from the Smoky Shot of the Plumbbob Test, in Nevada, from side-on pressure gages and Q-gages oriented along rising and falling slopes of terrain at the test site. The observed pressure-time profiles of the shock wave for the slope positions showed higher maximum overpressures than did the pressure-time profiles measured along the flat surface. Since the gages were in the Mach pressure region for the shot, it was thought that this had caused the shock wave to have a higher maximum overpressure.

As a part of the topography study, the BRL Shock Tube Facility was requested to perform the present experiment. The experiment was, therefore, designed to determine how the shock wave profile is changed when the pressure gages are in a known Mach region oriented along a slope.

#### DESCRIPTION OF THE EXPERIMENT

A symmetric model was made from 5 x 10 foot, 1/2-inch steel plates welded together to form a "hill" with equal rising and falling slopes. The included angle between either of the slopes and the bottom plate was approximately 30 degrees.

The model was instrumented on both slopes with flush mounted piezo-electric crystal gages to measure side-on shock overpressure. A similar type gage was used in the face-on probes, oriented along the slopes, to measure the stagnation overpressure. The stagnation probe was made by threading the gage into the end of a 1/2-inch pipe nipple, 3-inches long; a 90 degree elbow and another nipple completed the probe.

The model was exposed to shock overpressures of 5.5 and 12.2 psi produced at the open end of the detonation driven shock tube. Both side-on and stagnation pressure measurements were recorded at two

positions on the front rising slope and also at two positions on the rear falling slope. Figure A1 is a sketch of the model hill with the gage positions shown. The lengths of the mounting pipe nipples for the stagnation probes were varied in length so that the gage face centers were 2-1/2 in., 1 in., 2-1/2 in., 2-1/2 in., and 2-5/8 in. above the surface, respectively, for positions I, II, III, IV, and V.

## RESULTS

The results are presented graphically in Figures A2 through A3 as sets of pressure-time traces which show the observed pressures from the model hill with the corresponding input pressures from the control position in front of the model.

For comparison with the undisturbed condition, pressure values were taken from the record traces at a time of about 50  $\mu$ sec. These comparisons are presented in Table A1 and plotted in Figures A4 thru A7. For the rising slope of the model, for the 12.2 and 5.5 psi input waves respectively, the observed overpressures are about 1.8 and 2.2 times those of the level condition. The overpressures for the falling slope were 0.4 and 0.5 times that for the undisturbed level condition for the two pressure levels tested.

The increase in pressure for the rising surface is a result of the formation of a Mach reflection as the shock wave travels up the inclined surface. As the shock wave moves over the top of the model an expansion occurs which relieves the pressure to a lower value. References 1 and 2 illustrate photographically the growth process for a Mach reflection from an inclined slope. References 3 and 4 report pressure measurements taken from both rising and falling slopes. Calculations made from the data given in Reference 2 are shown in Table AII. The present data falls at the low end of the table, but appears to be in fair agreement with it.

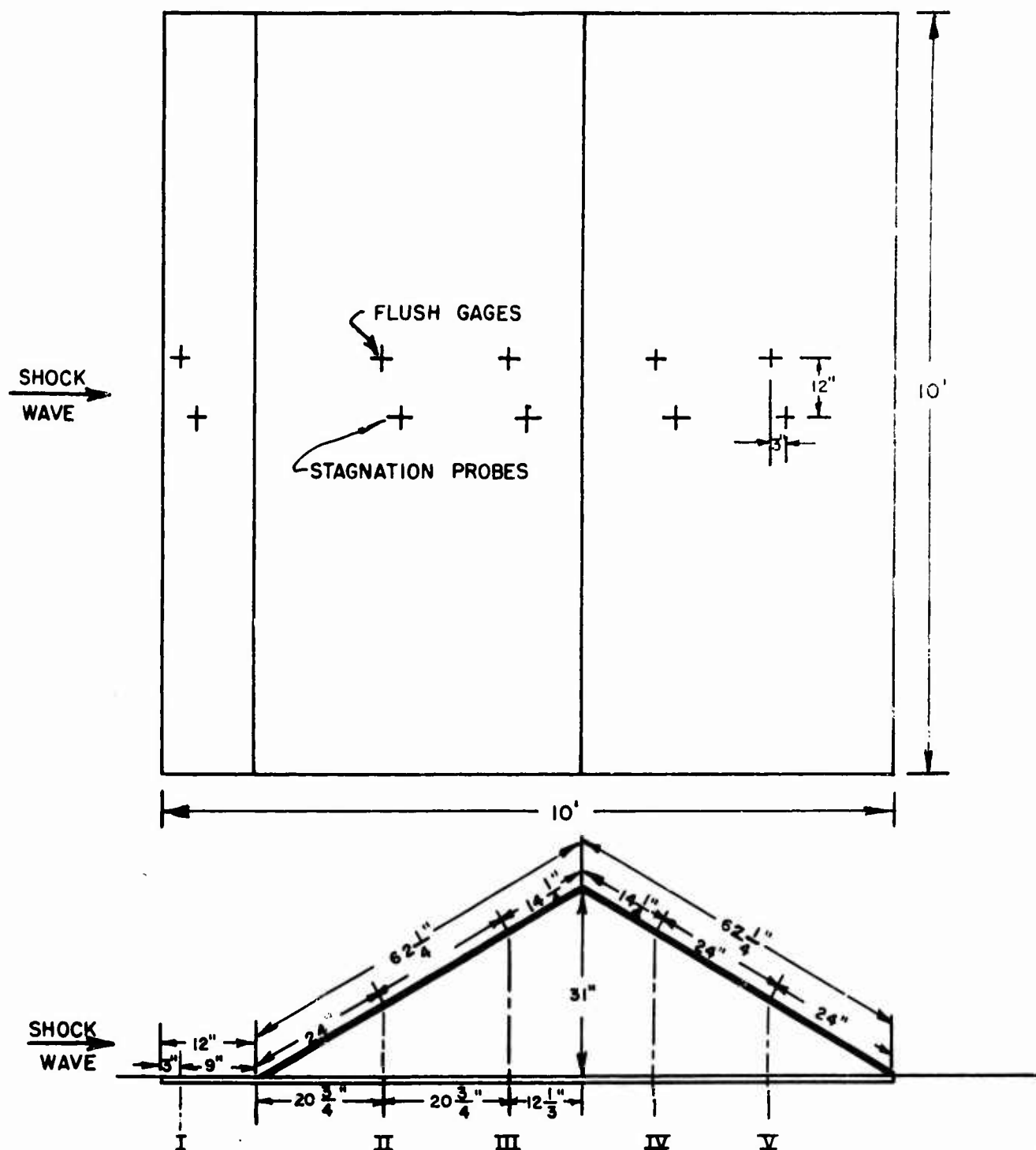


FIGURE A1 A SKETCH OF THE MODEL HILL WITH GAGE POSITIONS

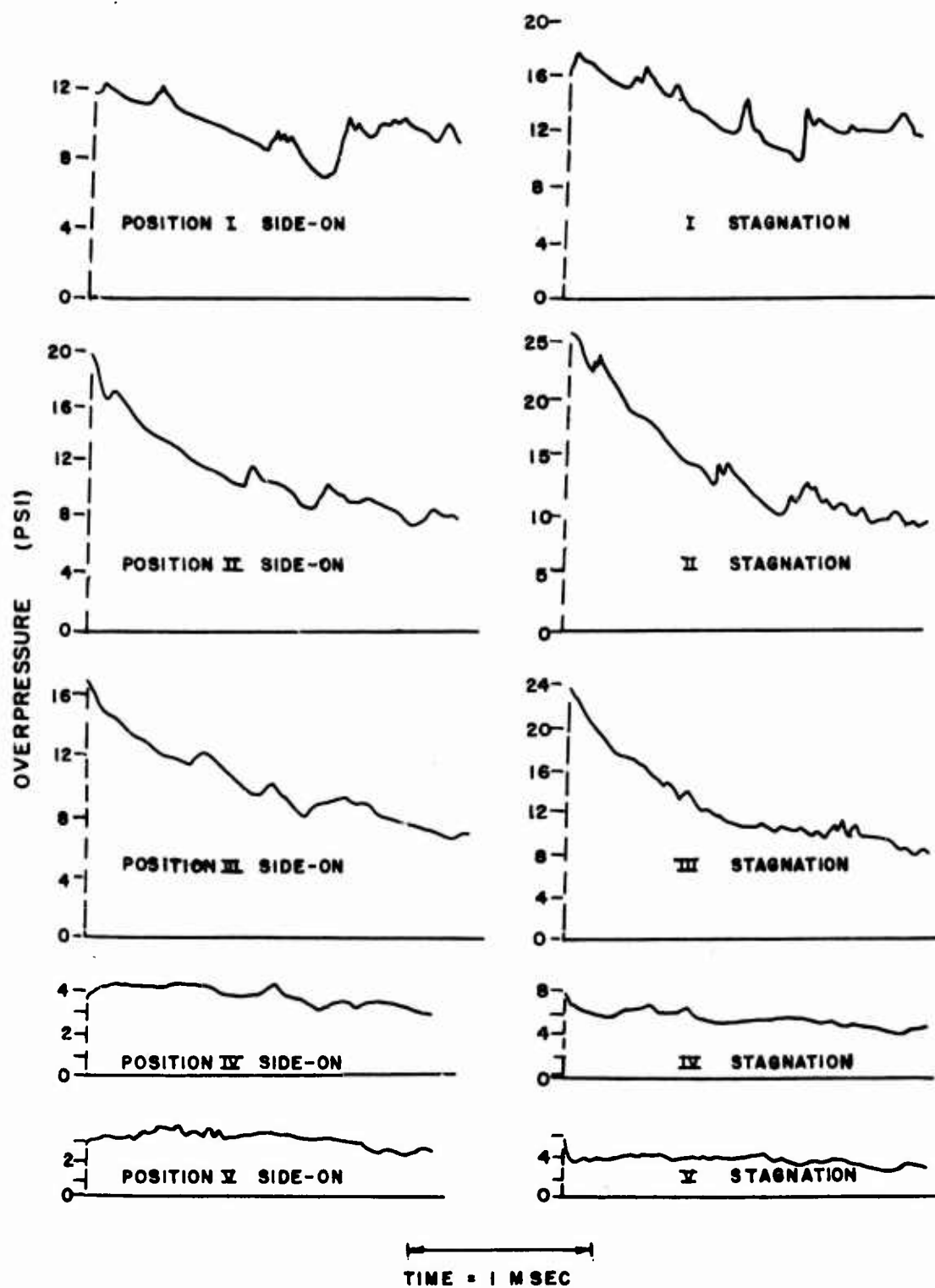


FIGURE A2 PRESSURE-TIME RESULTS

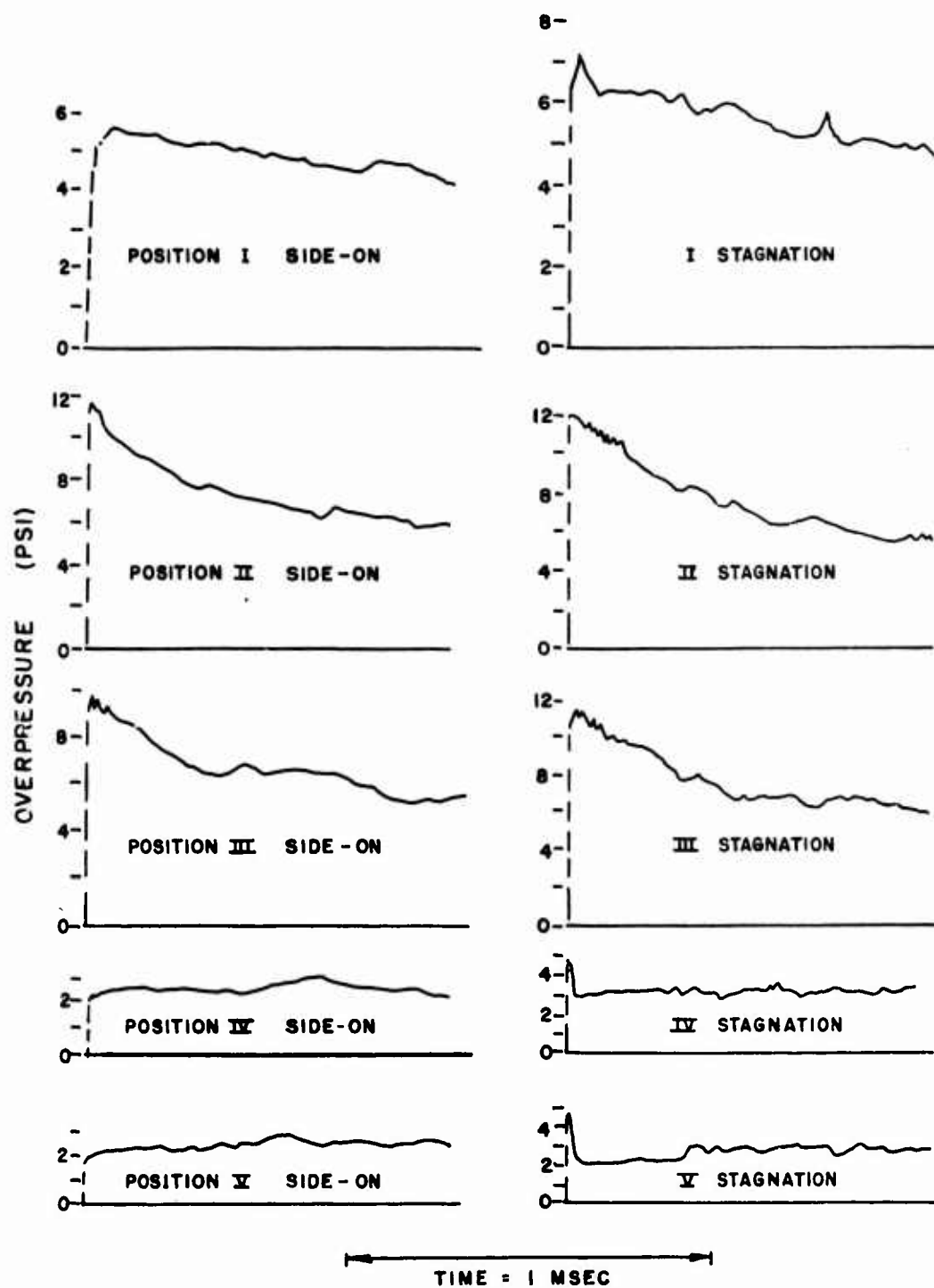


FIGURE A3 PRESSURE-TIME RESULTS



Table A-I. Observed Pressures - 30° Model Hill

Gage Position	Ratio of Pressure on the Model to that on the Level			
	For Input Pressure, 5.5 psi		For Input Pressure, 12.2 psi	
	Side-On	Stagnation	Side-On	Stagnation
I	1.0	1.0	1.0	1.0
II	2.2	2.2	1.9	2.0
III	2.2	2.3	1.8	1.9
IV	0.6	0.7	0.5	0.6
V	0.6	0.5	0.4	0.4

Gage Position	Normal Attenuation Along the Level For Input Waves			
	For Input Pressure, 5.5 psi		For Input Pressure, 12.2 psi	
	$P_s$ , psi	$P_{stag}$ , psi	$P_s$ , psi	$P_{stag}$ , psi
I	5.5	6.2	12.2	15.6
II	4.9	5.5	10.8	13.4
III	4.5	5.0	9.9	12.2
IV	4.0	4.3	8.7	10.5
V	3.6	3.9	7.7	9.1

Symbols used in Table A-I:

$P_s$  Shock Front Overpressure

$P_{stag}$  Shock Front Stagnation Overpressure

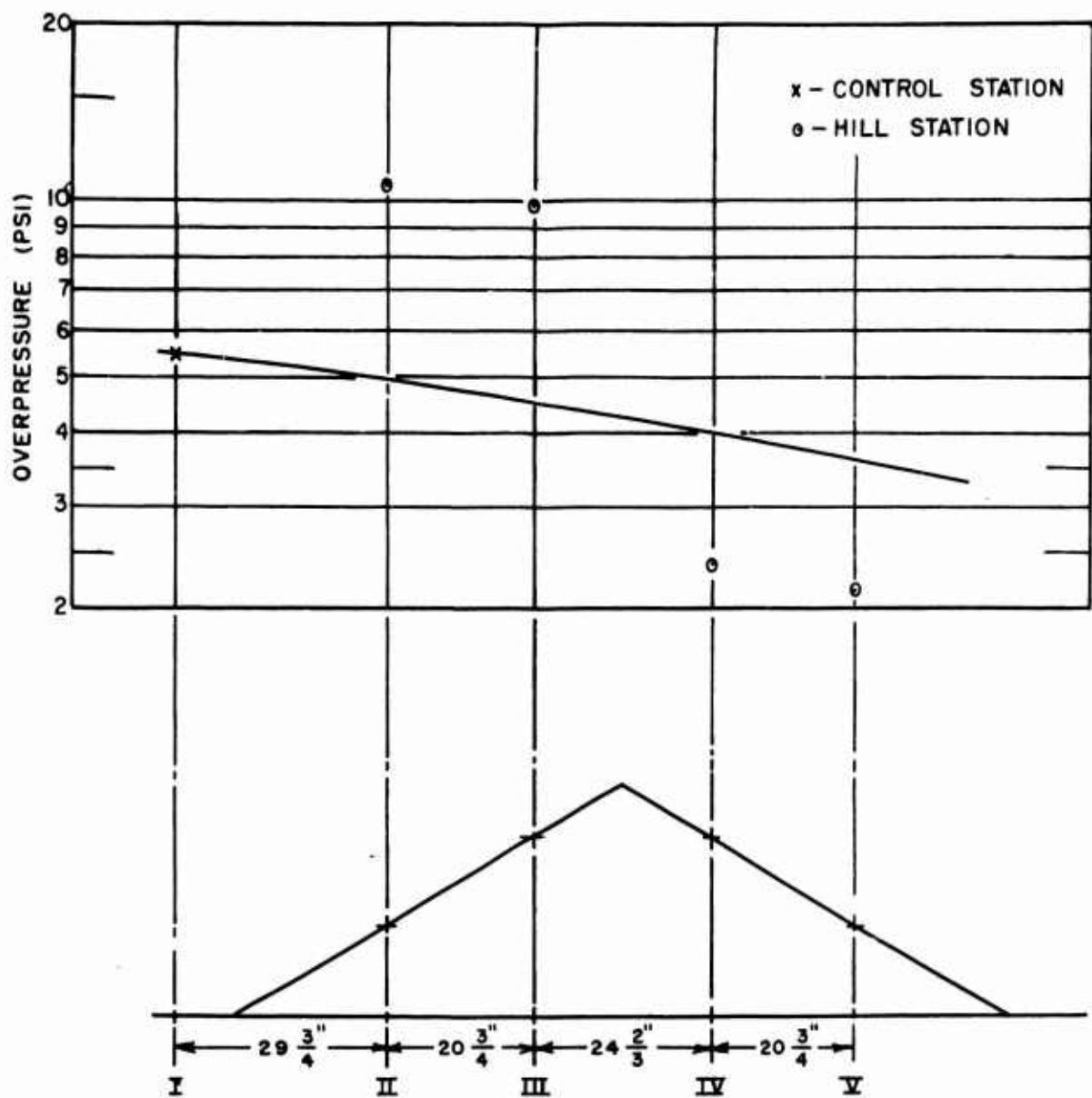


FIGURE A4 MEASURED OVERPRESSURE ON TERRAIN MODEL COMPARED WITH FREE FIELD

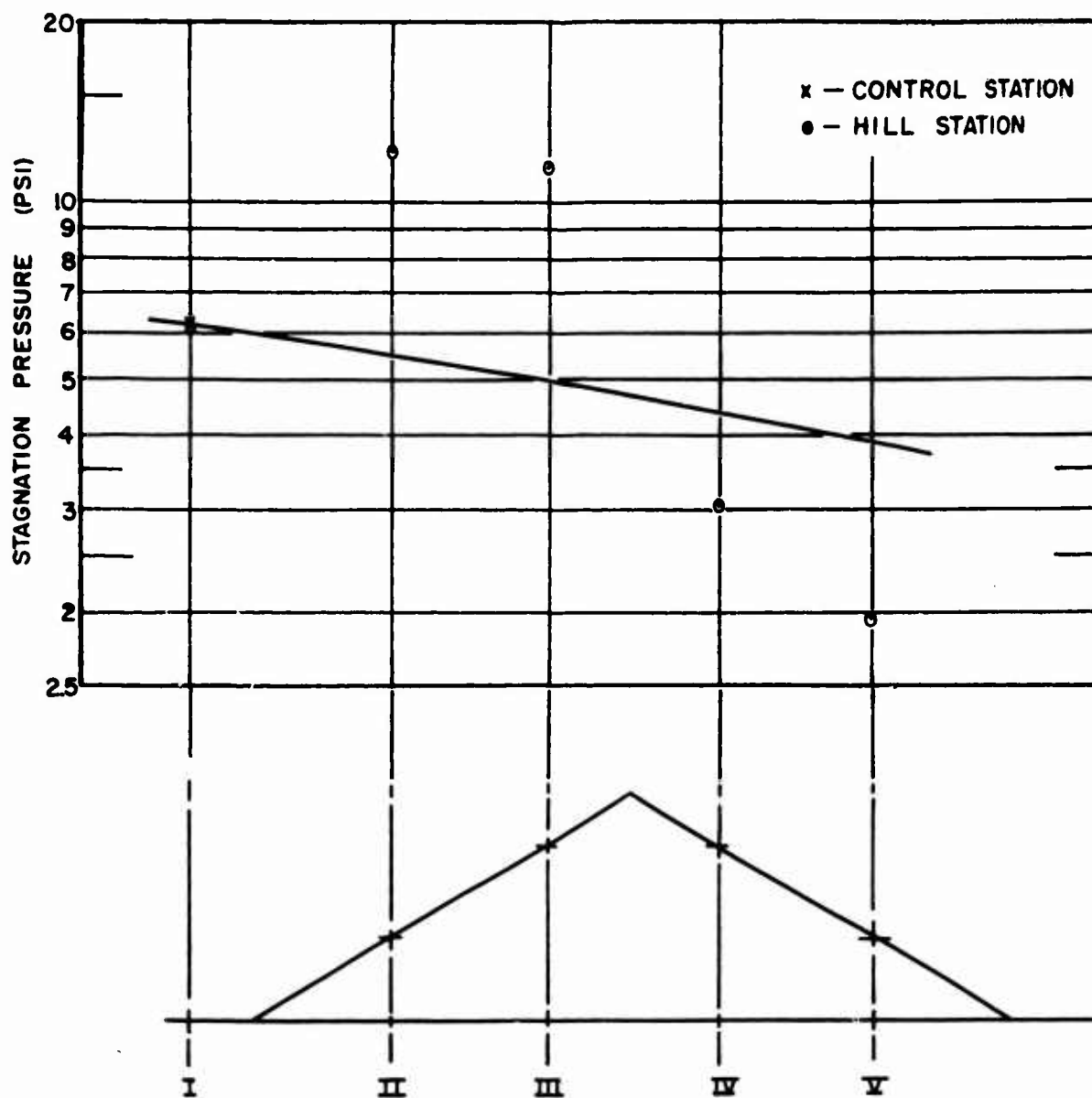


FIGURE A5 MEASURED STAGNATION PRESSURE TERRAIN MODEL COMPARED WITH FREE FIELD

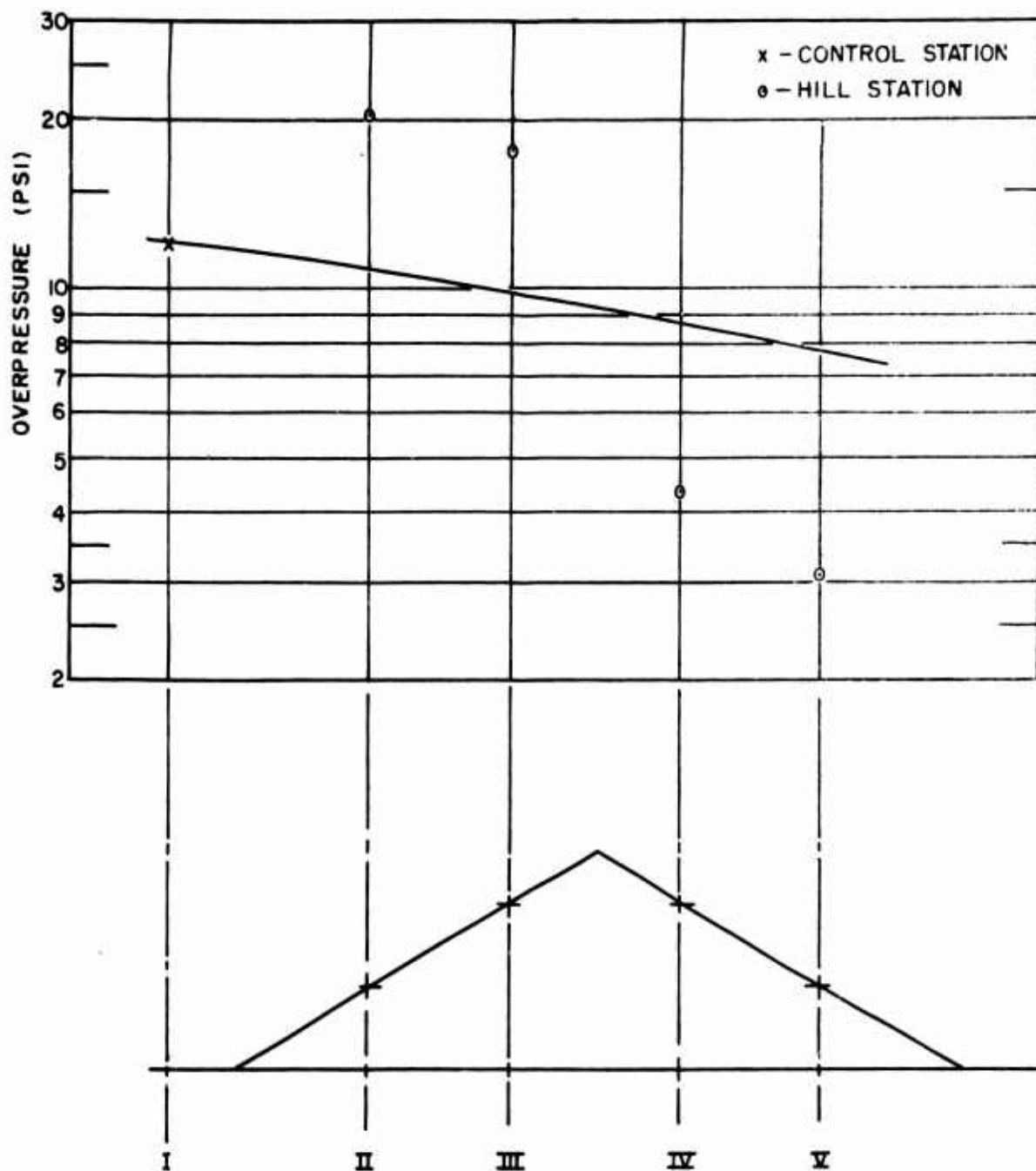


FIGURE A6 MEASURED OVERPRESSURE ON TERRAIN MODEL COMPARED WITH FREE FIELD

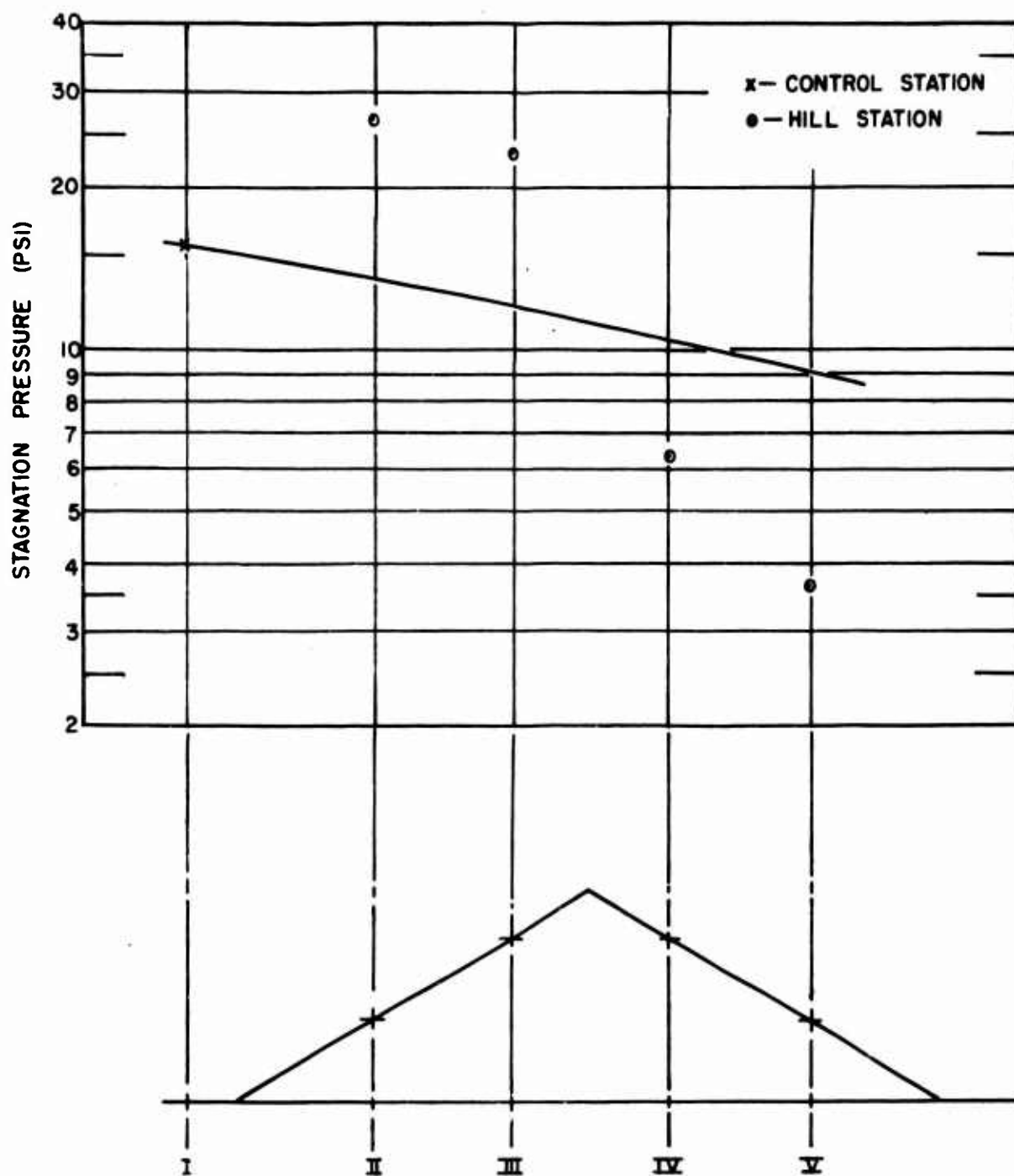


FIGURE A7 MEASURED STAGNATION ON TERRAIN MODEL COMPARED WITH FREE FIELD

Table A-II Calculations for a Rising Slope

Shock Overpressure psi	Shock Strength, $P_1/P_2$	Slope Angle deg	Angle X deg	Pressure on Slope psi
10	.595	30	4.0	22
20	.424	30	6.1	39
30	.328	30	6.8	55
60	.200	30	7.0	102
20	.424	15	15.0	28
50	.227	15	15.2	70

Symbols used in Table A-II:

- $P_1$  ambient pressure
- $P_2$  absolute shock pressure
- X angle between the slope and a line from the foot of the slope to the triple point of the shock wave Mach reflection.

One might reasonably expect to obtain similar results for large, scaled field models, or for natural topography made up of reasonably smooth rising or falling slopes.

#### SUMMARY AND CONCLUSIONS

Two major effects were noticed when a model hill was placed in the path of a shock wave. The first effect was a marked increase in pressure on the rising slope, when compared to the input pressure. Also, the pressure-time profile of the shock wave was steeper for about one-half millisecond after the shock wave arrived at the gage positions for the rising slope. No double peaks on the pressure-time records were observed, other than those present for the input waves. The stagnation probes were mounted at heights so as to be below the Mach reflection triple point in all cases. Had the gages been placed above the triple points, then two peaks should have been observed, one peak from the input wave and one peak from the reflected wave.

The second effect was a decrease in pressure on the rear slope. This was caused by the shock wave expansion as it moved down the rear slope; an opposite phenomenon to the increase in pressure from the Mach reflection at the front slope.

For an increasing input shock wave pressure, the ratio of measured slope pressure to the undisturbed shock pressure (where there is no model) was observed to decrease. According to the data of Table AII, the trend continues to higher pressures than those used in the present experiment. A similar trend held for the rear slope pressure values. A smaller percentage decrease of the input pressure was measured for the higher pressure input conditions.

#### REFERENCES

1. Smith, L. C. Photographic Investigation of the Reflection of Plane Shocks in Air. The Pentagon, Washington 25, D. C., Headquarters, Army Service Forces, NDRC Report No. A-350, November 1945.
2. White, Donald R. An Experimental Survey of the Mach Reflection of Shock Waves. Princeton University Department of Physics, Technical Report II-10, August 21, 1951.
3. Willoughby, A. B., et al. Effects of Topography on Shock Waves in Air. AFSWC-TR-57-9, August, 1956.
4. Broadview Bi-Monthly Progress Report. Burlingame, California, BRC 170-5, May 26, 1961.



PREVIOUS PAGE WAS BLANK, THEREFORE WAS NOT FILMED

APPENDIX B  
PRESSURE TIME PLOTS

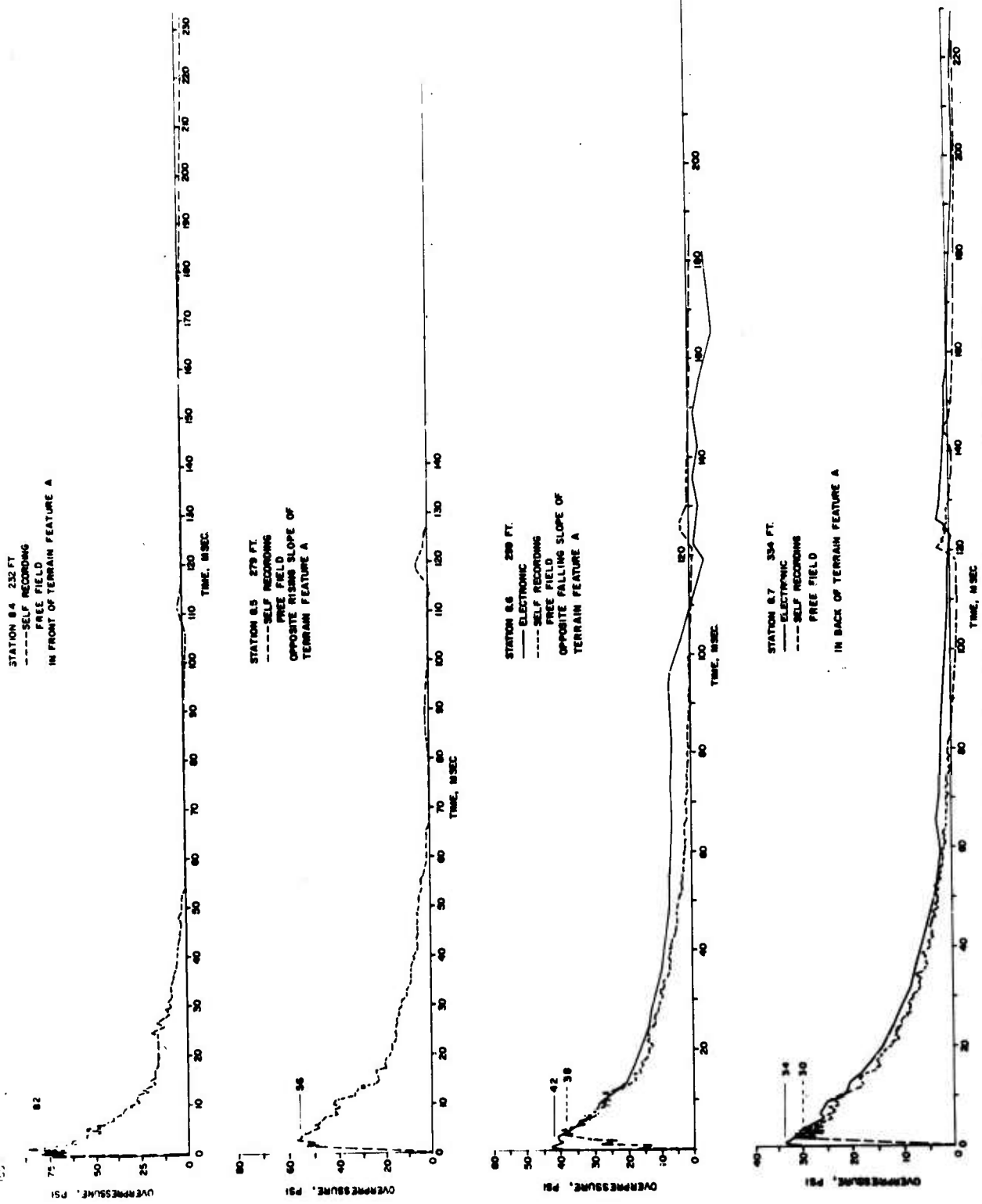


FIGURE B1 FREE FIELD OVERPRESSURE MEASUREMENTS

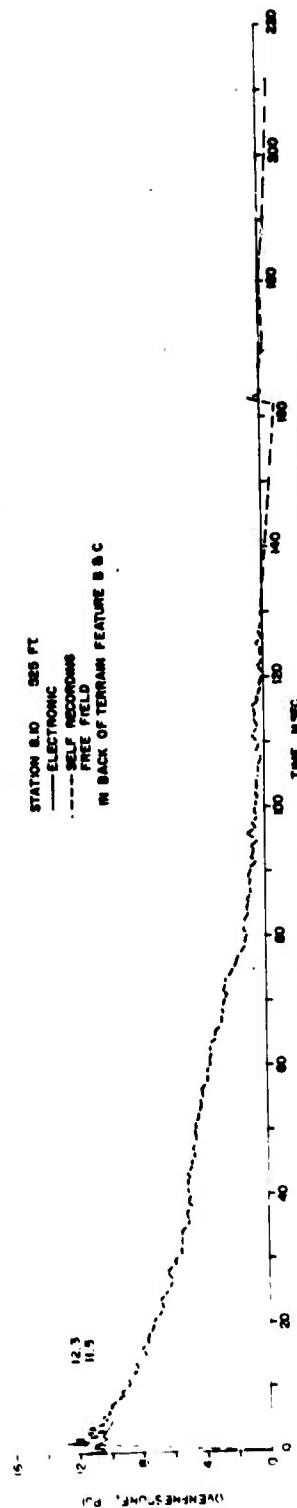
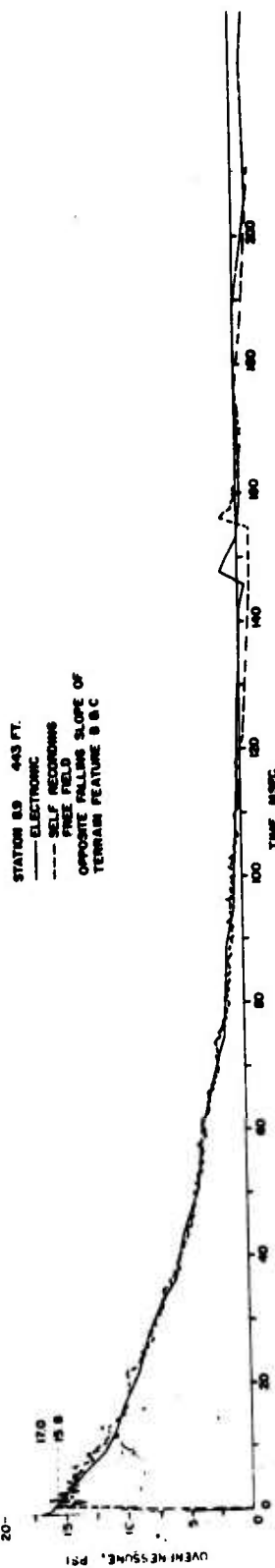
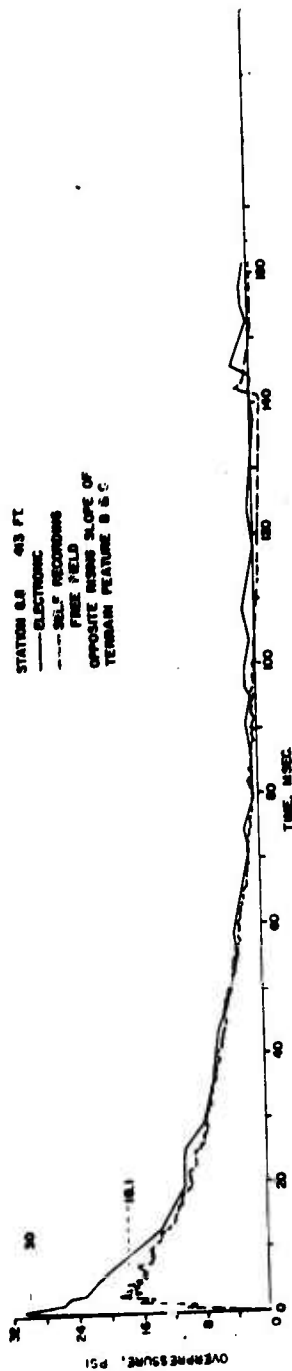
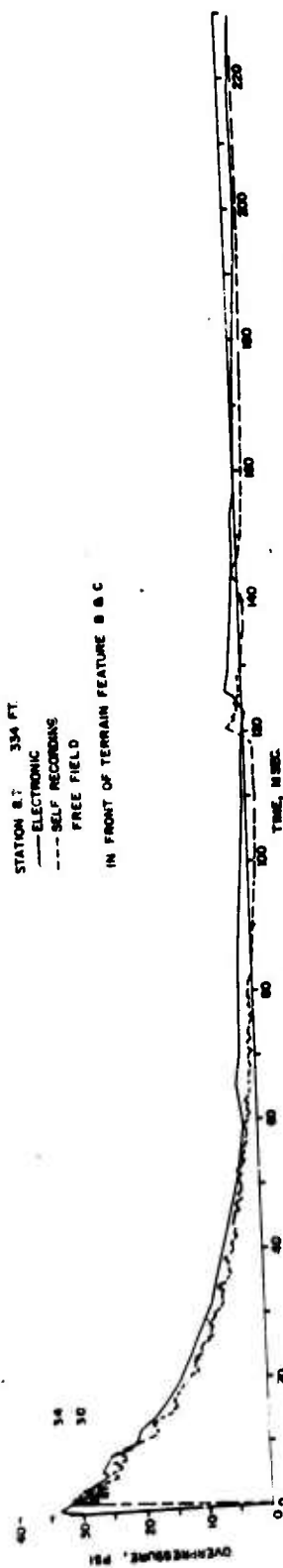


FIGURE B2 FREE FIELD OVERPRESSURE MEASUREMENTS

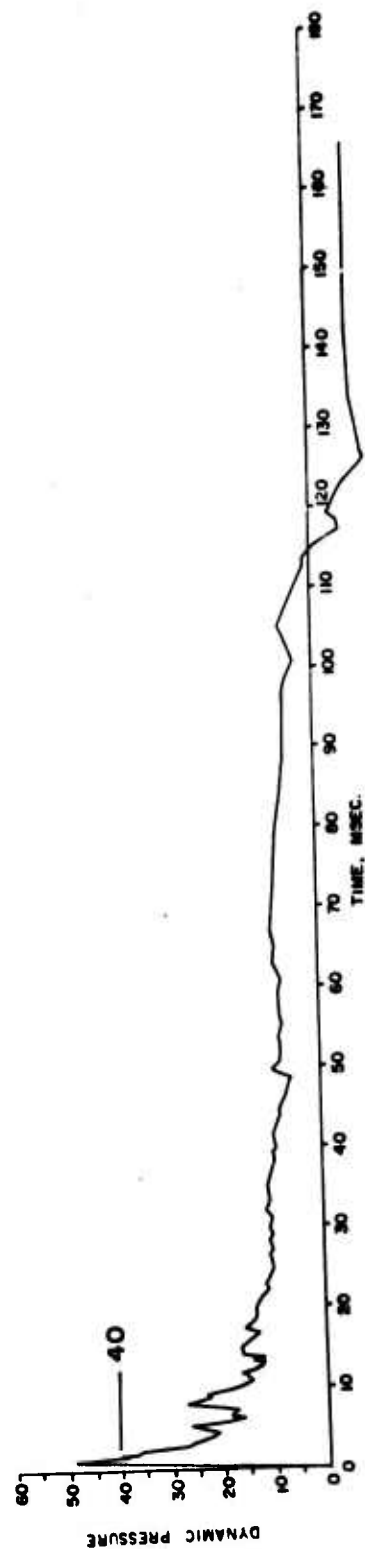
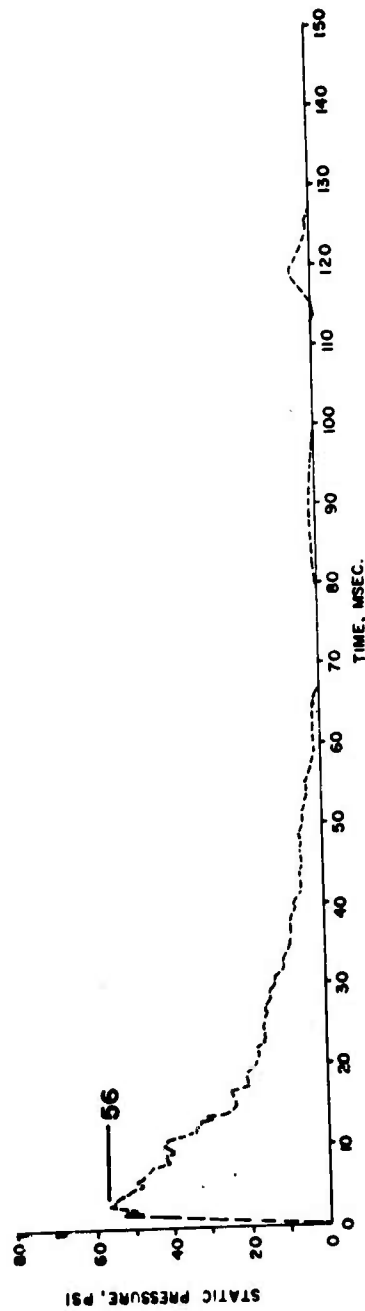
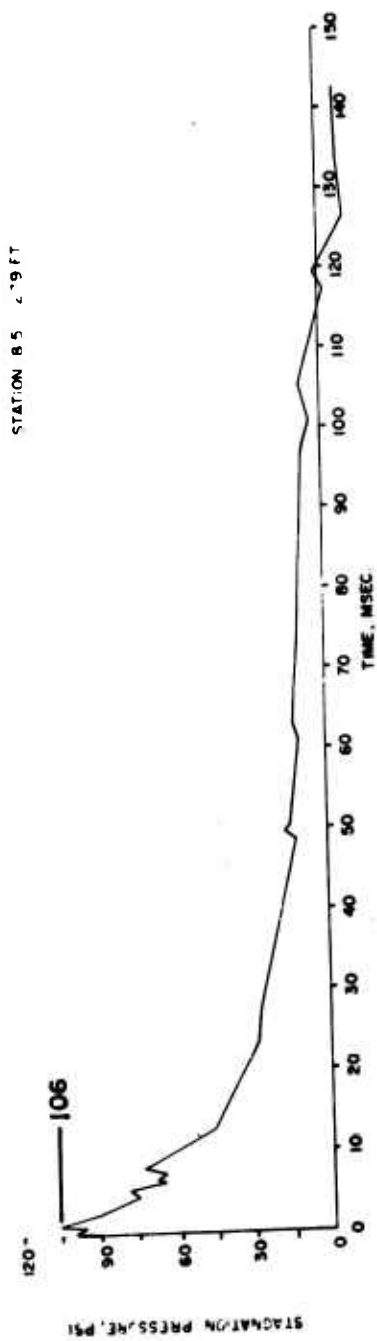


FIGURE B3 FREE FIELD PRESSURE MEASUREMENTS AT 279 FEET, STATION 8.5

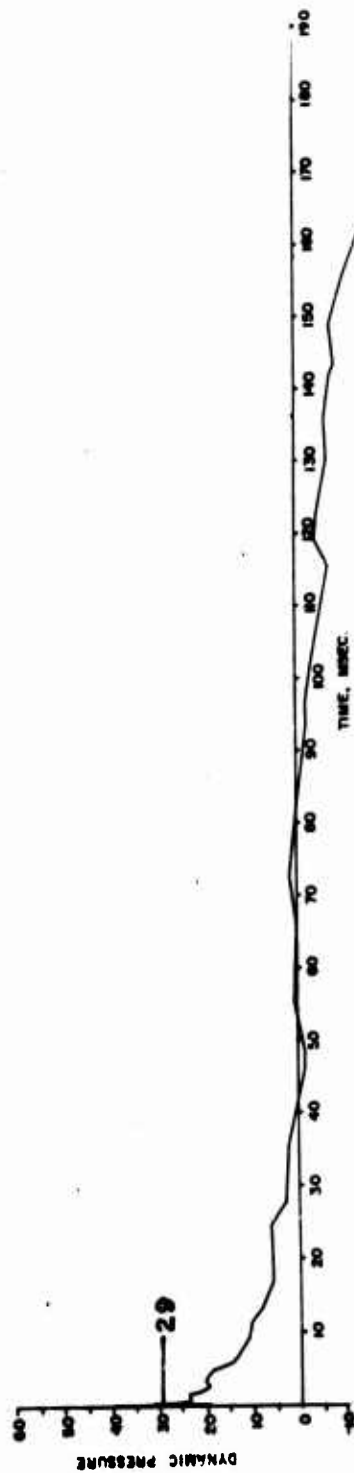
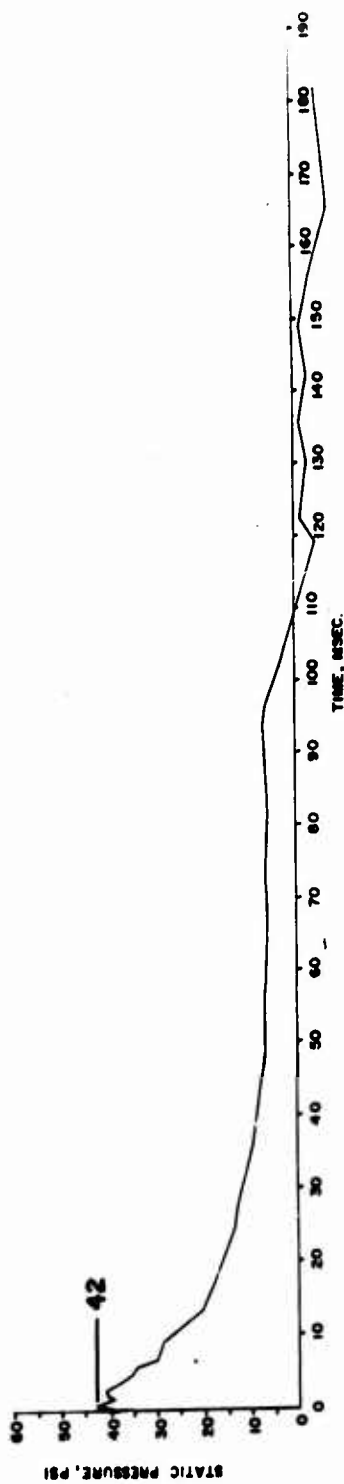
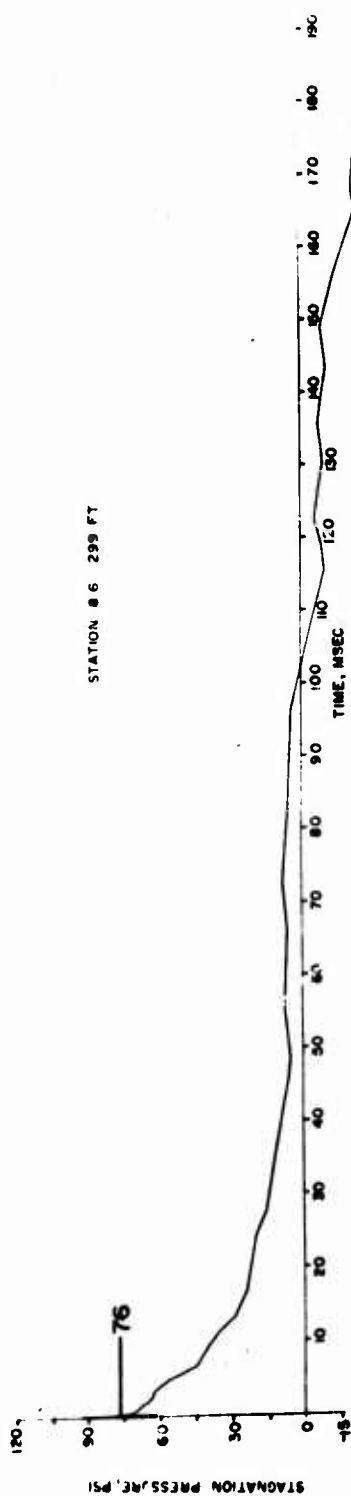


FIGURE B4 FREE FIELD PRESSURE MEASUREMENTS AT 299 FEET, STATION 8.6

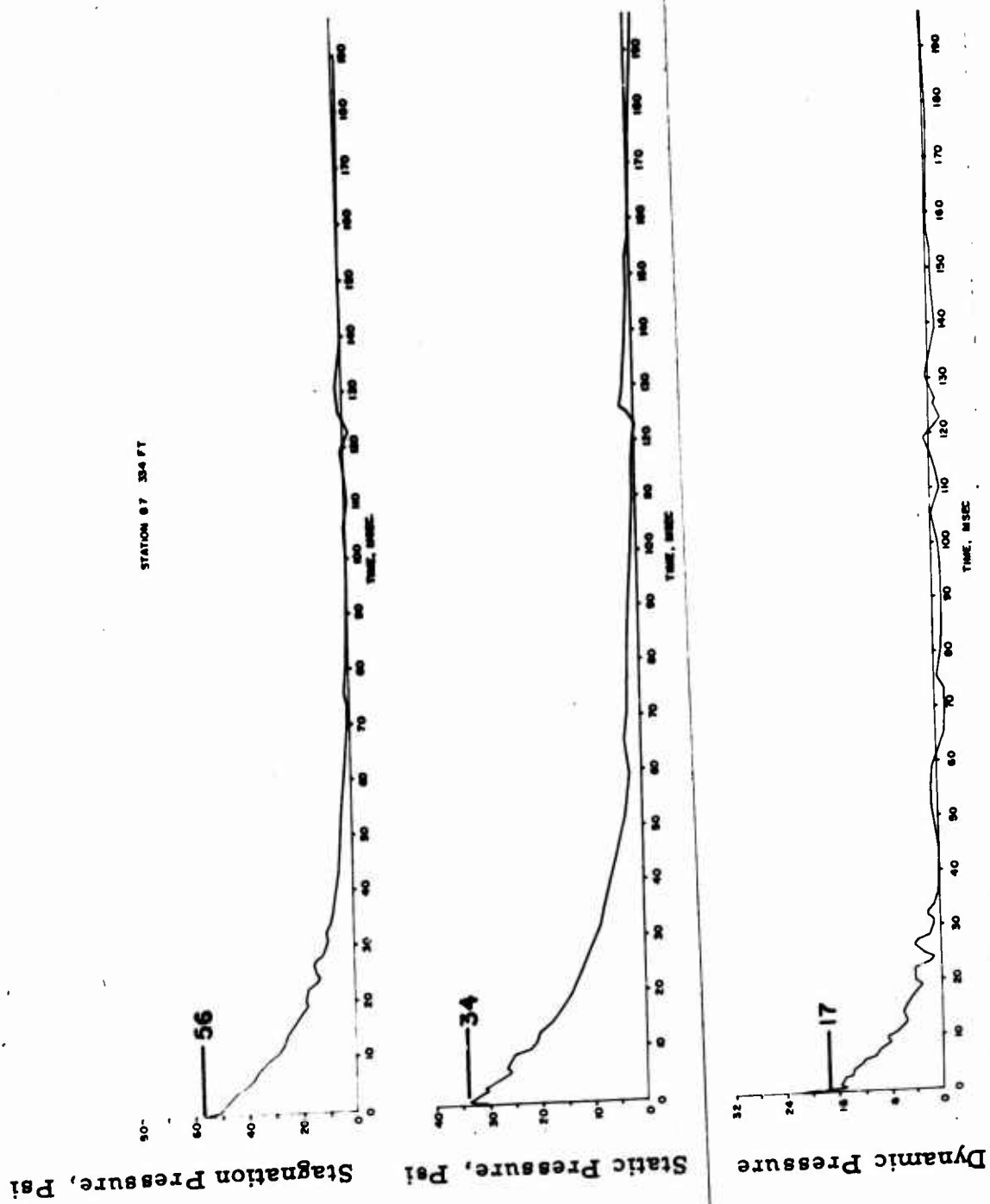


FIGURE B5 FREE FIELD PRESSURE MEASUREMENTS AT 334 FEET, STATION 8.7

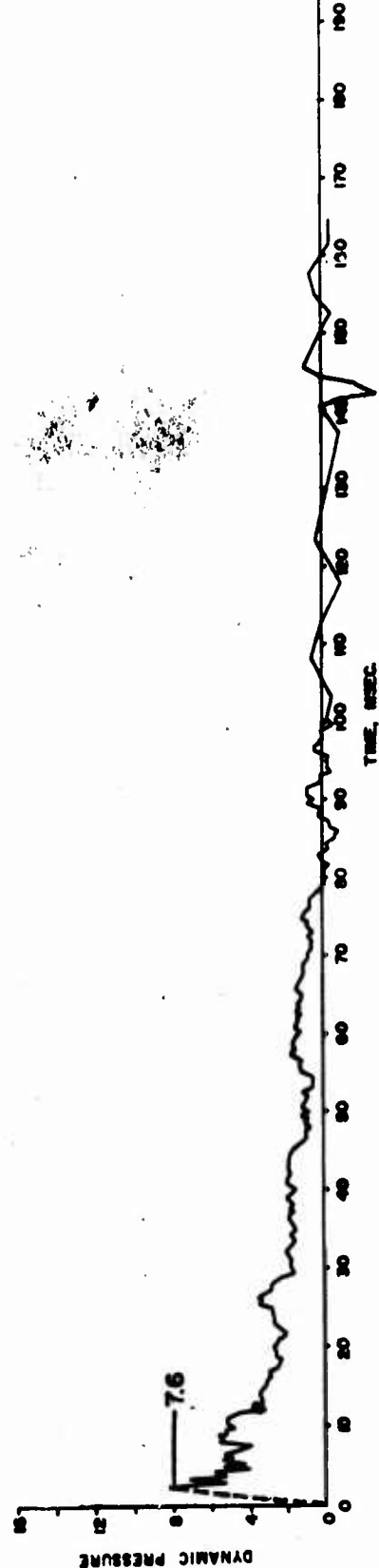
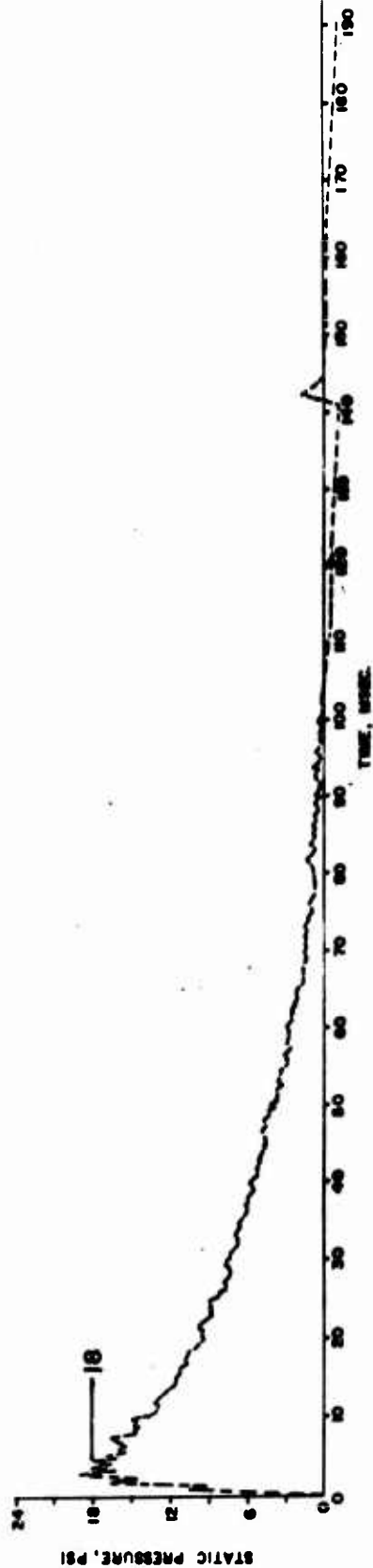
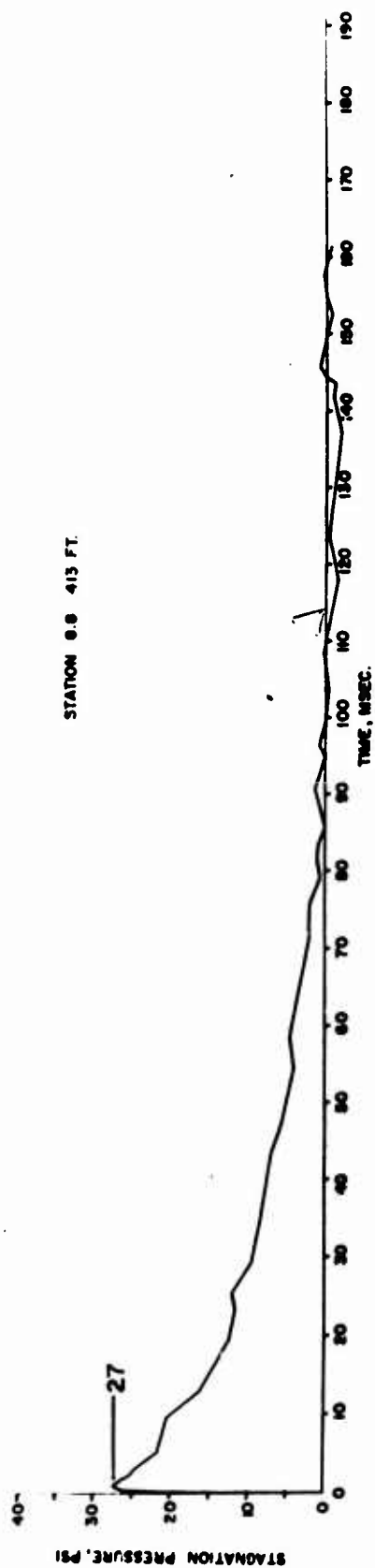


FIGURE B6 FREE FIELD PRESSURE MEASUREMENTS AT 413 FEET, STATION 8.8

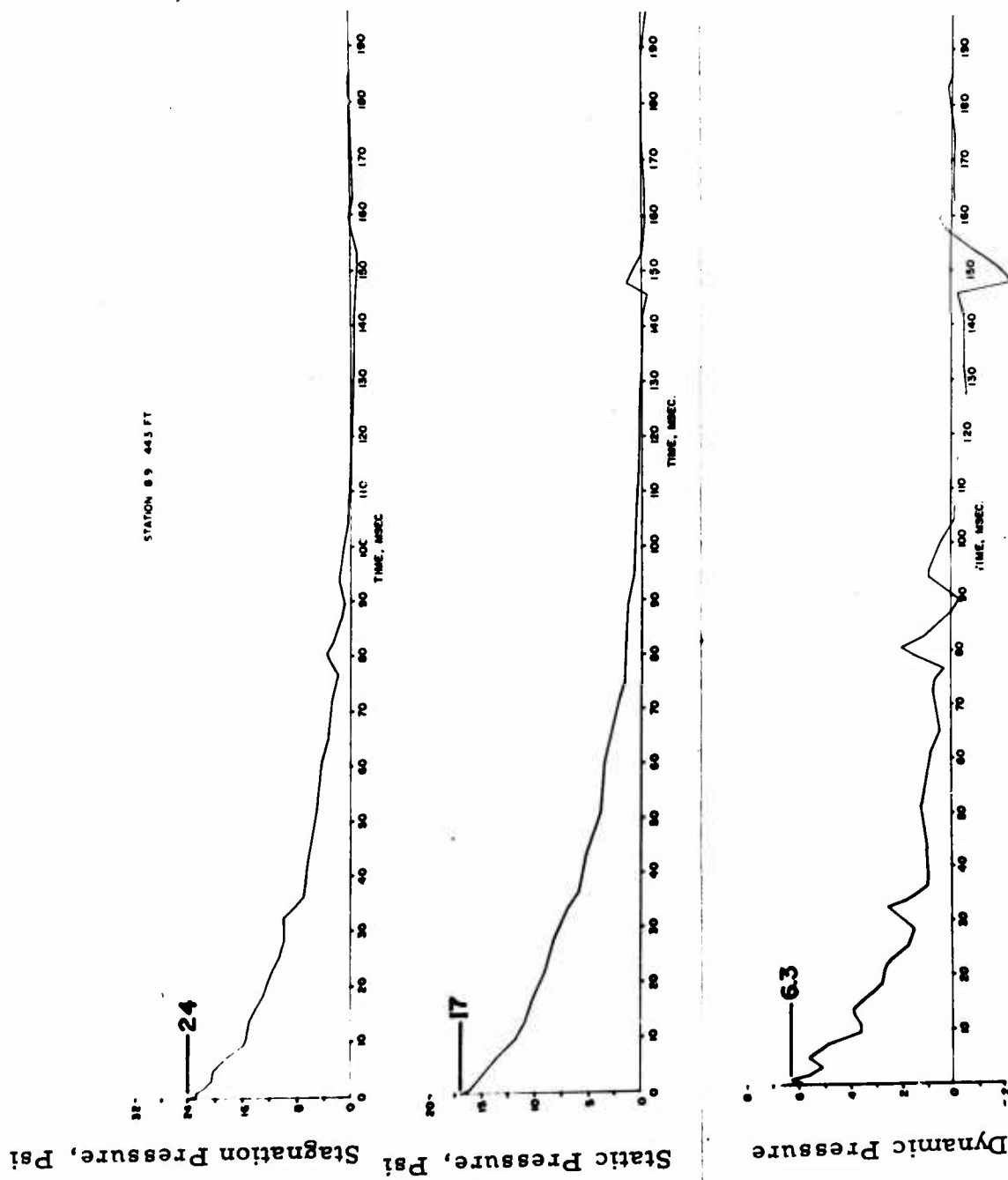


FIGURE B7 FREE FIELD PRESSURE MEASUREMENTS AT 443 FEET, STATION 8.9



8A-PI-40-60  
255.4 FT

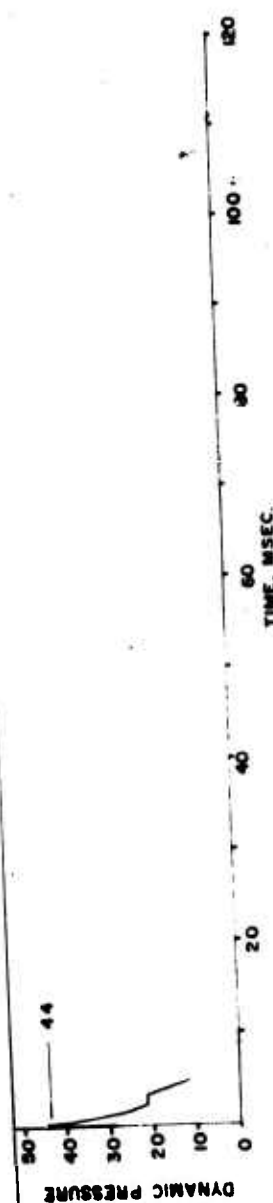
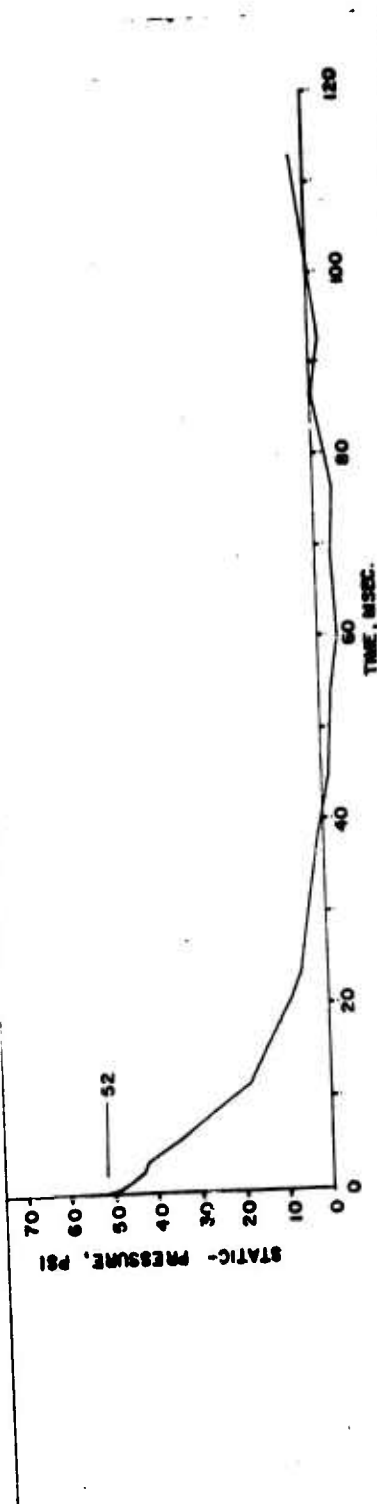
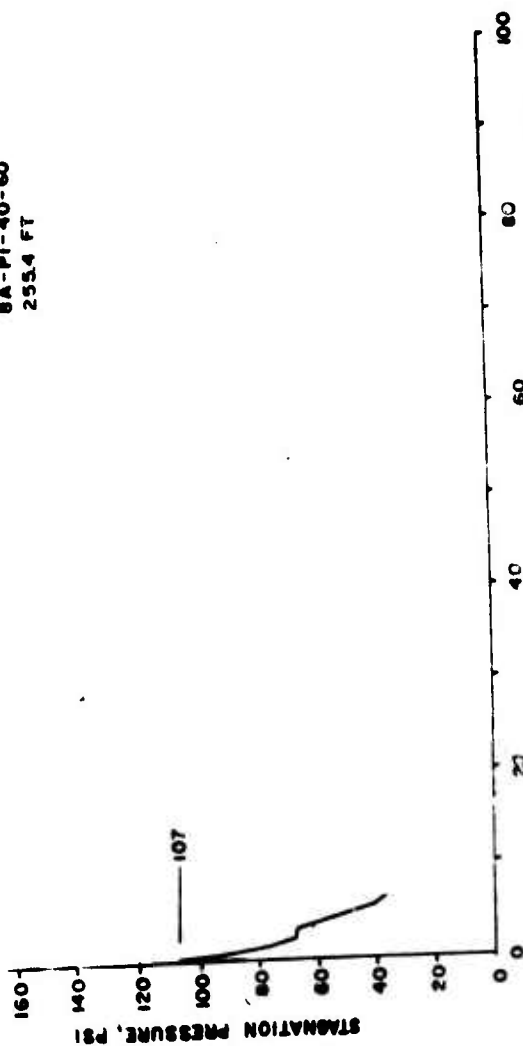


FIGURE B8 FREE FIELD PRESSURE MEASUREMENTS IN FRONT OF TERRAIN FEATURE A, STATION P1

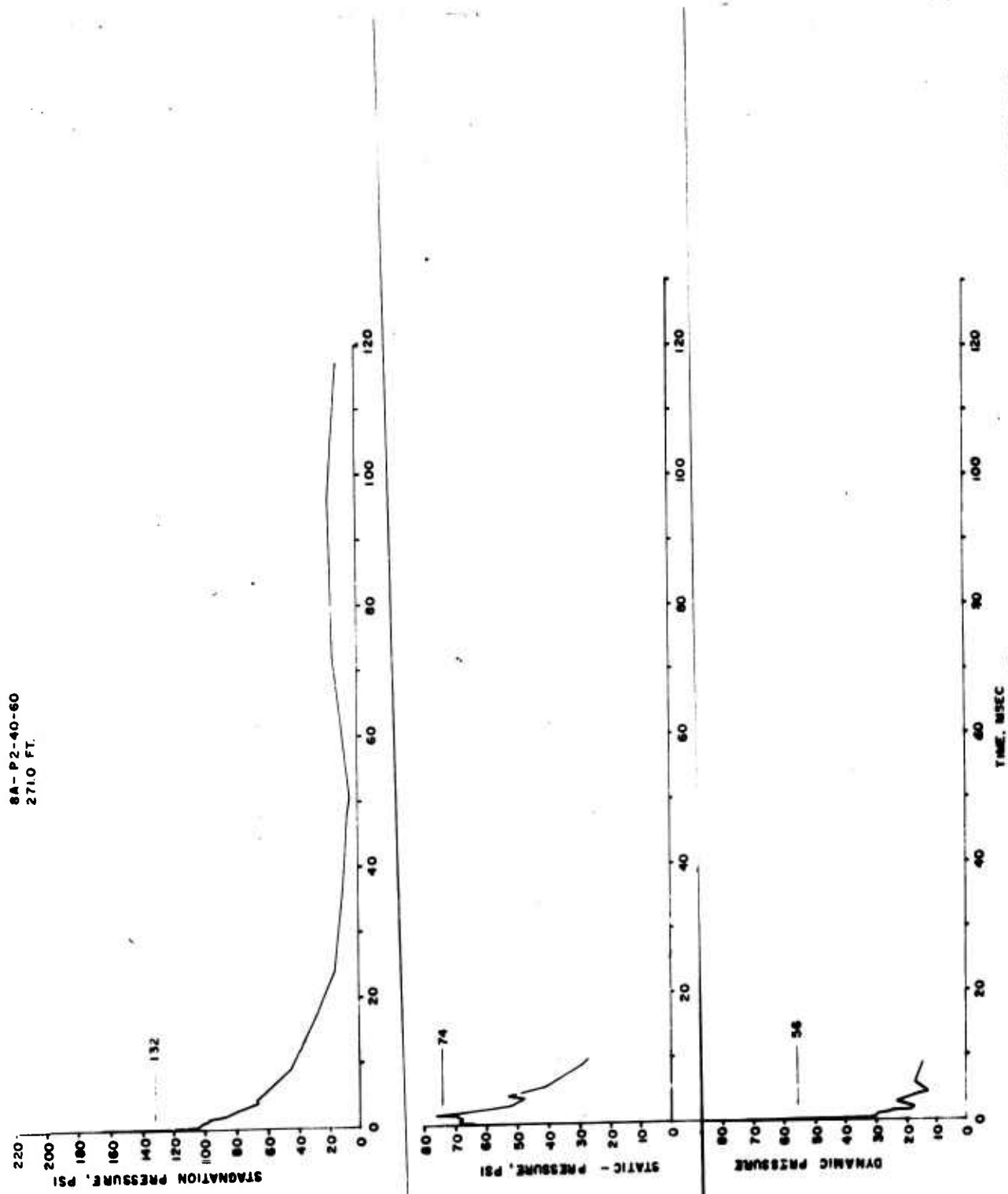


FIGURE B9 PRESSURE MEASUREMENTS ON 15° RISING SLOPE OF TERRAIN FEATURE A, STATION P2

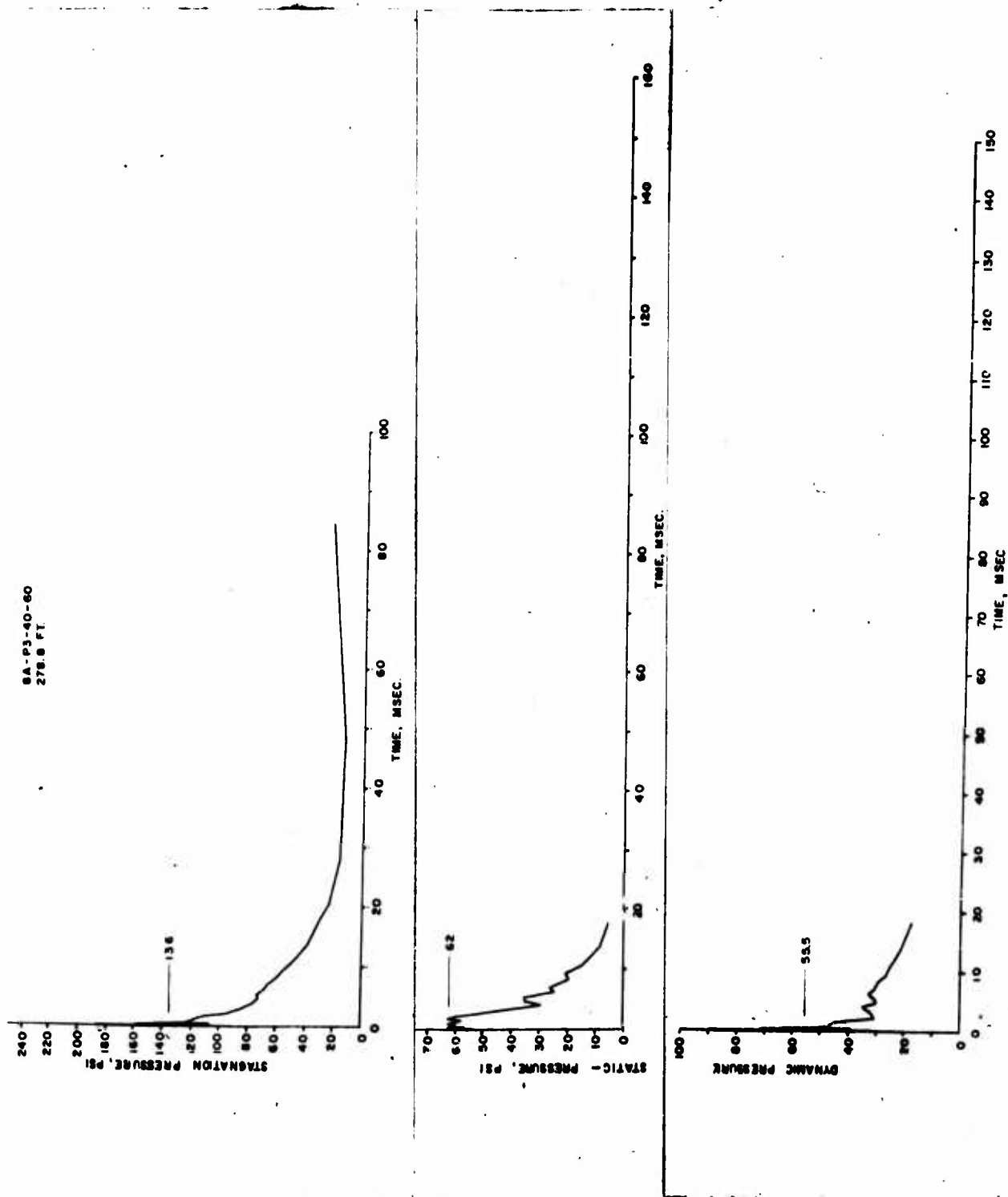


FIGURE B10 PRESSURE MEASUREMENTS ON 15° RISING SLOPE OF TERRAIN FEATURE A, STATION P3

88-P1-40-60  
391.1 FT.

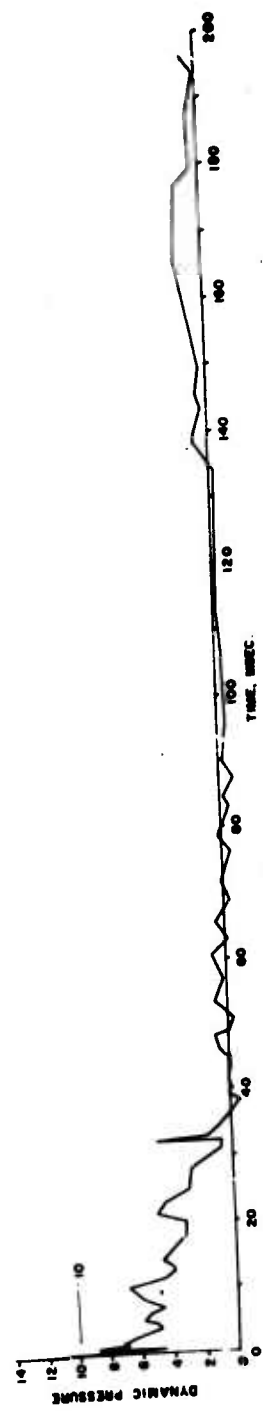
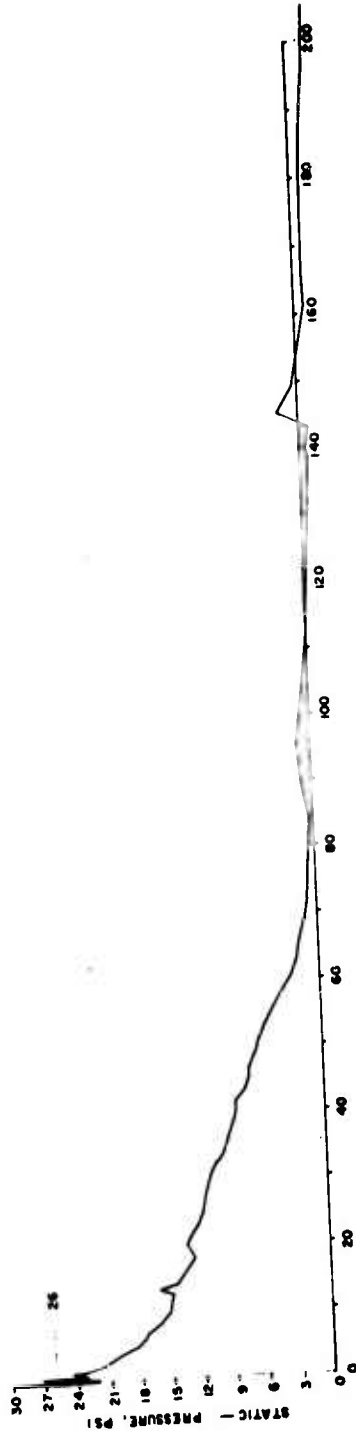
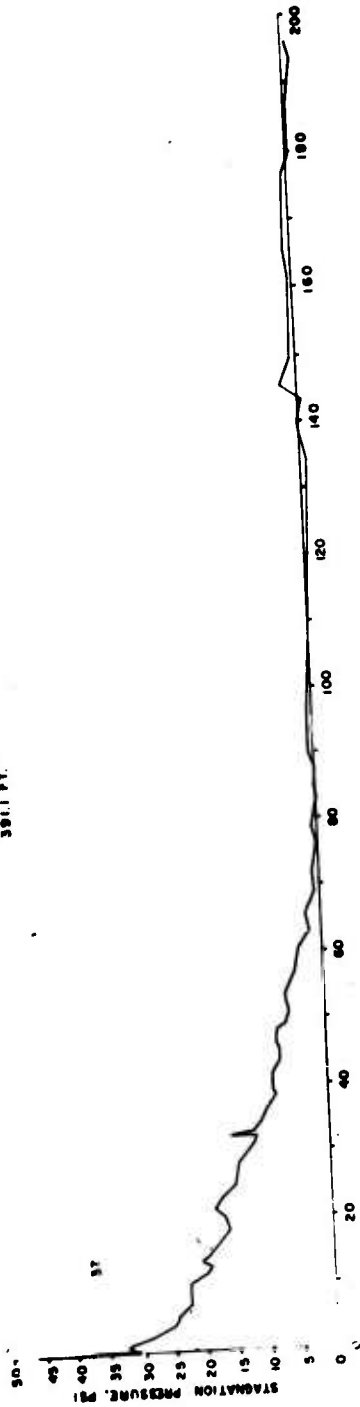


FIGURE B11 FREE FIELD PRESSURE MEASUREMENTS IN FRONT OF TERRAIN FEATURE B, STATION P1

88-P2-40-80  
400.8 FT

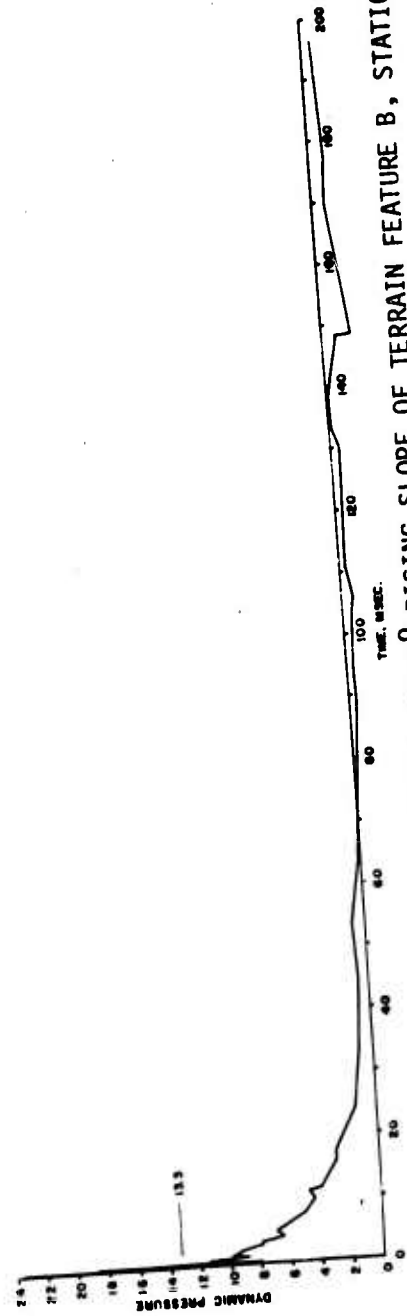
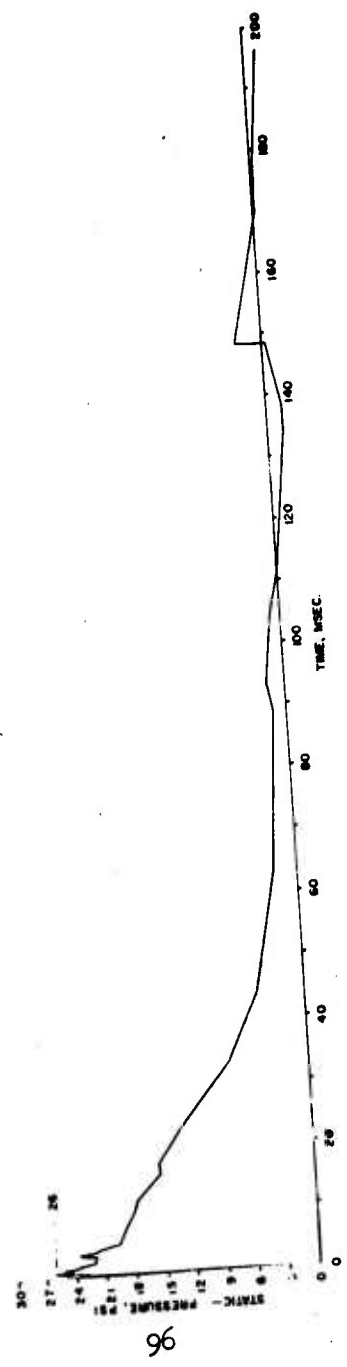
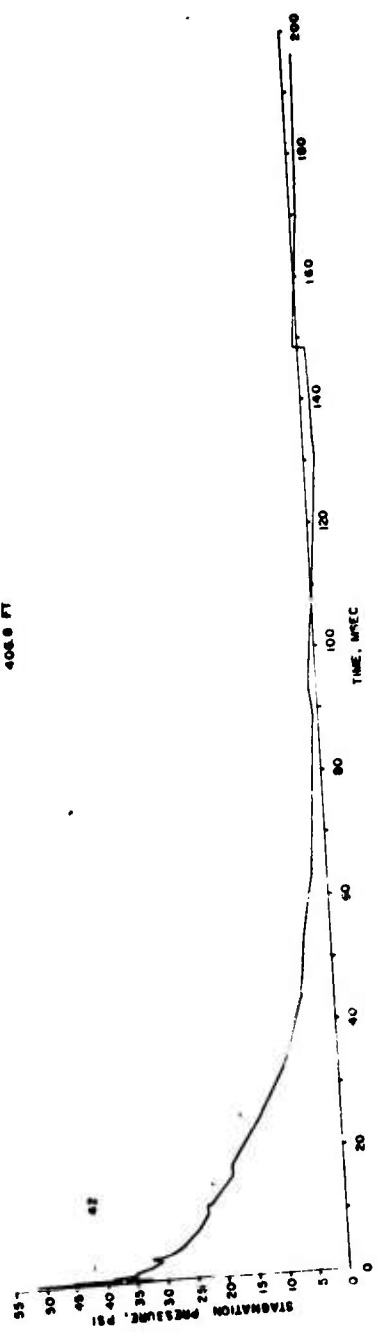


FIGURE B12 PRESSURE MEASUREMENTS ON 15° RISING SLOPE OF TERRAIN FEATURE B, STATION P2

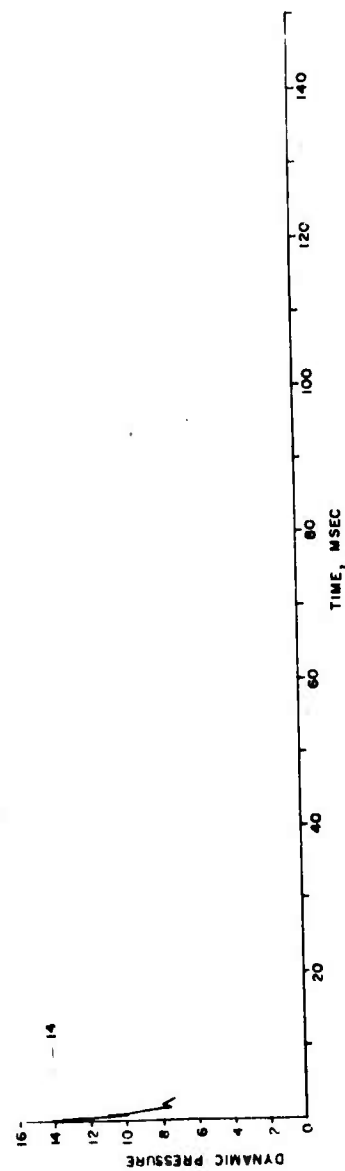
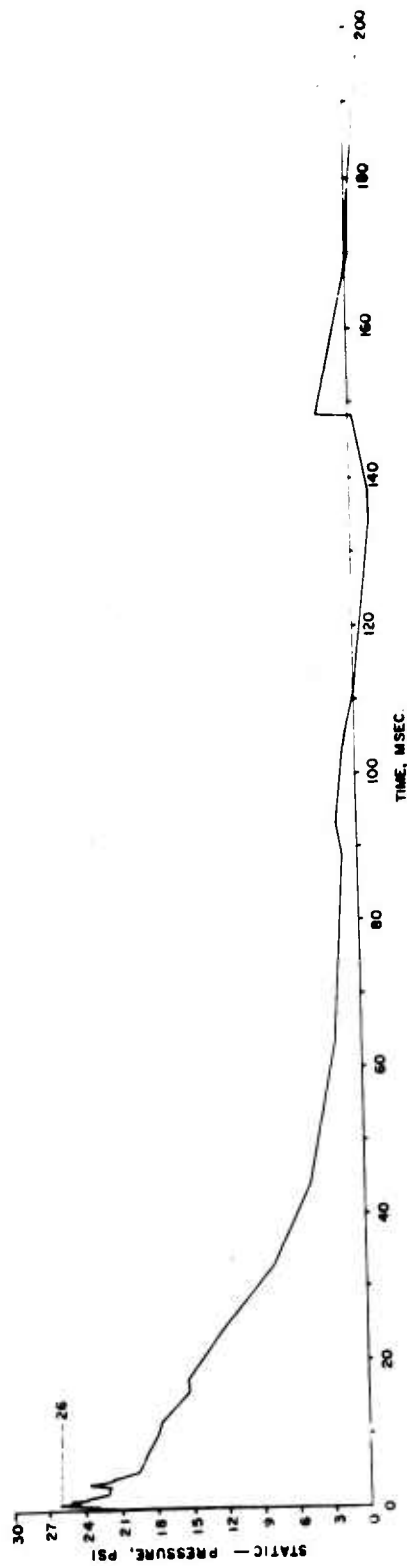
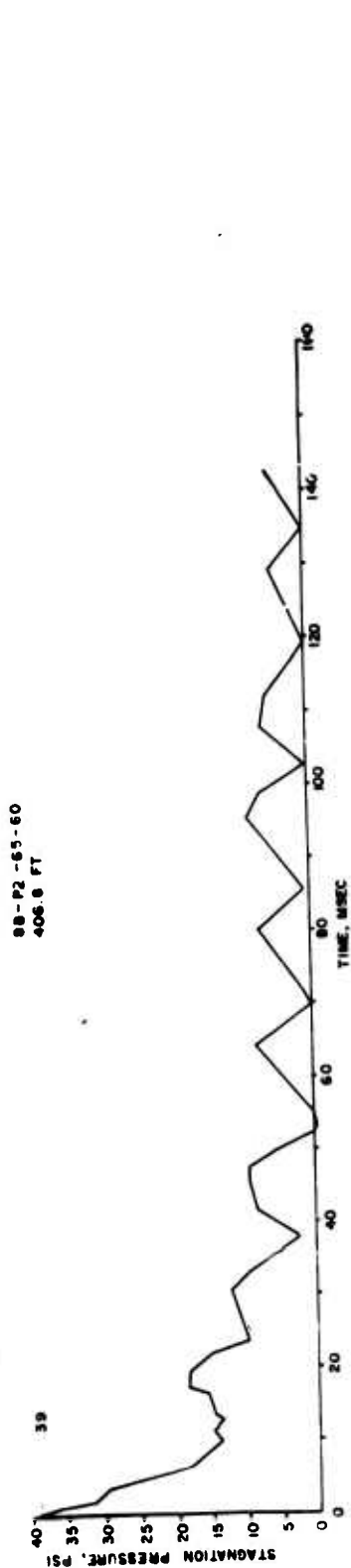


FIGURE B13 PRESSURE MEASUREMENTS ON 15° RISING SLOPE OF TERRAIN FEATURE B, STATION P2  
SURFACE LEVEL STAGNATION BLOCK

BB-P3-40-00  
4145 PY

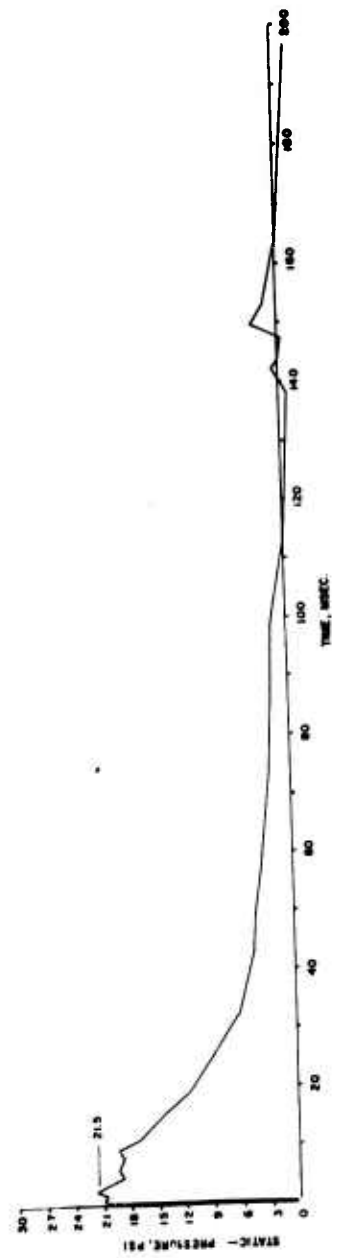
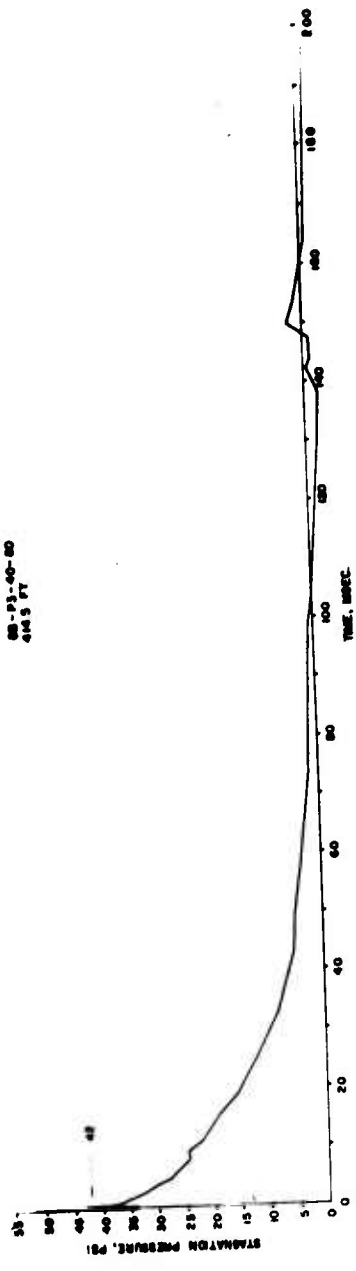


FIGURE B14 PRESSURE MEASUREMENTS ON 15° RISING SLOPE OF TERRAIN FEATURE B, STATION P3

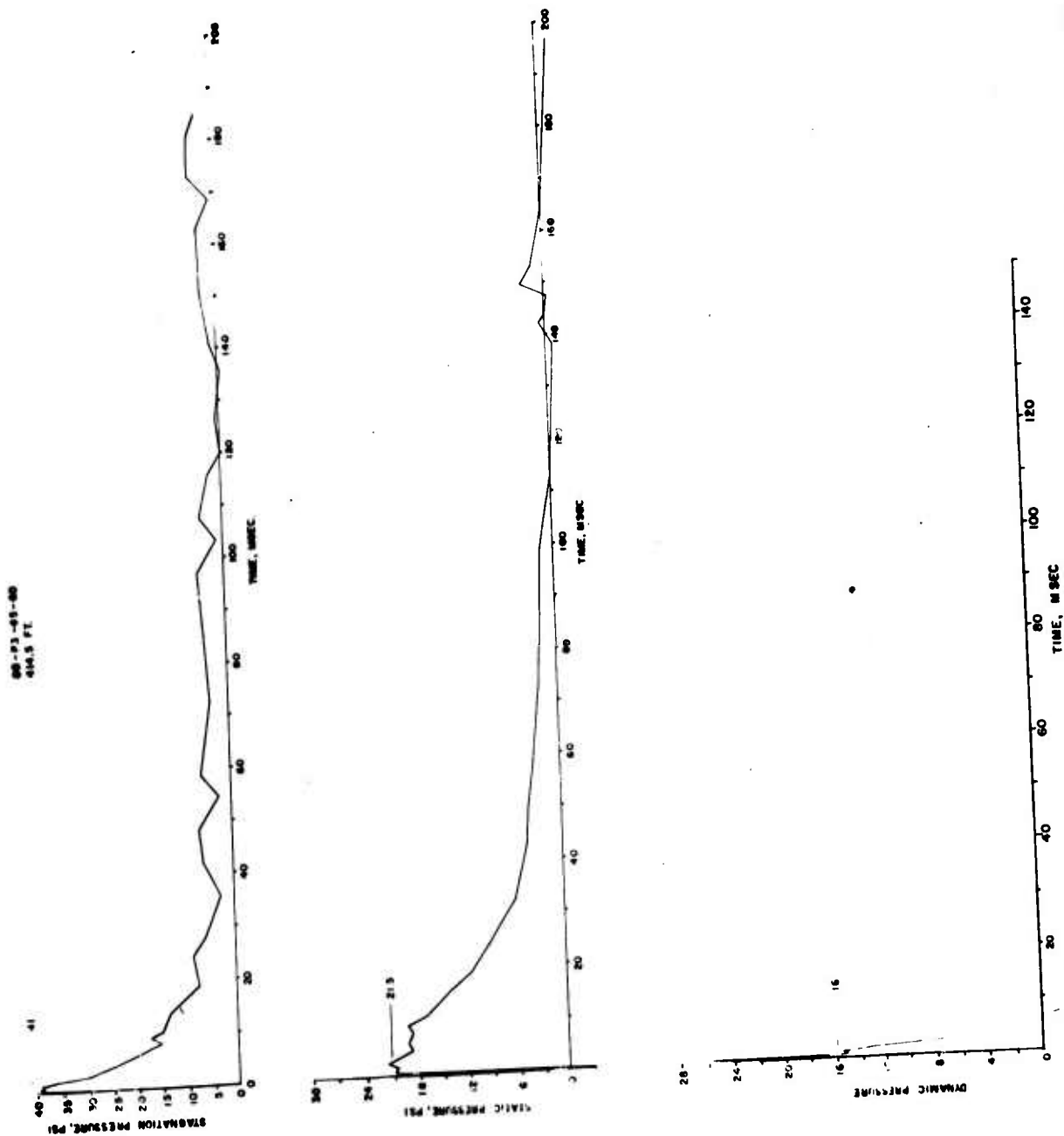


FIGURE B15 PRESSURE MEASUREMENTS ON 15° RISING SLOPE OF TERRAIN FEATURE B, STATION P3  
SURFACE LEVEL STAGNATION BLOCK



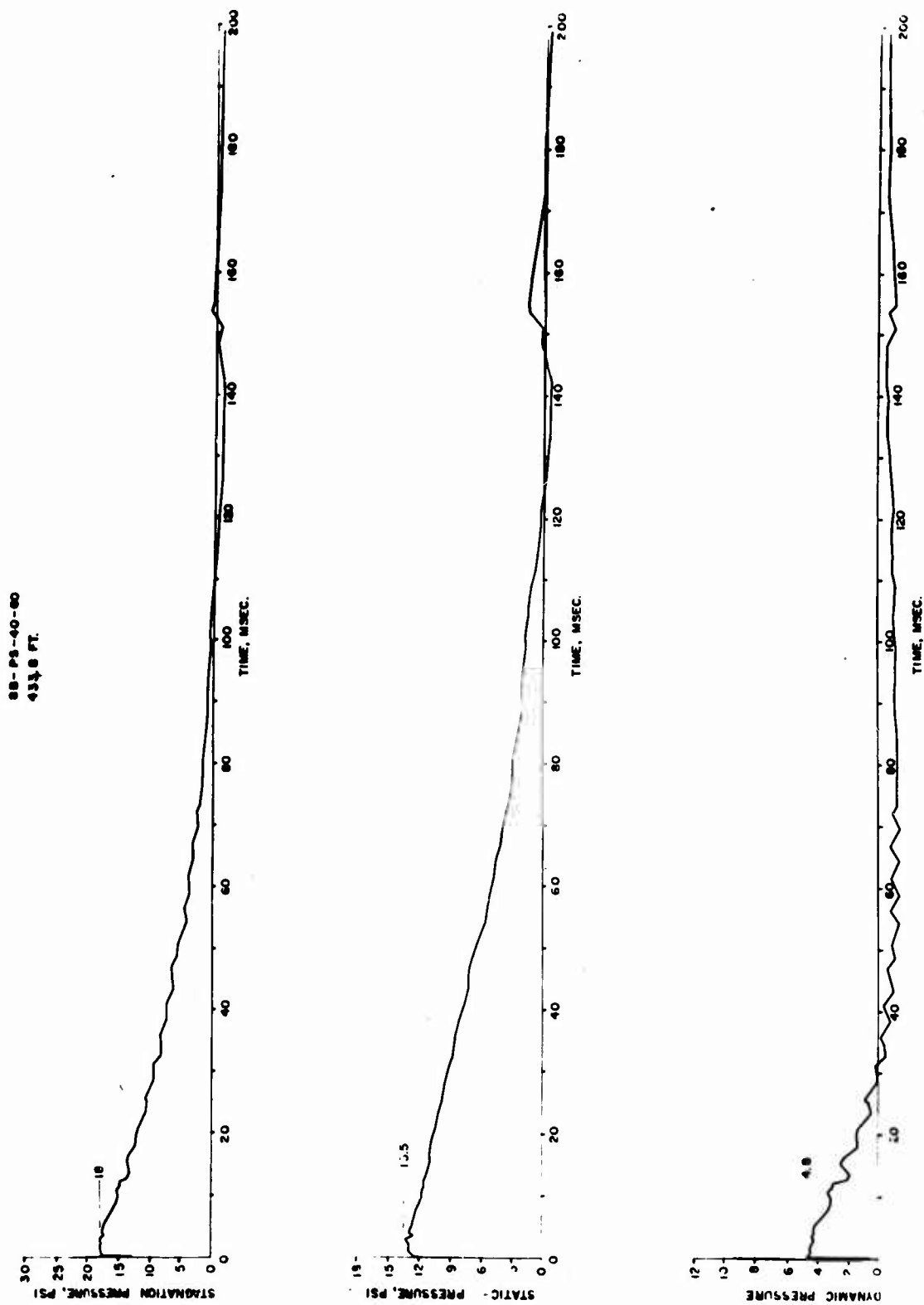


FIGURE B16 PRESSURE MEASUREMENTS ON  $15^{\circ}$  FALLING SLOPE OF TERRAIN FEATURE B, STATION P5

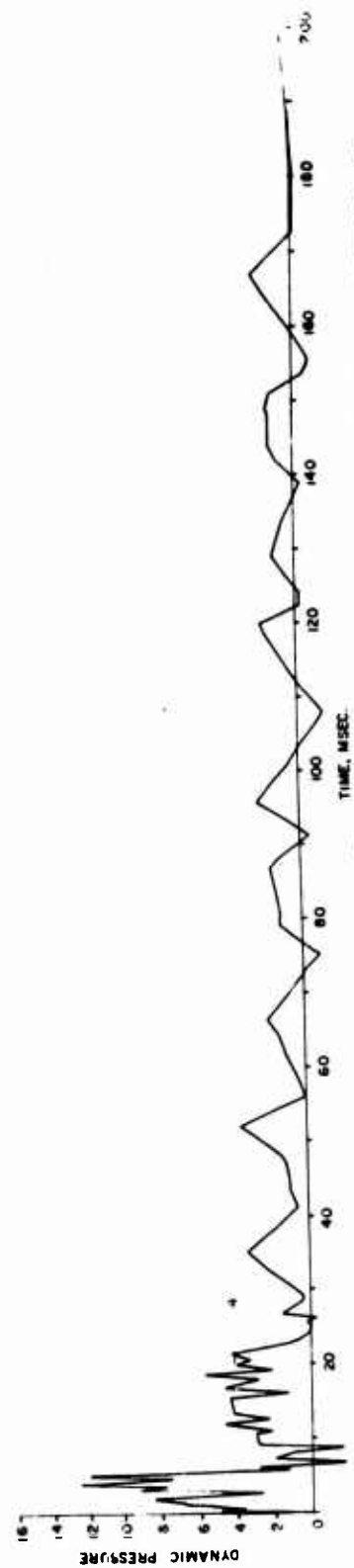
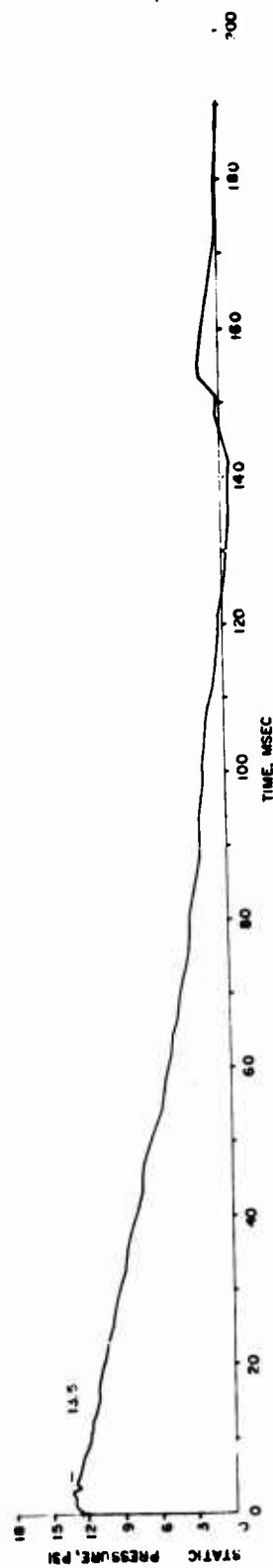
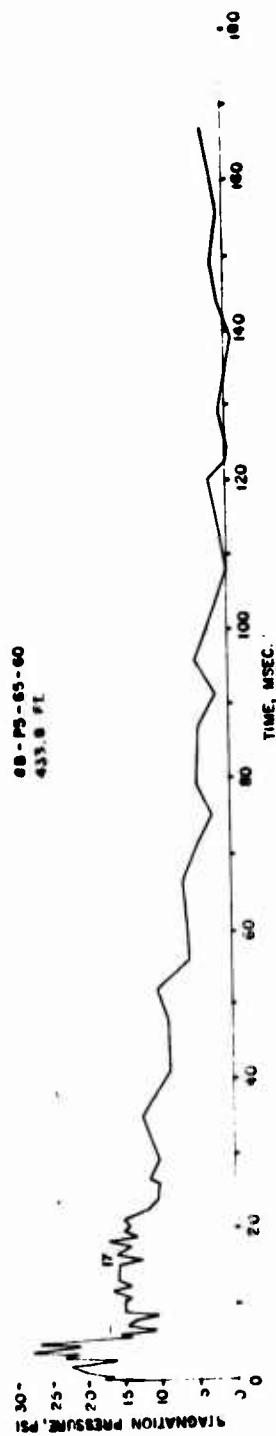


FIGURE B17 PRESSURE MEASUREMENTS ON 15° FALLING SLOPE OF TERRAIN FEATURE B, STATION P5  
SURFACE LEVEL STAGNATION BLOCK

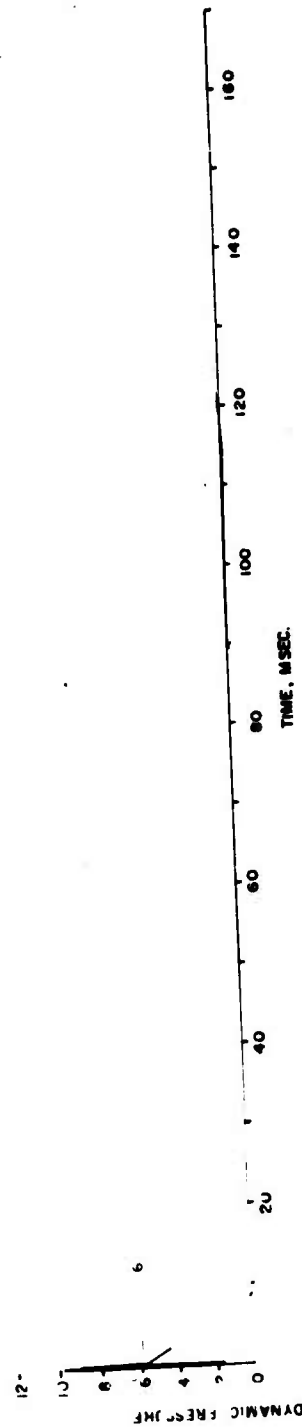
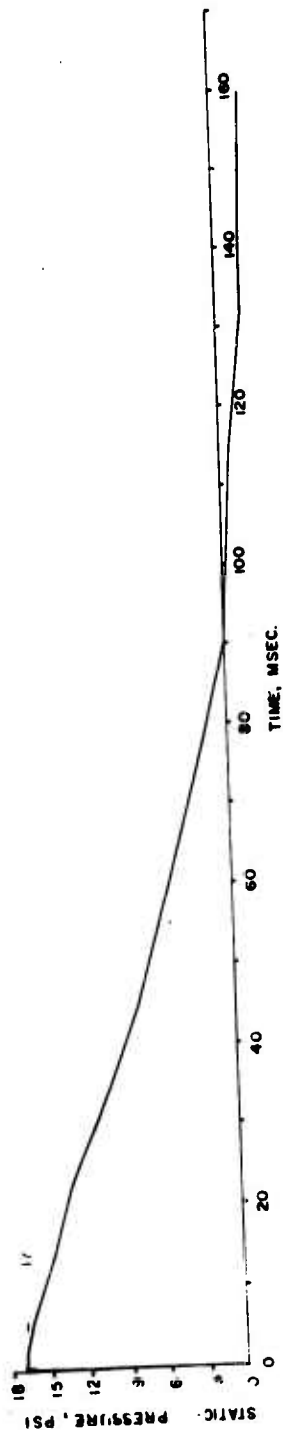
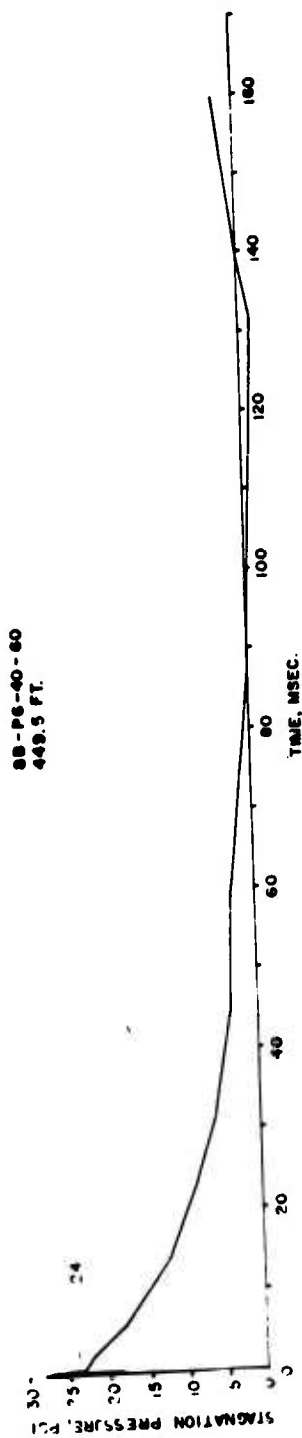


FIGURE B18 PRESSURE MEASUREMENTS IN BACK OF TERRAIN FEATURE B, STATION P6

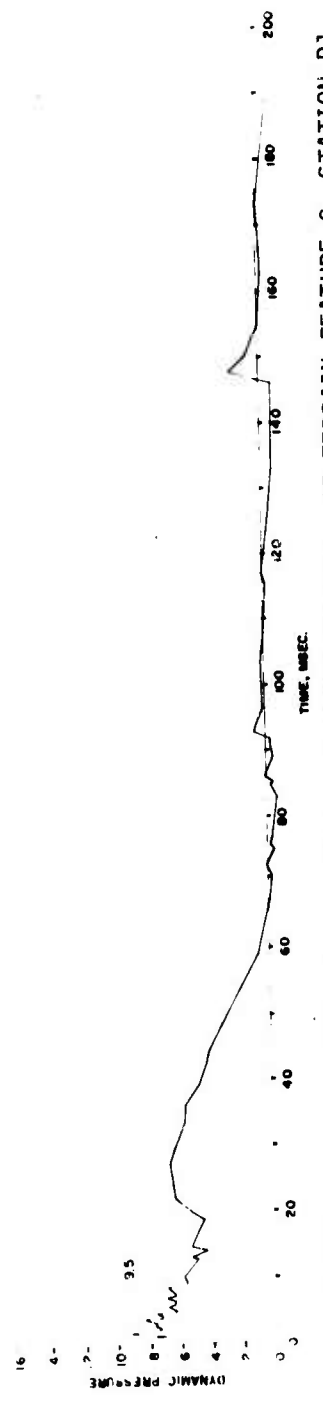
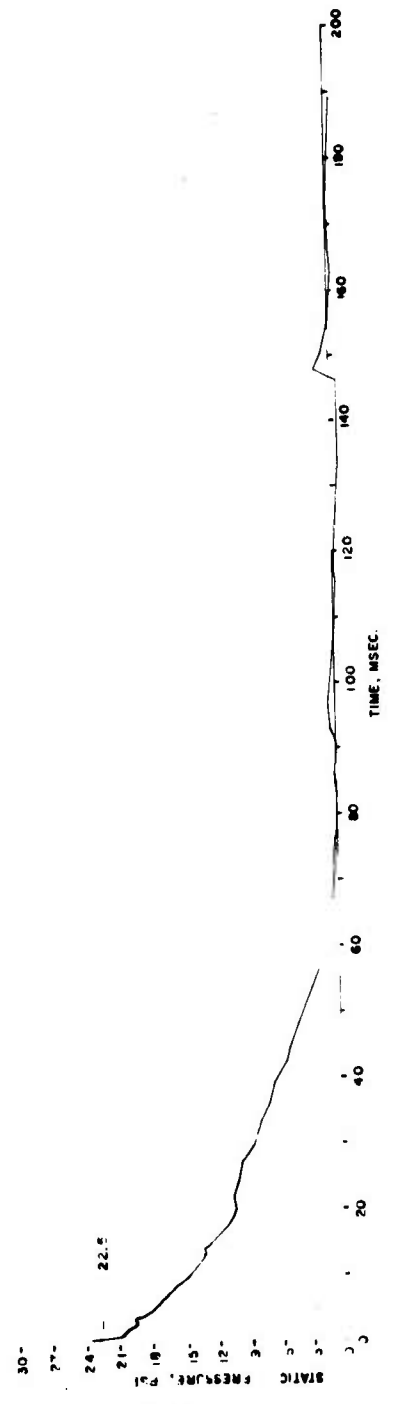
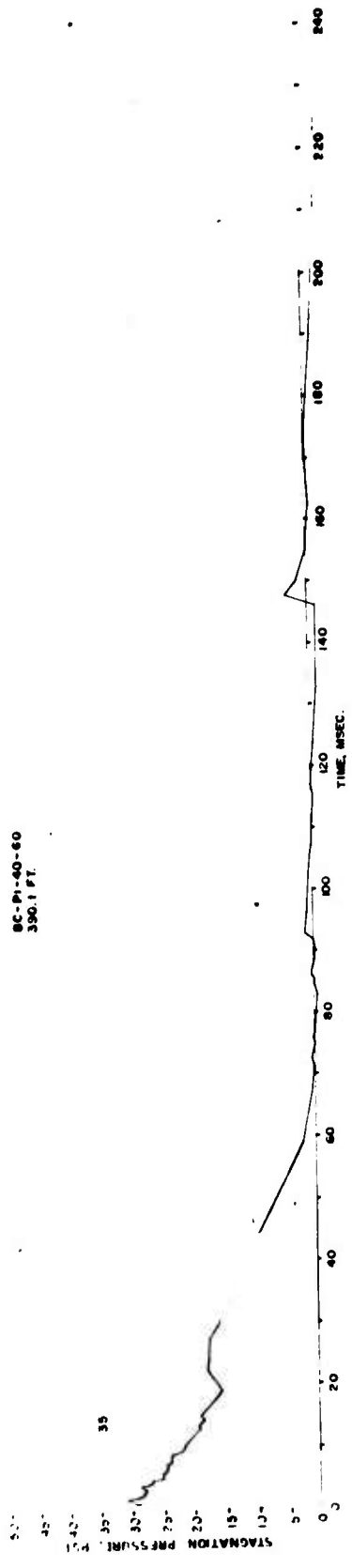


FIGURE B19 FREE FIELD PRESSURE MEASUREMENTS IN FRONT OF TERRAIN FEATURE C, STATION P1

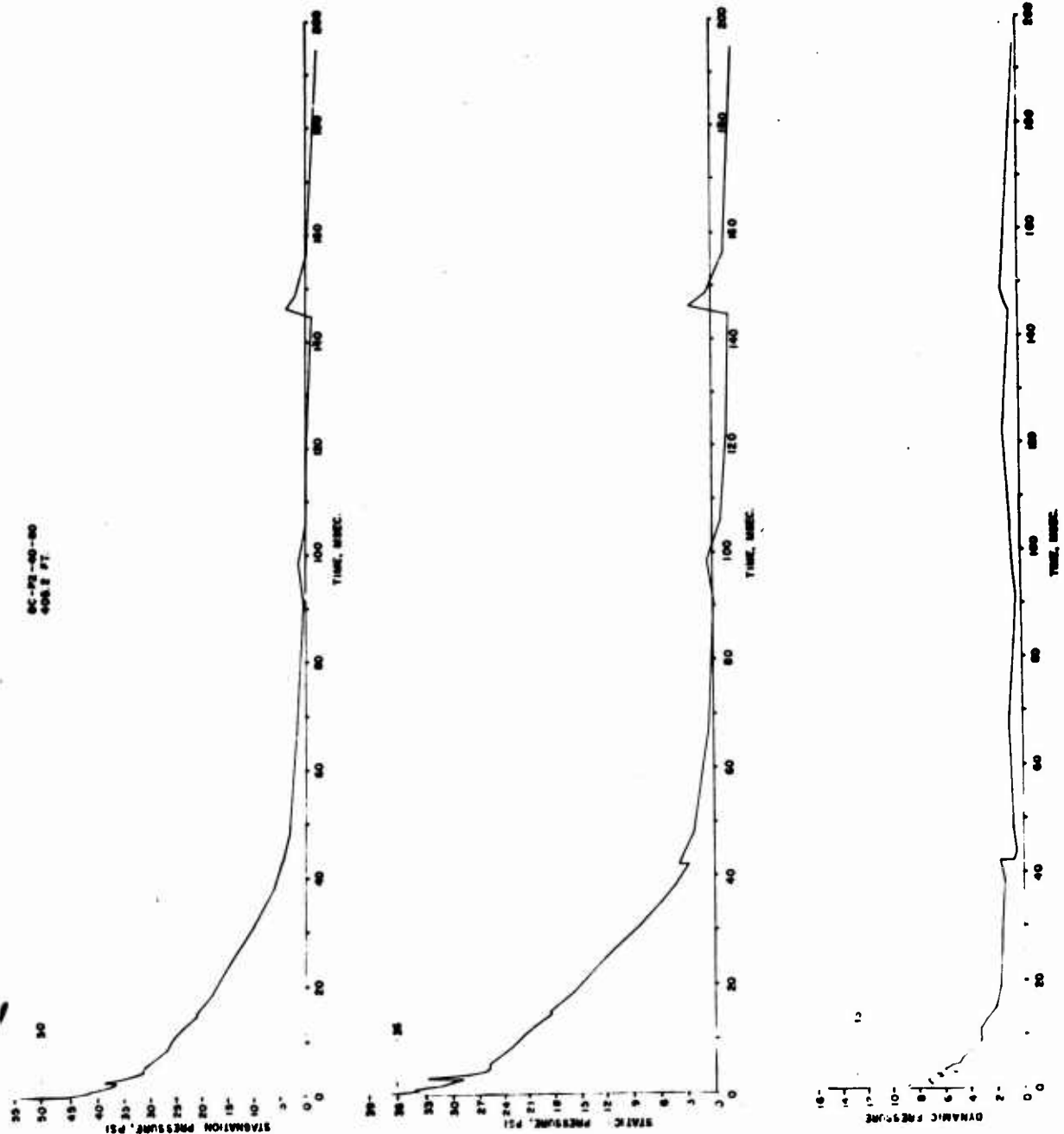


FIGURE B20 PRESSURE MEASUREMENTS ON 30° RISING SLOPE OF TERRAIN FEATURE C, STATION P2

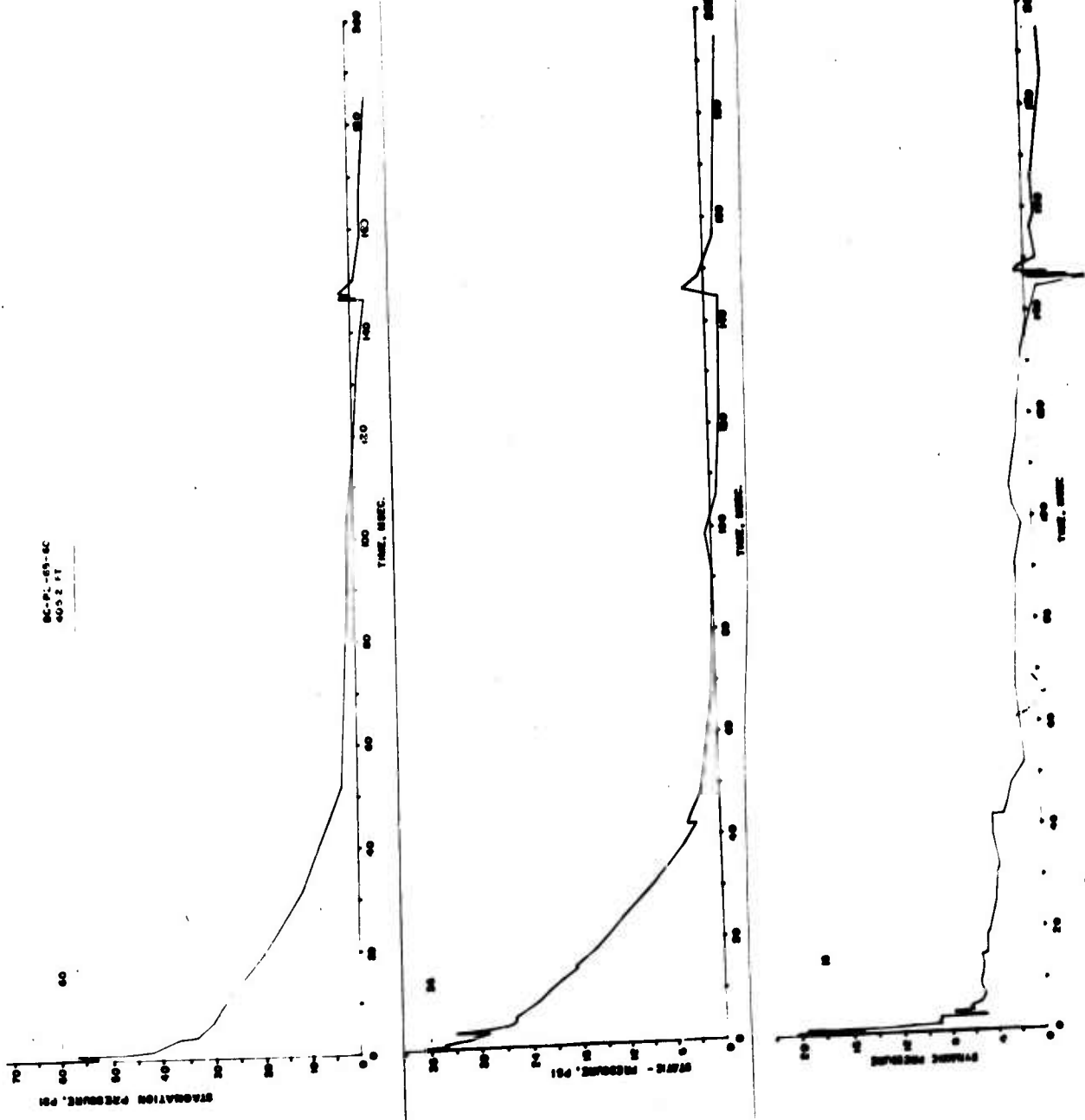


FIGURE B21 PRESSURE MEASUREMENTS ON 30° RISING SLOPE OF TERRAIN FEATURE C, STATION P2  
SURFACE LEVEL STAGNATION BLOCK

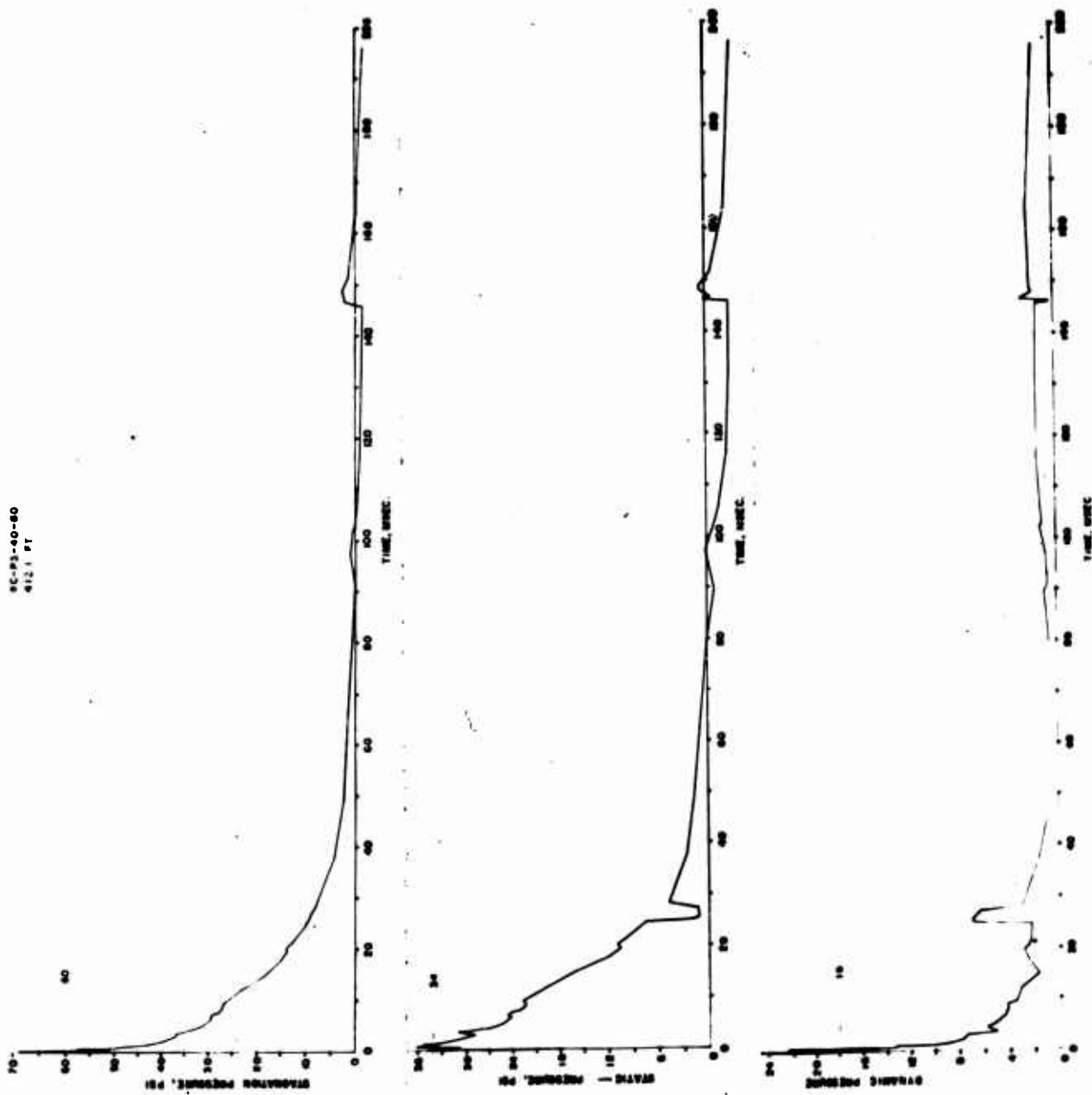


FIGURE B22 PRESSURE MEASUREMENTS ON 30° RISING SLOPE OF TERRAIN FEATURE C, STATION P3

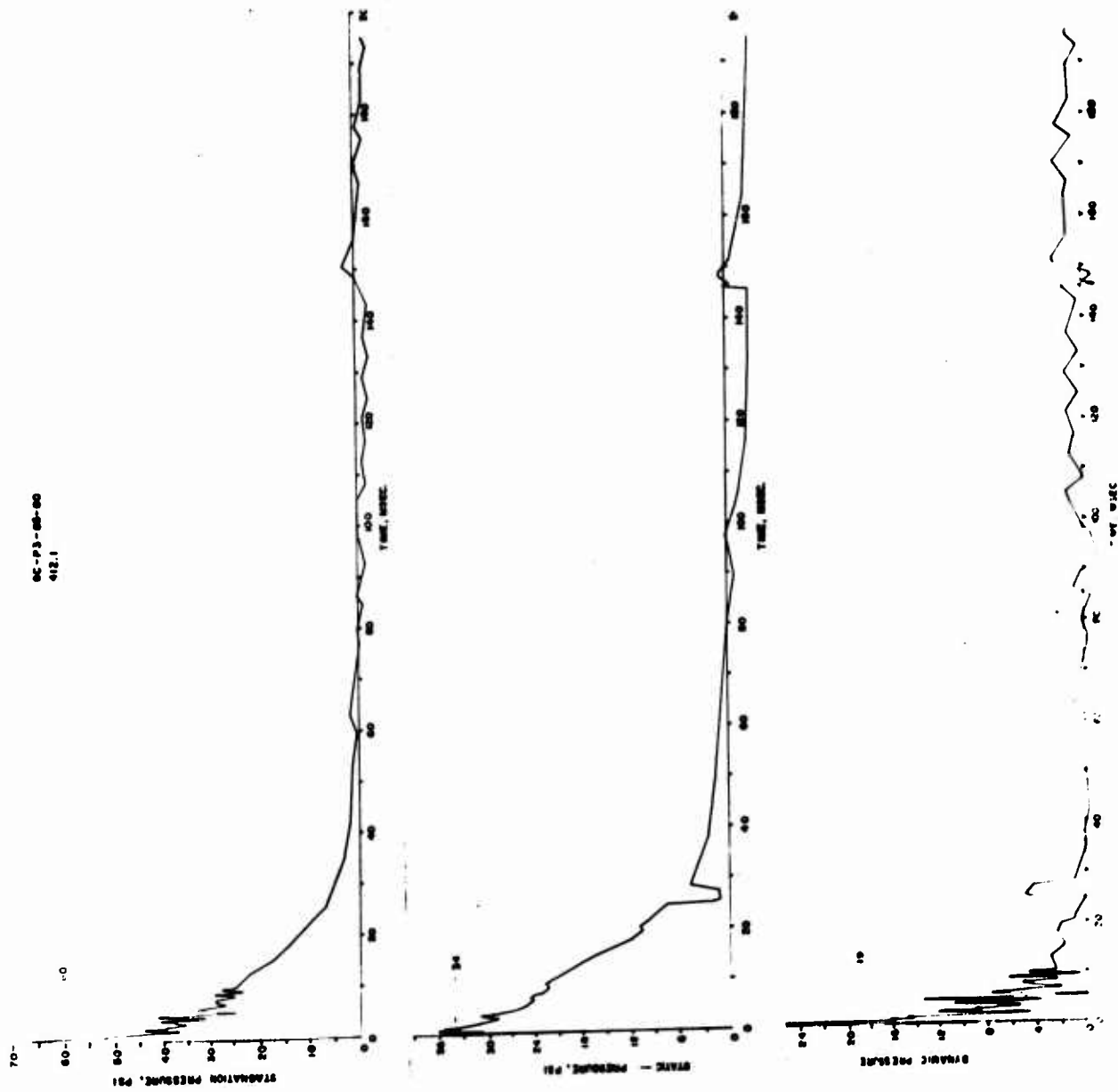


FIGURE B23 PRESSURE MEASUREMENTS ON 30° RISING SLOPE OF TERRAIN FEATURE C, STATION P3  
SURFACE LEVEL STAGNATION BLOCK



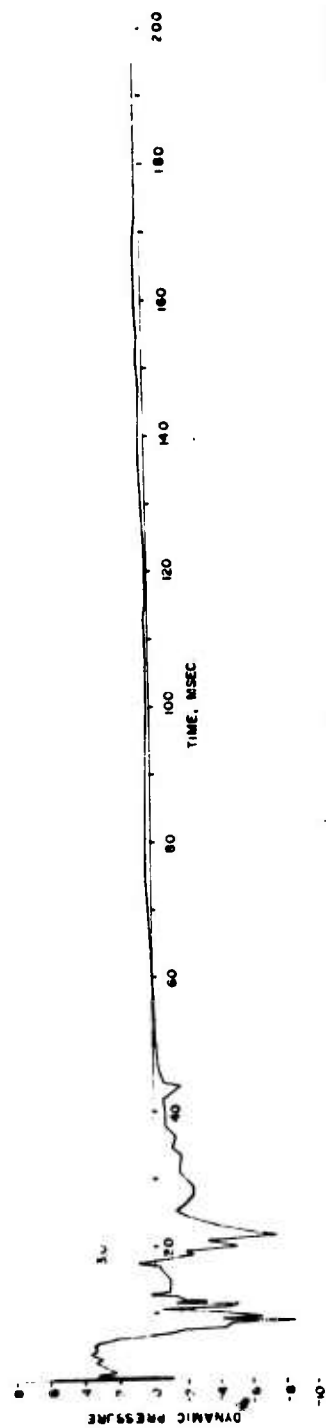
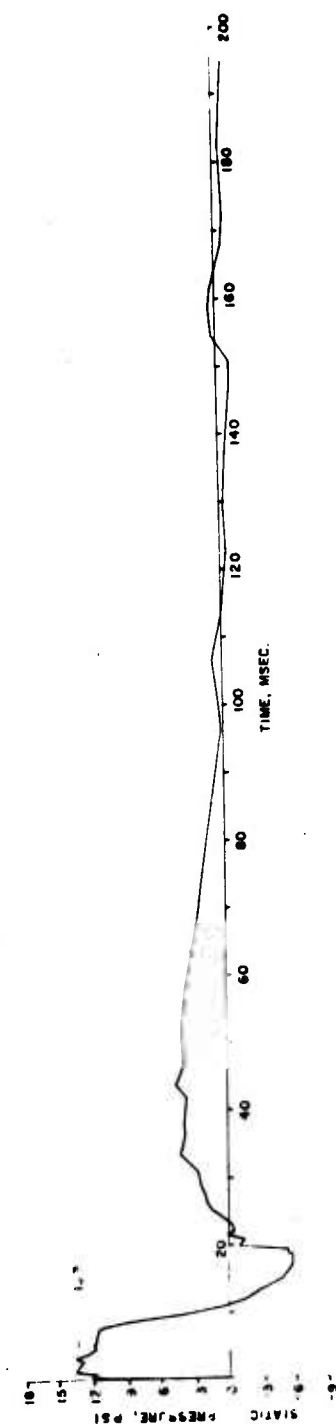
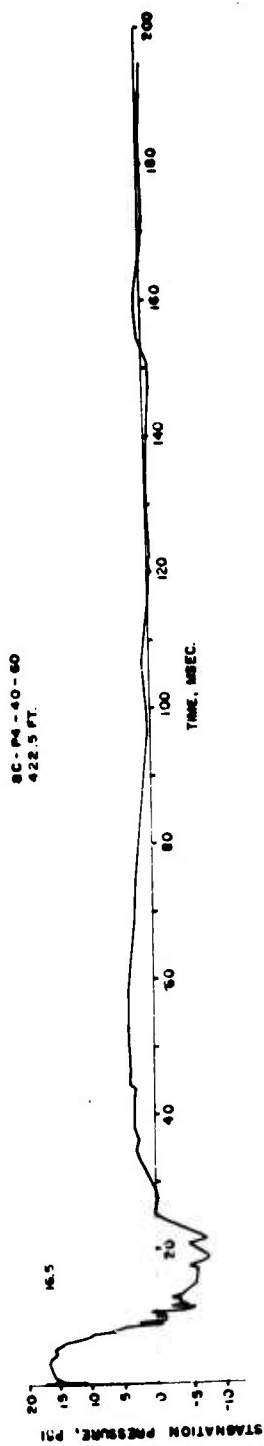


FIGURE B24 PRESSURE MEASUREMENTS ON 30° FALLING SLOPE OF TERRAIN FEATURE C, STATION P4

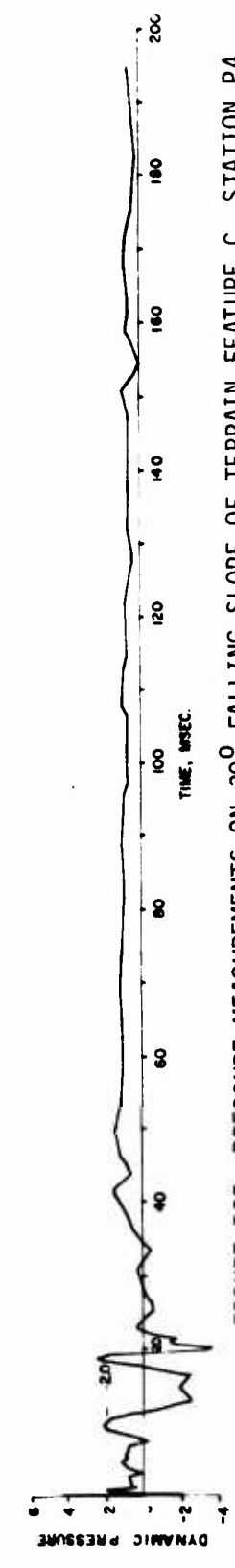
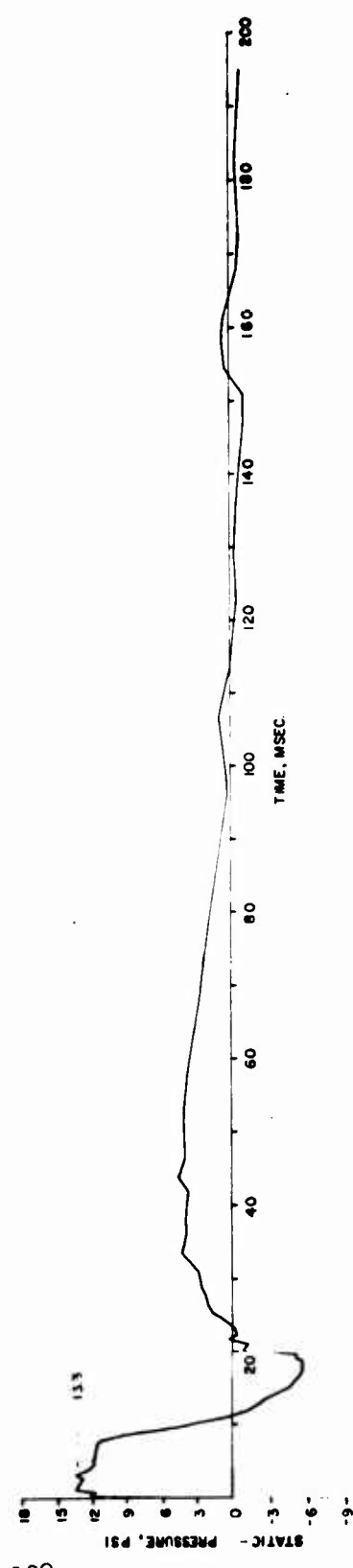
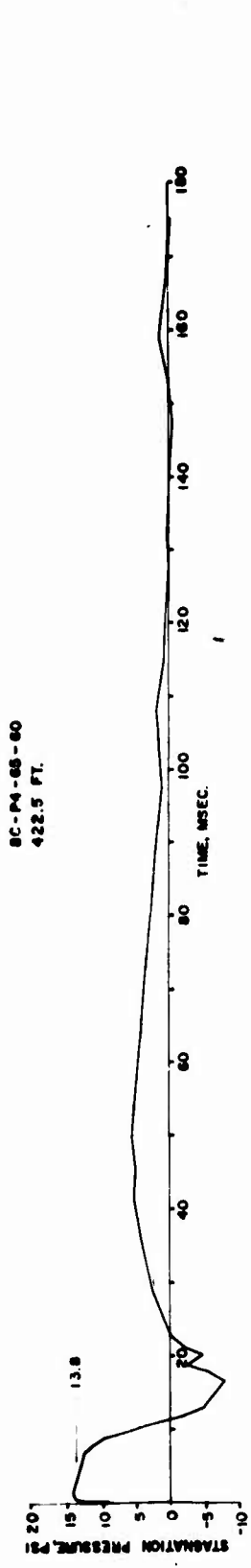
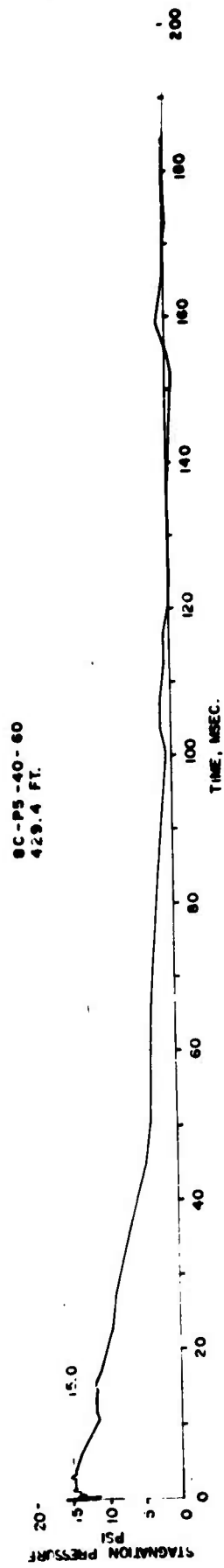


FIGURE B25 PRESSURE MEASUREMENTS ON 30° FALLING SLOPE OF TERRAIN FEATURE C, STATION P4  
SURFACE LEVEL STAGNATION BLOCK



110

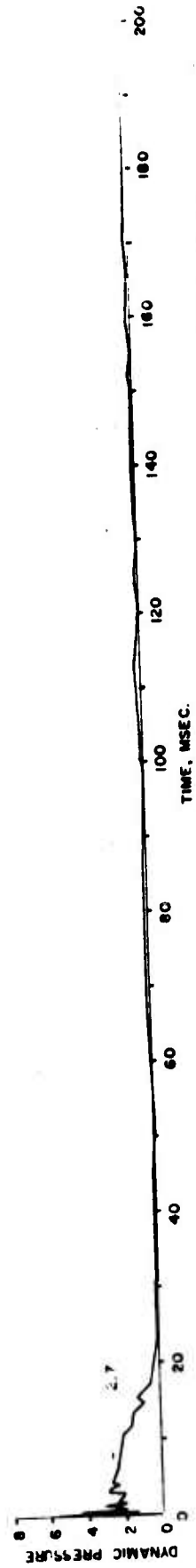
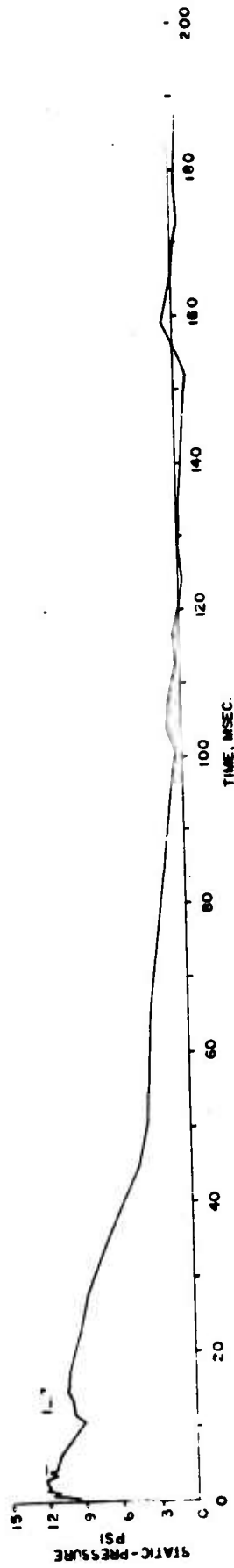


FIGURE B26 PRESSURE MEASUREMENTS ON 30° FALLING SLOPE OF TERRAIN FEATURE C, STATION P5

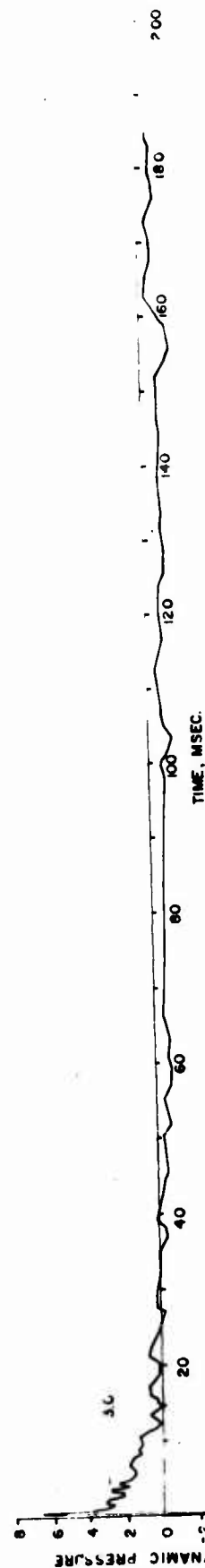
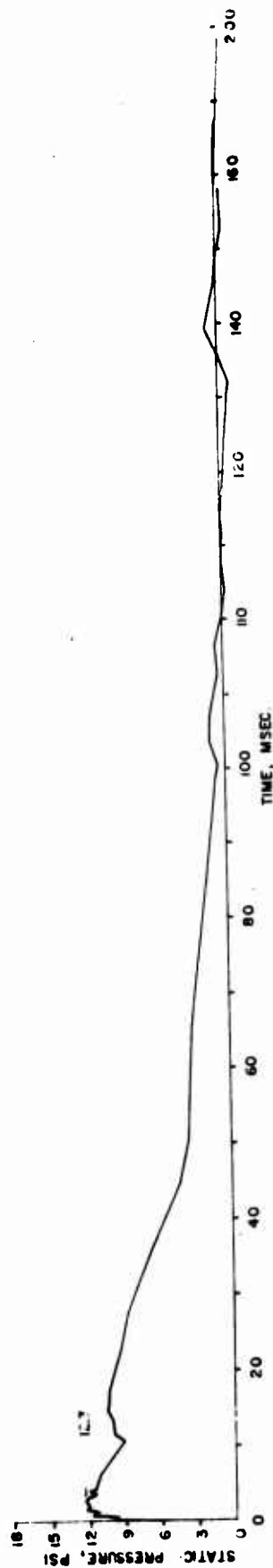
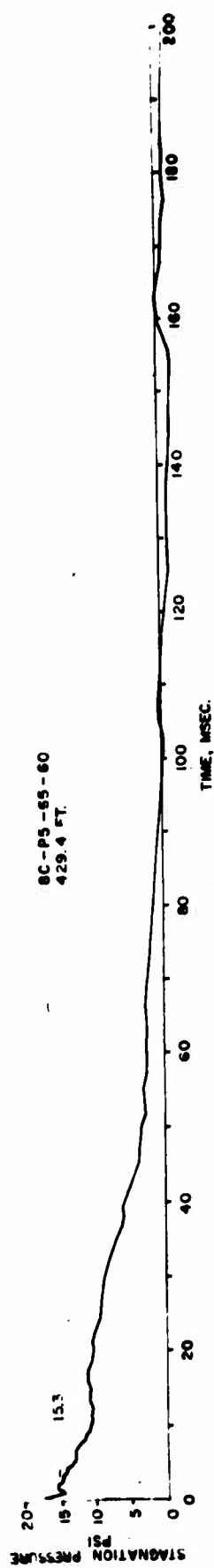


FIGURE B27 PRESSURE MEASUREMENTS ON 30° FALLING SLOPE OF TERRAIN FEATURE C, STATION P5  
SURFACE LEVEL STAGNATION BLOCK

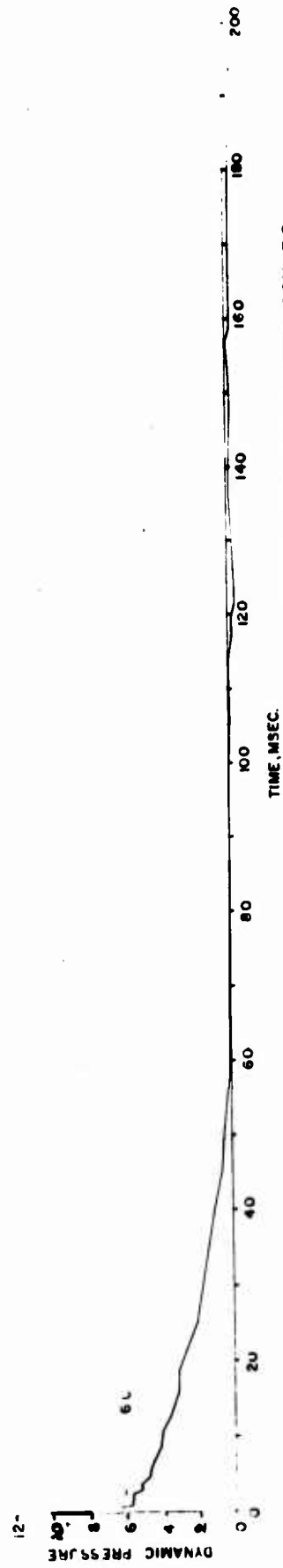
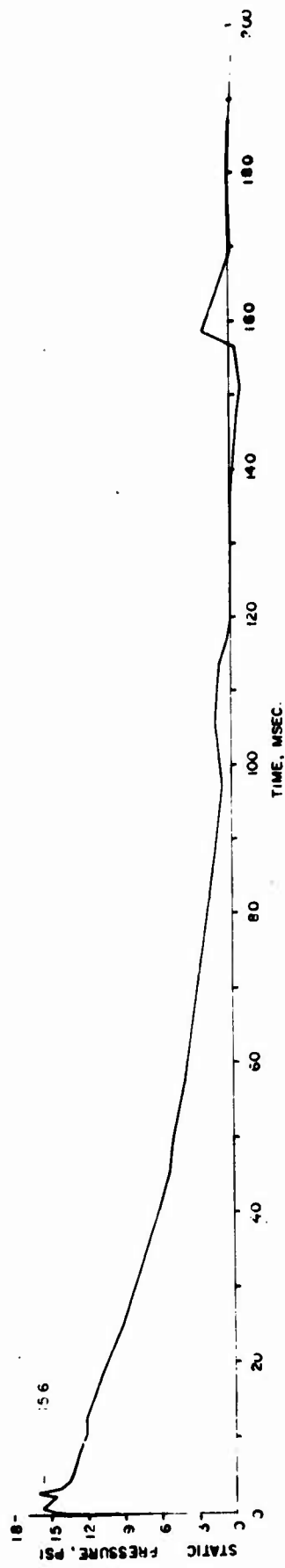
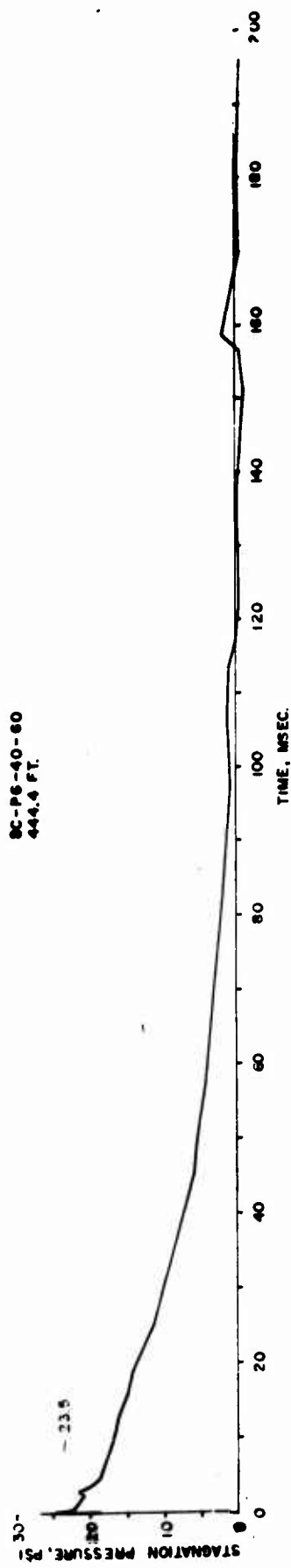


FIGURE B28 PRESSURE MEASUREMENTS IN BACK OF TERRAIN FEATURE C, STATION P6

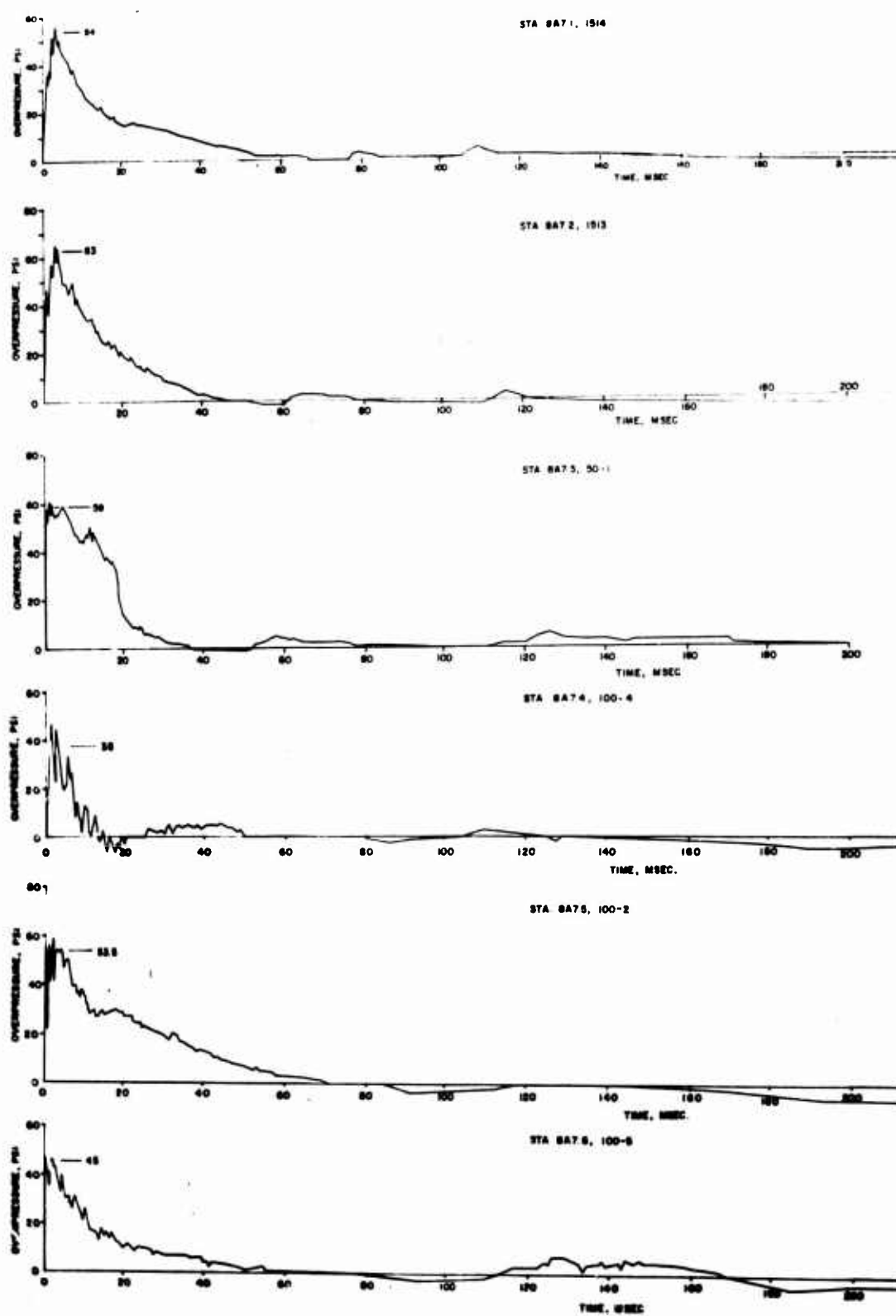


FIGURE B29 SELF-RECORDING OVERPRESSURE-TIME RECORDS FROM TERRAIN FEATURE A

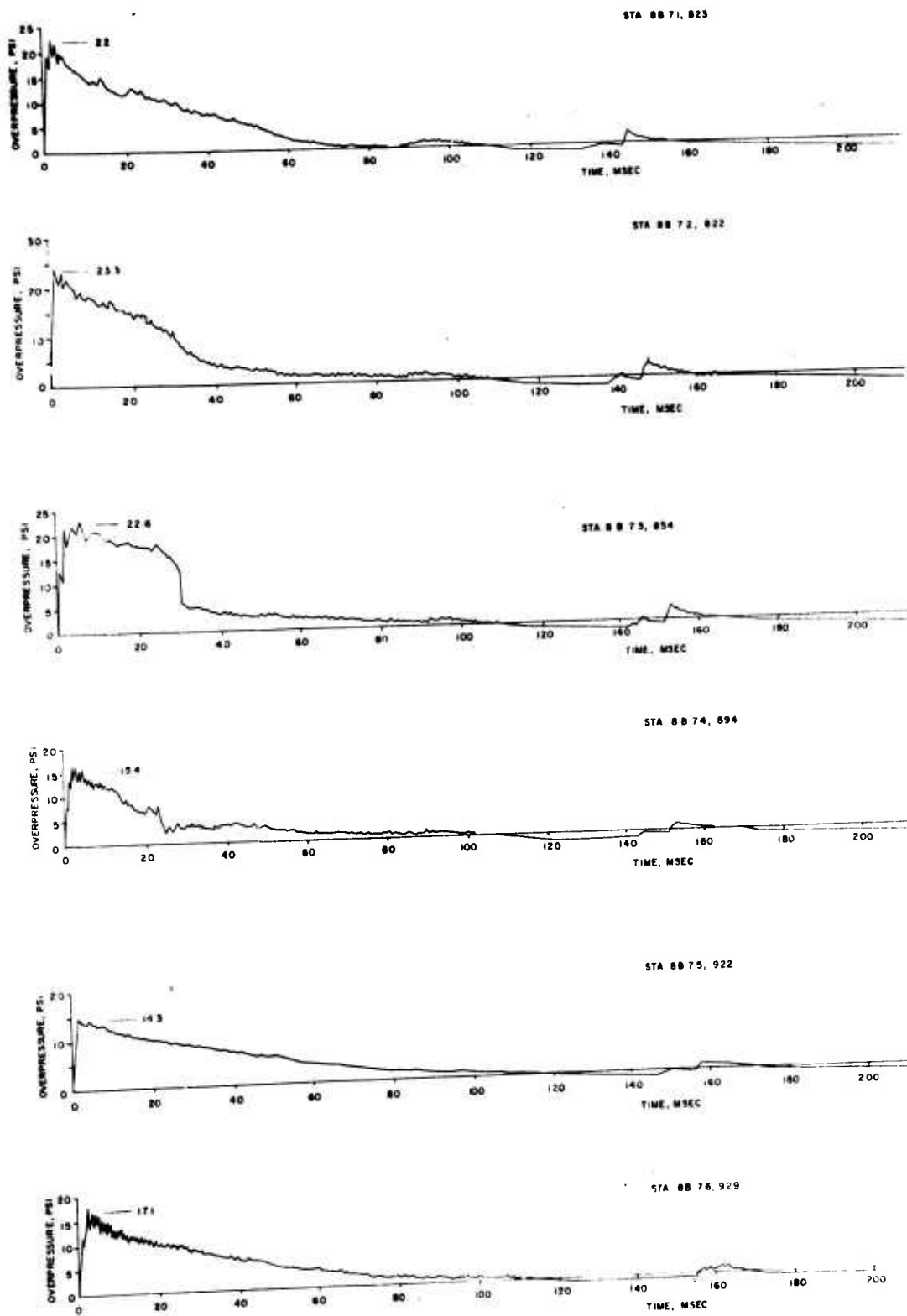


FIGURE B30 SELF-RECORDING OVERPRESSURE-TIME RECORDS FROM TERRAIN FEATURE B

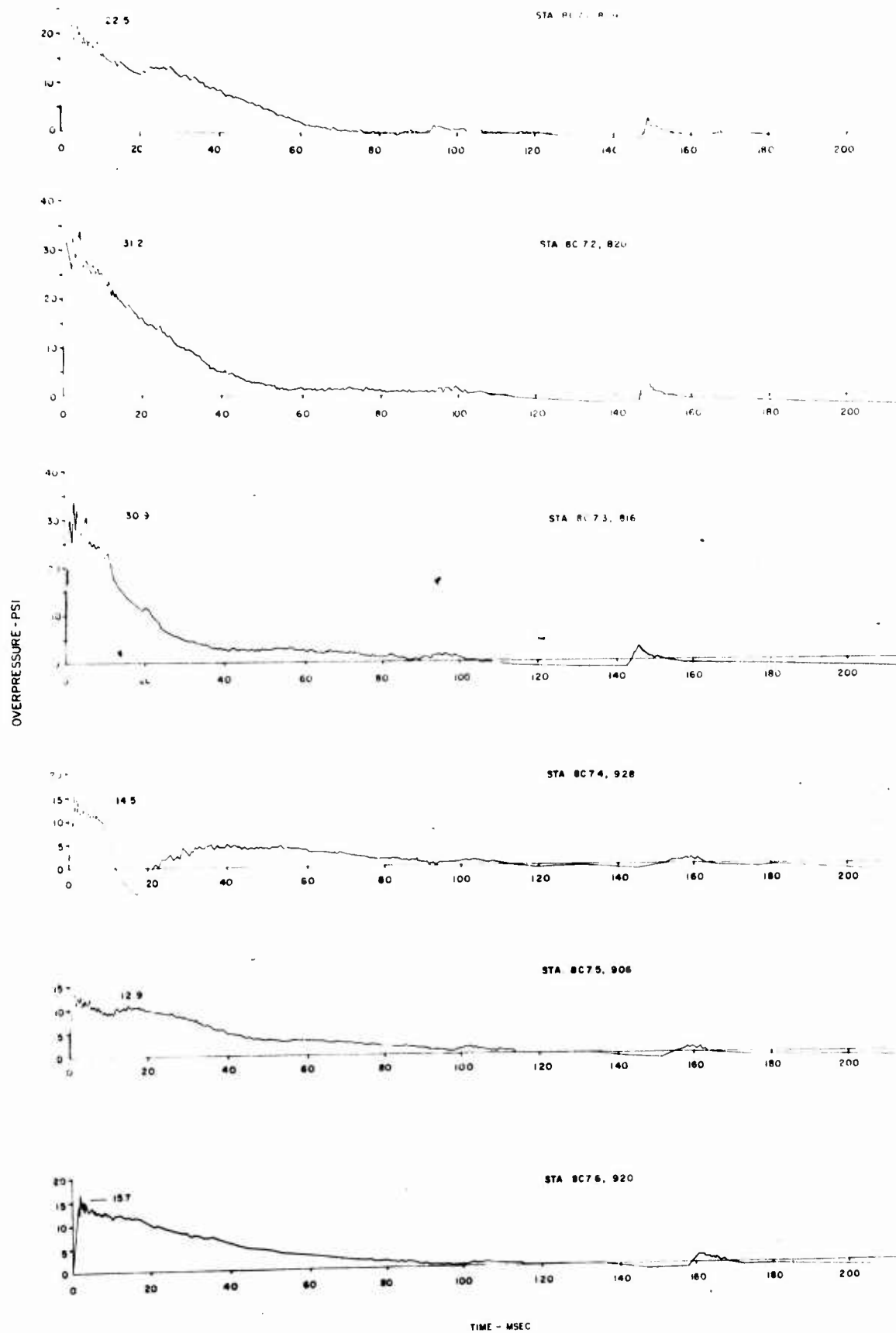


FIGURE B31 SELF-RECORDING OVERPRESSURE-TIME RECORDS FROM TERRAIN FEATURE C



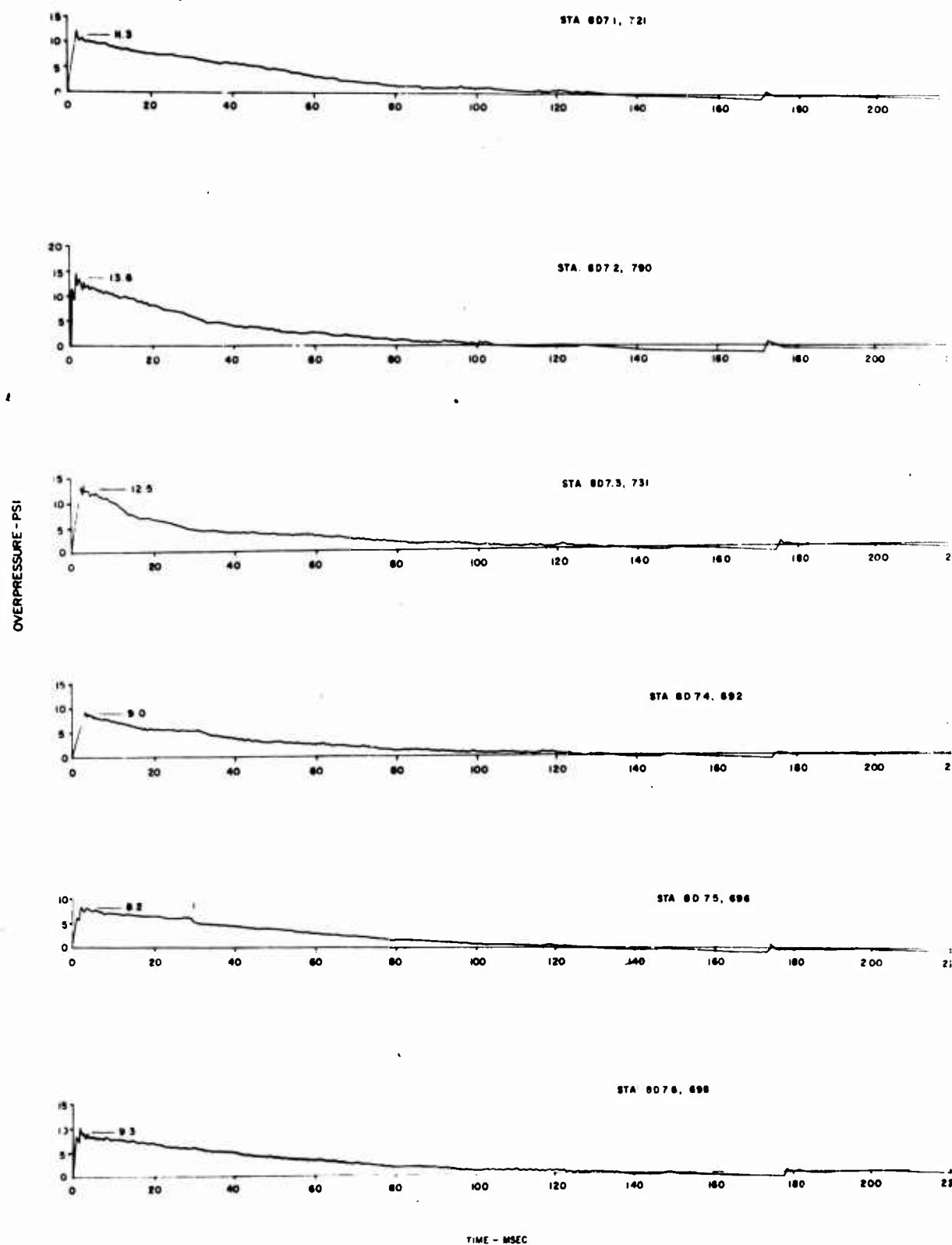


FIGURE B32 SELF-RECORDING OVERPRESSURE-TIME RECORDS FROM TERRAIN FEATURE D

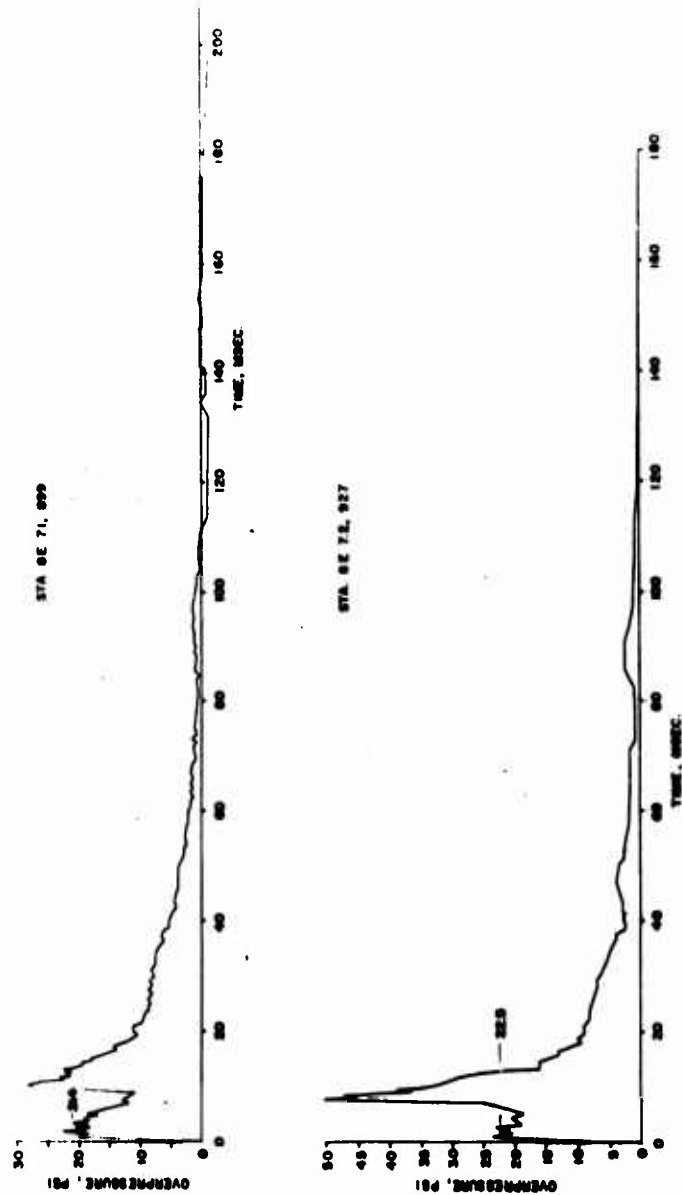


FIGURE B33 SELF-RECORDING OVERPRESSURE-TIME RECORDS FROM TERRAIN FEATURE E

Unclassified

Security Classification

DOCUMENT CONTROL DATA - R&D		
(Security classification of title, body of abstract and indexing annotation must be entered when the overall report is classified)		
1. ORIGINATING ACTIVITY (Corporate author) U.S. Army Ballistic Research Laboratories Aberdeen Proving Ground, Maryland		2a. REPORT SECURITY CLASSIFICATION Unclassified
		2b. GROUP
3. REPORT TITLE  TERRAIN EFFECTS ON BLAST WAVE PARAMETERS		
4. DESCRIPTIVE NOTES (Type of report and inclusive dates)		
5. AUTHOR(S) (Last name, first name, initial)  Keefer, John H. and Day, J. Donald		
6. REPORT DATE April 1966	7a. TOTAL NO. OF PAGES 123	7b. NO. OF REFS 11
8a. CONTRACT OR GRANT NO.	9a. ORIGINATOR'S REPORT NUMBER(S)  Report No. 1319	
b. PROJECT NO. RDT&E 1P014501A33E		
c.	9b. OTHER REPORT NO(S) (Any other numbers that may be assigned this report)	
d.		
10. AVAILABILITY/LIMITATION NOTICES This document is subject to special export controls and each transmittal to foreign governments or foreign nationals may be made only with prior approval of U.S. Army Materiel Command, Attn: AMCMU-IS, Washington, D. C.		
11. SUPPLEMENTARY NOTES	12. SPONSORING MILITARY ACTIVITY DASA, Washington, D. C. AMC, Washington, D. C.	
13. ABSTRACT  This report presents the results from large scale model terrain features exposed to the blast wave from a 100 ton TNT surface burst and a small scale terrain model exposed to the blast wave from the Ballistic Research Laboratories (BRL) high pressure shock tube.  The large scale model terrain study utilized five terrain features exposed to the blast at various pressure levels. The terrain features were equipped with various types of overpressure and dynamic pressure instrumentation. Ratios obtained from the pressure measured on the flat terrain and that measured on the rising and falling slopes are presented.  For the small scale model test, pressures were measured over the rising and falling slopes of a 30° model hill exposed to the blast wave from the mouth of the BRL detonation driven shock tube. The pressure time records measured are presented. The results compare favorably to previously reported model data.		

DD FORM 1473  
1 JAN 64

Unclassified

Security Classification

14. KEY WORDS	LINK A		LINK B		LINK C	
	ROLE	WT	ROLE	WT	ROLE	WT
Terrain effects Air blast parameters TNT air blast data						

**INSTRUCTIONS**

1. **ORIGINATING ACTIVITY:** Enter the name and address of the contractor, subcontractor, grantee, Department of Defense activity or other organization (*corporate author*) issuing the report.

2a. **REPORT SECURITY CLASSIFICATION:** Enter the overall security classification of the report. Indicate whether "Restricted Data" is included. Marking is to be in accordance with appropriate security regulations.

2b. **GROUP:** Automatic downgrading is specified in DoD Directive 5200.10 and Armed Forces Industrial Manual. Enter the group number. Also, when applicable, show that optional markings have been used for Group 3 and Group 4 as authorized.

3. **REPORT TITLE:** Enter the complete report title in all capital letters. Titles in all cases should be unclassified. If a meaningful title cannot be selected without classification, show title classification in all capitals in parenthesis immediately following the title.

4. **DESCRIPTIVE NOTES:** If appropriate, enter the type of report, e.g., interim, progress, summary, annual, or final. Give the inclusive dates when a specific reporting period is covered.

5. **AUTHOR(S):** Enter the name(s) of author(s) as shown on or in the report. Enter last name, first name, middle initial. If military, show rank and branch of service. The name of the principal author is an absolute minimum requirement.

6. **REPORT DATE:** Enter the date of the report as day, month, year, or month, year. If more than one date appears on the report, use date of publication.

7a. **TOTAL NUMBER OF PAGES:** The total page count should follow normal pagination procedures, i.e., enter the number of pages containing information.

7b. **NUMBER OF REFERENCES:** Enter the total number of references cited in the report.

8a. **CONTRACT OR GRANT NUMBER:** If appropriate, enter the applicable number of the contract or grant under which the report was written.

8b, 8c, & 8d. **PROJECT NUMBER:** Enter the appropriate military department identification, such as project number, subproject number, system numbers, task number, etc.

9a. **ORIGINATOR'S REPORT NUMBER(S):** Enter the official report number by which the document will be identified and controlled by the originating activity. This number must be unique to this report.

9b. **OTHER REPORT NUMBER(S):** If the report has been assigned any other report numbers (*either by the originator or by the sponsor*), also enter this number(s).

10. **AVAILABILITY/LIMITATION NOTICES:** Enter any limitations on further dissemination of the report, other than those imposed by security classification, using standard statements such as:

- (1) "Qualified requesters may obtain copies of this report from DDC."
- (2) "Foreign announcement and dissemination of this report by DDC is not authorized."
- (3) "U. S. Government agencies may obtain copies of this report directly from DDC. Other qualified DDC users shall request through \_\_\_\_\_."
- (4) "U. S. military agencies may obtain copies of this report directly from DDC. Other qualified users shall request through \_\_\_\_\_."
- (5) "All distribution of this report is controlled. Qualified DDC users shall request through \_\_\_\_\_."

If the report has been furnished to the Office of Technical Services, Department of Commerce, for sale to the public, indicate this fact and enter the price, if known.

11. **SUPPLEMENTARY NOTES:** Use for additional explanatory notes.

12. **SPONSORING MILITARY ACTIVITY:** Enter the name of the departmental project office or laboratory sponsoring (*paying for*) the research and development. Include address.

13. **ABSTRACT:** Enter an abstract giving a brief and factual summary of the document indicative of the report, even though it may also appear elsewhere in the body of the technical report. If additional space is required, a continuation sheet shall be attached.

It is highly desirable that the abstract of classified reports be unclassified. Each paragraph of the abstract shall end with an indication of the military security classification of the information in the paragraph, represented as (TS), (S), (C), or (U).

There is no limitation on the length of the abstract. However, the suggested length is from 150 to 225 words.

14. **KEY WORDS:** Key words are technically meaningful terms or short phrases that characterize a report and may be used as index entries for cataloging the report. Key words must be selected so that no security classification is required. Identifiers, such as equipment model designation, trade name, military project code name, geographic location, may be used as key words but will be followed by an indication of technical context. The assignment of links, rules, and weights is optional.